University of Alberta

Expression in the yeast *Saccharomyces cerevisiae* and purification of the human erythrocyte Anion Exchanger (AE1)

By

Haley Jean Shandro 

A thesis submitted to the Faculty of Graduate Studies and Research in partial fulfilment of the requirements for the degree of

Master of Science

Department of Biochemistry

Edmonton, Alberta, Canada
Fall 2007

Your file Votre référence
ISBN: 978-0-494-33347-1
Our file Notre référence
ISBN: 978-0-494-33347-1

I dedicate this thesis to my husband, and my family, whose continued support throughout my education has made this work possible.

Abstract

The human Anion Exchanger, AE1, facilitates the electroneutral exchange of chloride for bicarbonate across the erythrocyte membrane. AE1, which comprises 50% of the erythrocyte integral membrane protein, plays a central role in CO_2 metabolism and pH regulation. The 55 kDa membrane domain of AE1 (AE1MD) has 12-14 transmembrane segments and is alone responsible for the transport function of the protein. A high-resolution x-ray crystallographic structure has not been determined for the membrane domain. The current study describes a method for the expression and purification of the membrane domain of AE1 expressed in *Saccharomyces cerevisiae*. The AE1 membrane domain alone, modified with both a 6-His and GST tag, was expressed to 0.5-0.8 mg/l culture. This yeast expression system allows for expression of AE1MD in a eukaryotic membrane, processing through the endoplasmic reticulum for proper folding, and reproducible, large-scale expression and purification of homogeneous protein.

Acknowledgements

I would like to thank my supervisor, Dr. Joe Casey, for the opportunity to grow and learn in his laboratory. He has challenged and supported me throughout my degree, and I am grateful for his guidance.

I would like to thank the past and present members of the Casey lab, who made the lab environment so enjoyable to be in. I would like to particularly acknowledge Dr. Bernardo Alvarez and Dr. Patricio Morgan for their friendship, expertise, and occasional Spanish lessons. Anita Quon and Carmen Rieder have been amazingly helpful and supportive, and are excellent resources in the lab. Fellow graduate students Danielle Johnson, Pamela Bonar have been great colleagues. I would like to acknowledge a graduate student who has gone before me, Heather McMurtrie, who was a great friend, sounding board, and an inspiration to choose my own true path in life.

I would like to thank my committee members Dr. Larry Fliegel and Dr. Mark Glover, who have constantly supported me throughout my project. So many people in the departments of Biochemistry and Physiology at the University of Alberta have helped me with techniques and equipment that I can't mention them all. Without such a collaborative environment, this research would never have been possible.

I would like to acknowledge the Canadian Institute of Health Research Strategic Training Initiative in Membrane Proteins and Cardiovascular Disease for financial support.

Table of Contents

List of Tables

List of Figures

Abbreviations

2D, two-dimensional

3D, three-dimensional

AE, anion exchanger

AE1Ct, AE1 C-terminal domain

AE1MD, yeast expressed AE1 membrane domain

Amp, ampicillin

BAD, biotin acceptor domain

BCA, bicinchoninic acid

BSA, bovine serum albumin

BT, bicarbonate transporter

$C_{12}E_8$, octaethylene glycol monododecyl ether

CA, carbonic anhydrase

cAE1MD, cleaved AE1MD

CBP, calmodulin binding protein

CD, circular dichroism spectroscopy

CIP, calf intestinal alkaline phosphatase

Ct or C-terminus, carboxyl-terminal

DIC, differential interference contrast

DIDS, 4,4'-diisothiocyanostilbene-2,2'-disulfonate

DDM, dodecyl maltoside

dNTP, deoxynucleotide triphosphates

dRTA, distal renal tubular acidosis

DTT, dithiothreitol

ECL, enhance chemiluminescence

EDTA, ethylenediaminetetraacetic acid

E. coli, Escherichia coli

FC, Fos-choline

GAL-AE1MD, galactose induced AE1MD

GSH, reduced glutathione

GST, glutathione S-transferase

GST-AE1Ct, GST fusion protein of AE1Ct

HEK, human embryonic kidney

HRP, horseradish peroxidase

HS, hereditary spherocytosis

IPB, immunoprecipitation buffer

IPTG, isopropylthiogalactoside

kb, kilobases

kDa, kiloDalton

LB, Luria-Bertani

MBP, maltose binding protein

LPC, lysophosphatidylcholine

NBC, sodium bicarbonate co-transporter

Nt or N-terminus, amino-terminal

OG, octyl glucoside

PBS, phosphate buffered saline

PCR, polymerase chain reaction

PGK, phosphoglycerate kinase

pI, isoelectric point

PMSF, phenylemthanesulfonyl fluoride

PNGase F, peptide-N-glycosidase F

PVDF, polyvinylidene difluoride

RNaseA, Ribonuclease A

S. cerevisiae, Saccharomyces cerevisiae

SAO, Southeast Asian Ovalocytosis

SDS, sodium dodecyl sulfate

SDS-PAGE, SDS-polyacrylamide gel electrophoresis

SERCA, sarco/endoplasmic reticulum calcium ATPase

SITS, 4-acetamido-4′-isothiocyanostilbene-2,2′-disulfonate

SLC, solute carrier family

TM, transmembrane segment

Chapter 1

Introduction

1.1 Chloride/Bicarbonate exchange proteins

Actively metabolizing tissues produce acid; for respiratory oxidation to proceed, this acid waste must be removed. Acid equivalents are removed from the body in several ways. Buffers throughout the body neutralize the buildup of acid, the base bicarbonate (HCO_3^-) is reabsorbed in the kidney as protons are excreted in the urine, and carbon dioxide is exhaled at the lung. These processes prevent the buildup of acid equivalents in the body. If acid is allowed to accumulate, the result could be whole body metabolic acidosis and a loss of pH homeostasis. To maintain pH homeostasis, plasma membrane bicarbonate transporters are expressed throughout the body. These transporters move membrane-impermeant bicarbonate across biological membranes, thereby facilitating removal of metabolic waste.

There are several classes of bicarbonate transporters, the major one being the Cl^-/HCO_3^- exchangers. Two distinct families of polytopic membrane proteins, the SLC4 family, and the SLC26 family, contain members that function as Cl^-/HCO_3^- exchangers. The families are designated "SLC" by the Human Genome Organization (HUGO), which stands for "solute carrier" (1). Chloride/bicarbonate exchangers are found in both the SLC4 and SLC26 families, but there is no significant evolutionary relationship between the two families. Therefore the two families are distinct, as represented in Figure 1.1 (Milton Saier, UCSD, personal communication). The SLC4 family can further be divided into sodium-dependent (Na^+ Bicarbonate Co-transporters (NBCs)), and sodium-independent (anion exchangers (AEs)) transporters. The AEs have been well studied, and serve as a model for other bicarbonate transporter proteins. The anion exchangers (AE1-AE3) mediate electroneutral Cl^-/HCO_3^- exchange

across the plasma membrane of cells throughout the body. AE1 is expressed in erythrocytes and kidney, while AE3 is expressed in metabolically active tissues such as retina, heart, and brain. AE2 is expressed widely in many tissues. AE proteins are targeted to the basolateral membrane of epithelial cells. AE1, the best characterized of the Cl^-/HCO_3^- exchangers, serves as a model for functional and structural studies of the other anion exchangers.

1.2 Human Erythrocyte Anion Exchanger, AE1

1.2.1 Physiological role

AE1 (Band 3) is a member of a family of membrane proteins that carry out the electroneutral exchange of Cl^- for HCO_3^- across the plasma membrane (2). Members of this family, mammalian anion exchangers (AE), help to regulate cell volume and intracellular pH (2, 3). There are three forms of AE1. Erythrocyte AE1 is the full-length form. Kidney AE1 (kAE1) is truncated and transcribed from an alternate promoter. A novel truncated splicing variant of AE1, AE1n, is expressed in rat neonatal cardiomyocytes (4) and AE1n mRNA transcripts are observed in adult rat heart (5). The function of AE1n is unknown.

Erythrocyte AE1 accounts for ~50% of the total integral membrane protein in the human erythrocyte (6) and is present at 1.2×10^6 copies per cell (6, 7) where it functions to increase the total CO_2 carrying capacity of the blood (8). AE1 was originally named Band 3 due to the protein's position on polyacrylamide gels following electrophoresis of erythrocyte membranes.

CO_2 metabolism and HCO_3^- transport in erythrocytes is well characterized (Fig. 1.2). Metabolic activity in tissues produces the waste product, CO_2/HCO_3^-,

through respiratory oxidation. Metabolic acidosis occurs if waste CO_2 is allowed to accumulate in tissue. Thus, an efficient removal system for CO_2 is in place in the body. Membrane-permeant CO_2 diffuses into erythrocytes in peripheral capillaries, where it is rapidly converted to membrane-impermeant HCO_3^- by the cytosolic enzyme, carbonic anhydrase II (CAII) (9). The reversible hydration of CO_2 to HCO_3^- also produces a proton (9). The erythrocyte plasma membrane Cl^-/HCO_3^- exchanger, AE1, driven by the outward gradient of HCO_3^-, exports HCO_3^- into the blood plasma in exchange for Cl^- (10). At the lung, a low CO_2 environment causes the process to reverse. HCO_3^- is driven into the erythrocyte by the inward concentration gradient through AE1, in exchange for Cl^-. In the erythrocyte, CAII catalyses the formation of CO_2, which subsequently diffuses into the alveoli and is excreted via exhalation. By exhaling CO_2, metabolic acidosis and sustained respiratory oxidation are prevented. Therefore, the erythrocyte bicarbonate transport cycle is vital for whole body pH homeostasis. The conversion of CO_2 to the more soluble form, HCO_3^-, increases the carrying capacity of the blood for CO_2, and increases the body's ability to remove metabolic waste (8). Since AE1 activity in the erythrocyte may be the rate-limiting factor in cardiovascular performance (11), AE1 plays a very significant physiological role.

AE1 has a central role in protein complexes in the erythrocyte. It serves as an anchoring site for many erythrocyte membrane-associated proteins such as the adaptor protein ankyrin (12), which links AE1 to the cytoskeleton, protein 4.2 (13), protein 4.1 (14), glyceraldehyde-3-phosphate-dehydrogenase (15), phosphofructokinase (16), hemoglobin (17), and protein tyrosine kinase $p72^{syk}$ (18). Through interactions with the spectrin/actin cytoskeleton, AE1 helps to

maintain the biconcave structure of the erythrocyte, and helps control cell shape and flexibility (19). In order to fit through the small diameter of the capillaries during blood flow, erythrocytes must be flexible and able to bend. AE1 helps maintain the required flexibility through its interactions with other proteins. The majority of intracellular protein-protein interactions that AE1 is involved in occur in the large cytosolic N-terminal domain.

AE1 may also play a role regulating the metabolism of glucose (20), and also acts as a senescence antigen to clear aged and damaged erythrocytes from the blood stream (21). When AE1 clusters in the membrane, antibodies bind to the extracellular surface of the erythrocyte to facilitate removal of aged or damaged erythrocytes in the spleen (22-24). AE1 may form a portion of the site of erythrocyte invasion of the malarial parasite, *Plasmodium falciparum* (25, 26)

AE1 forms multiple blood group antigens (27). The antigens are located primarily on extracellular loop 3 and 4, and also 1 and 7. The Wright blood group antigen is formed by an interaction between the erythrocyte integral membrane protein, glycophorin A, and transmembrane segment 8 of AE1 (28). Glycophorin A may also stabilize AE1 structure, increase the processing of AE1 to the erythrocyte plasma membrane, and increase the transport activity of AE1 by 30% (29-31).

While the erythrocyte has a central role in CO_2 metabolism, the role of the kidney is centred around fluid and electrolyte balance in addition to pH homeostasis. In order to perform these vital functions, the kidney has multiple mechanisms for secretion of acid or base equivalents as fluid moves through the nephron, and also for the absorption of salt (NaCl) (32). The truncated form of AE1 in the kidney, kAE1, functions to acidify the urine, and reabsorb bicarbonate

to help maintain pH homeostasis. The majority of HCO_3^- absorption occurs in the proximal tubule, mediated by basolateral NBC1 (33-36). kAE1 functions in the distal renal tubule and the collecting duct, where the fine-tuning of urine composition takes place. kAE1 is found in the renal distal tubule, and is targeted specifically to the basolateral membrane of renal α-intercalated cells by information in the C-terminal tail (37-42). Approximately 5% of the total filtered HCO_3^- is reabsorbed in the distal tubule and collecting duct (43). Intercalated cells in the collecting duct are termed alpha (α-, A-type, acid secreting), or beta (β-, B-type, base secreting), depending on the role they play in HCO_3^- handling. Alpha intercalated cells reabsorb HCO_3^-, and beta intercalated cells secrete HCO_3^-, but only in the rare instance of metabolic alkalosis. kAE1 is found in the alpha intercalated cells of the collecting duct, and is expressed at the basolateral membrane (Fig 1.3) (37, 40-42).

S. cerevisiae expresses a homologue of AE1, YNL275w. While this protein shares some sequence similarity to AE1, its role in yeast is unclear, and it is not known if it conducts HCO_3^- transport in yeast (44). YNL275w may transport Cl^-, Br^-, HCO_3^- and NO_3^- as evidenced by the ability of these anions to inhibit binding of YNL275w to the stilbene disulfonate inhibitor SITS (44). YNL275w shares 27% sequence identity with the plant boron transporter BOR1, and YNL275w may act as a boron transporter in yeast (45). YNL275w binds the anion exchanger inhibitor DIDS (4,4'-diisothiocyanostilbene-2,2'-disulfonate) (discussed in section 1.2.5), and may have a similar transmembrane domain structure to AE1 (44).

1.2.2 Diseases associated with AE1

Several diseases are associated with mutations in AE1. These diseases include hereditary spherocytosis (HS) (OMIM: +109270), and distal renal tubular acidosis (dRTA) (OMIM: #179800 and #602722) (46). South-east Asian Ovalocytosis (SAO) OMIM: +109270), is a condition associated with AE1, that does not result in any adverse symptoms. Severe hemolytic anemia results from the deletion of AE1 in knockout mice (47, 48). Since AE1 stabilizes the shape and structure of erythrocytes through interactions with the spectrin/ankyrin cytoskeleton, AE1-null mice have very fragile erythrocyte plasma membranes, presumably due to the loss of an AE1-mediated interaction between the plasma membrane and the cytoskeleton (47, 48). Also, $AE1^{-/-}$ mice exhibit a high rate of neonatal mortality (47, 48). Homozygous loss of the AE1 gene has not been seen in humans, and is presumed to be lethal *in utero*.

SAO, a condition widespread in Southeast Asia arises from the deletion of residues 400-408 at the end of the N-terminal cytoplasmic domain and the beginning of the first transmembrane segment of AE1 (49). AE1 with this deletion mutant is not functional (50, 51). A heterodimer of mutant and wildtype AE1 monomers is functional, although with a 40% reduction in overall transport activity (50, 51). A homozygous SAO mutation is lethal *in utero*. SAO mutant AE1 binds the cytoskeleton more strongly than wildtype, and this strong interaction enhances the rigidity of the erythrocyte membrane (52). Patients with SAO exhibit erythrocytes with altered shape, but no clinical pathology. In fact, the enhanced plasma membrane rigidity seems to confers resistance to cerebral malaria (53, 54).

HS is a form of familial haemolytic anemia caused by abnormal erythrocyte plasma membrane structure. Among HS cases, 20% are caused by mutations in AE1; cases of HS are also caused by mutations in the cytoskeletal components ankyrin and spectrin. HS is characterized by fragile erythrocytes, with reduced surface area (55, 56). Hemolytic anemia results from this loss of erythrocyte stability. Interestingly, HS is not associated with renal pathology. The autosomal dominant form of HS makes up the largest group of AE1 mutations associated with HS. These mutants are mis-folded and are generally mis-targeted to the plasma membrane, thereby decreasing contact between the plasma membrane and underlying cytoskeleton (47). Mutants E40K, G130R and P327R are located in the N-terminal cytoplasmic domain of AE1. Mutations in this region may inhibit interactions between AE1 and cytoskeletal components (57). R290C (Band 3 Bicetrel) is retained in the endoplasmic reticulum and causes wild type protein to be retained also, since AE1 is found in erythrocytes associated as dimers (58). Mutations in the membrane domain of AE1 that cause HS are also retained intracellularly (59). Some HS mutants don't bind immobilized anion exchange inhibitor, since they are probably mis-folded (60).

Renal pathology also results from mutations in AE1, although different mutations cause renal and erythroid diseases. Distal renal tubule acidosis (dRTA) is caused by a loss of Cl^-/HCO_3^- exchange activity in the distal tubule of the kidney, and is associated with failed acid secretion. Consequences of dRTA include metabolic acidosis, decreased urinary acid secretion, hypokalemia, and hypercalciuria (61, 62). Recessive dRTA results from mutants that are retained intracellularly, such as G701D. Dominant dRTA is caused by AE1 mutants that are either retained in the ER, such as R598H (63, 64), or mis-targeted, such as

901X which has a deletion of the last 11 residues in the C-terminus. AE1 901X is found apically and basolaterally in α-intercalated cells, while wild-type kAE1 is only expressed basolaterally (65, 66). Mutants associated with dominant dRTA retain normal transport function, but the phenotype results from a deficiency in overall Cl^-/HCO_3^- exchange in the distal renal tubule. SAO is highly prevalent in dRTA patients from Thailand (67), New Guinea and Malaysia (68). SAO may be a pre-disposing factor for dRTA as the incidence of SAO is high in Malay patients with dRTA (69). A common genetic basis between SAO and dRTA has been suggested (68, 70).

1.2.3 Transport activity

AE1 mediates the electroneutral exchange of Cl^- for HCO_3^- across the plasma membrane, with a turnover rate of about $5 \times 10^4/s$, which is only one order of magnitude slower than ion channels (71). A ping-pong model has been proposed for AE1 transport activity in which a conformational change causes the transport site to alternately face the extracellular space and the cytosol (72, 73). Anion binding causes a conformational change, which shifts the binding site from one face of the membrane to the other. The anion then diffuses away from the binding site. Another anion binds the unoccupied site and, following a conformational change, the anion binding site returns to face the original side (74-76). AE1 is able to transport a wide variety of substrates. AE1 transports Br^- and F^- at the same rate as HCO_3^- and Cl^- (8). I^- and HPO_3^{2-} are transported 10-fold slower, and SO_4^{2-} is transported 10^4 slower than Cl^- (8). Since AE1 facilitates electroneutral anion transport, transport of divalent cations results in a net electrogenic movement of one negative charge. To satisfy the negative charge, a

proton may be co-transported with divalent cations, resulting in net electroneutral transport (73). Therefore, transport of divalent cations may be slower. AE1 expressed in HEK 293 cells is capable of Cl^-/OH^- exchange (77). AE1 can also bind small organic phosphates and anions, such as N-(4-azido-2-nitrophenyl)-2-aminoethylsulfonate (NAP-taurine) (78). AE1 is capable of transport over a broad pH range (pH 5-11) and at low pH can carry out slow H^+/divalent anion co-transport (3, 74, 79). Flexibility in modes of transport and substrate selectivity is likely due to flexibility in the membrane domain. Residues involved in anion exchange activity, the anion selectivity filter, translocation pore and permeability barrier of the transport site have been defined (80, 81), but without a high resolution structure, a clear and detailed model of transport cannot be described. For instance, one residue identified in the anion translocation pathway and permeability barrier is E681 in transmembrane segment 8 (82, 83). E681 provides the proton in AE1-mediated $H^+/SO_4^=$ co-transport (84, 85). When the corresponding residue in mouse AE1, E699, is mutated to Q, electroneutral Cl^-/Cl^- exchange is inhibited (86). While this residue has been identified as part of the membrane permeability barrier, a high-resolution structure would place the residue in context, and help explain some of the alternative modes of transport of which AE1 is capable.

Other proteins influence the transport activity of AE1. For example, AE1 transport in erythrocytes that lack the integral membrane protein Glycophorin A (M^kM^k cells) is reduced by 40% (87). Glycophorin A is proposed to play a role in the biosynthesis and folding of AE1 in red blood cells (87). Glycophorin A may play a role as a chaperone, and assist in processing of AE1 to the erythrocyte plasma membrane (67, 88). Glycophorin A also enhances AE1 transport activity

(30). Decreased transport may result in M^kM^k cells due to a decrease in AE1 at the plasma membrane, and consequent decrease in total activity. The enzyme carbonic anhydrase II (CAII), which catalyzes the reversible hydration of CO_2 to HCO_3^- and H^+ facilitates the maximal activity of AE1 through an interaction with the C-terminal tail of AE1 (89, 90). In an interaction that has been termed the bicarbonate transport metabolon, CAII binding to AE1 increases the local HCO_3^- gradient at the active site of AE1, therefore enhancing transport activity (91). A controversy has arisen over the interaction between CAII and AE1 (92). A physical interaction between SLC4 bicarbonate transport proteins and CAII has been found previously based on ELISA binding assays of GST-fusion proteins, and co-immunoprecipitation (89, 90, 93, 94). Recently, however, an interaction was not seen between pure AE1 C-terminal peptide and immobilized CAII and *vice versa* (92). This issue remains unresolved.

1.2.4 AE1 structure

Cl^-/HCO_3^- exchangers of the SLC4 family share a common architecture (Fig. 1.4), consisting of three domains. The N-terminal cytoplasmic domain is 400-700 residues long. The cytoplasmic domains of AE2 and AE3 share 53% identity and are 300 residues longer than that of AE1. The function and structure of the cytoplasmic domain of AE1 is well characterized, but little is known about the function and structure of the cytoplasmic domains of AE2 and AE3. Second is the transmembrane domain, which is the site of Cl^-/HCO_3^- exchange. The membrane domain is made up of 10-14 transmembrane segments. AE2 and AE3 are 90% identical in the membrane domain. The third domain is a short C-

terminal cytosolic tail, which contains the acidic CAII binding motif. AE1 and AE2 share 60% sequence similarity in the C-terminal domain.

AE1 serves as a model for structural and functional studies of the other anion exchangers. Human AE1 is 911 amino acids long. The 43 kDa amino-terminal cytoplasmic domain (residues 1-360) interacts with the cytoskeleton (95) and glycolytic enzymes (18). Kidney AE1 (kAE1) is a truncated form of AE1, which lacks the N-terminal 65 amino acids. Through interactions with the cytoskeleton, AE1 helps to maintain the biconcave disc structure of erythrocytes (96). The region linking the N-terminal cytosolic region and the membrane domain (residues 361-403) is thought to be flexible and may act as a hinge between the two domains (97). The 55 kDa membrane domain is necessary and sufficient for transport function (98). There is a single site of N-linked glycosylation at Asn642 on the fourth extracellular loop, which is not required for protein transport function or structure (99, 100). The membrane domain is predicted to span the membrane 12-14 times (10). The third domain is a short cytoplasmic C-terminal domain of 4.5 kDa. This domain is required for correct processing of AE1 to the plasma membrane (101), and interacts with the enzyme carbonic anhydrase II, which is required for optimal transport function (102). Both termini of AE1 are cytosolic.

As a consequence of its abundance in the erythrocyte, AE1 is the most extensively studied of the SLC4 exchangers, and there is consequently a wealth of biochemical and structural data available for AE1. As such, AE1 is a model for the study of polytopic membrane proteins. The structure of AE1 is the best understood of the anion exchangers. The membrane domains of AE1, AE2, and AE3 are highly conserved, with 70% sequence identity in the membrane domain.

AE1 in the erythrocyte membrane exists as dimers and tetramers, and forms the tight dimer through interactions in the membrane domain. Monomeric AE1 is the functional unit and the dimer can only be disrupted to monomers with protein denaturation (103, 104). Kinetic studies indicate that both subunits of the AE1 dimer interact allosterically, but are distinct (105, 106). When one monomer of the dimeric unit is inhibited, the uninhibited monomer retains normal transport activity (103, 104).

As the membrane domain is required for transport activity, a high-resolution structure of this domain is essential for insight into the transport function of AE1. The structure of the N-terminal half of the AE1 membrane domain has been well predicted by hydropathy analysis and biochemical analysis such as cysteine-scanning mutagenesis (107-109). The topology of the C-terminal half of the membrane domain is controversial, and suggested topology models indicate re-entrant loops, and non-helical membrane regions (81, 108, 110, 111). Several biochemical approaches have been used to clarify the structure of the region, including cysteine-scanning mutagenesis (107, 110), protease accessibility studies (112), N-glycosylation site scanning mutagenesis (108, 113), and epitope mapping (114). The last transmembrane segments may be more flexible due to the non-helical conformation and may be easily shifted into different conformations required for transport activity.

The crystal structure of the N-terminal cytoplasmic domain (residues 1-379) has been solved to 2.6 Å resolution (115). The crystal structure of the cytoplasmic domain revealed a dimer of 75 x 55 x 45 Å, and each monomer is made up of 11 β-strands and 10 helical segments. The cytoplasmic domain was crystallized as dimers and tetramers. A low-resolution 20 Å structure of dimeric

AE1 membrane domain has been described by electron microscopy and image reconstruction (116) with a thickness of 80 Å. 3D crystals of AE1 have also been described to 14 Å resolution (117). The membrane domain appears to contain a flexible region that results in two distinct crystal forms (118). The two forms may represent two conformations that are achieved during the transport process. The 20 Å dimeric structure shows a canyon-like structure with large cytosolic protrusions. A high-resolution representation of the membrane domain would give insight into the transport mechanism of AE1.

1.2.5 Inhibition of AE1

The stilbene disulfonates are the best known class of Cl^-/HCO_3^- exchanger inhibitors (119). These inhibitors bind with high affinity, with binding constants less than 1 μM. The structure of stilbene disulfonates facilitates anion exchanger inhibition in two ways. First, localization to the hydrophobic membrane is facilitated by the hydrophobic stilbene structure. Second, the negatively charged sulfonate groups have affinity for anion binding sites in proteins. The best known stilbene disulfonate anion exchange inhibitor is DIDS (4,4′-diisothiocyanatostilbene-2,2′-disulfonic acid), which reacts with free lysine residues on the extracellular face of the exchangers (120). DIDS binds to the extracellular face of AE1 at lysine 539 and 851, and locks it in an outward facing conformation (119-122). The binding sites for stilbene disulfonates and Cl^- are distinct but interact (123). There are two stages of inhibitor binding. The first stage is a rapid, low affinity interaction. The second stage is a slow conformational change to a high affinity state. Cl^- affects the dissociation rate of

stilbene disulfonate inhibitors, indicating an interaction between the two distinct sites (123). In the context of membrane protein crystallization, the use of inhibitors such as DIDS to lock the anion exchanger into a single conformation could aid in crystal formation by restricting the high rate of dynamic movement the exchanger undergoes during transport.

1.3 Mammalian membrane proteins expressed in yeast and subsequently crystallized

1.3.1 SERCA1a Ca^{2+}-ATPase

The Sarcoplasmic Endoplasmic Reticulum Calcium ATPase 1a (SERCA1a) is a polytopic membrane protein that functions in calcium homeostasis. By pumping calcium into the sarcoplasmic reticulum, SERCA1a maintains a low cytosolic calcium concentration. The crystal structure of native SERCA1a has been solved in several conformations in part due to its abundant expression in rabbit sarcoplasmic reticulum, where it make up roughly 75% of ER membrane protein. In order to study the structure of SERCA1a mutants, a recombinant yeast expression system was examined. The crystal structure solved for yeast-expressed SERCA1A is identical to that of the native protein (124, 125), and the protein was functional. Thus a yeast expression system can produce functional mammalian membrane protein with identical structure to native protein and is therefore suitable for crystallographic studies. SERCA1a was expressed in *S. cerevisiae* and purified using a biotinylated acceptor domain tag. In this method, a biotin acceptor domain (BAD) is fused to the protein of interest, and is naturally biotinylated in yeast. Purification is achieved by binding biotinylated

protein to an avidin affinity resin, followed by proteolytic cleavage to separate the BAD tag from the protein of interest. SERCA1a was expressed on a plasmid with a galactose inducible promoter (126); this plasmid, pYeDP60, has also been used to expressed AE1 in *S. cerevisiae* (127). The detergent dodecyl maltoside (DDM) was used to isolate SERCA1a from isolated yeast membranes, followed by detergent replacement to $C_{12}E_8$ (125). DDM was chosen for this purification system over Lysophosphatidylcholine (LPC) because the protein purification was lower with LPC despite a higher degree of solubilization, and SERCA1a solubilized in DDM was more active than the protein solubilized with LPC (128).

1.3.2 Mammalian Voltage-Dependent Shaker Family K^+ Channel

Voltage-dependent potassium channels, present in all eukaryotic cells, function to modulate electrical activity in the cell. This is particularly important in excitable cells and tissues such a neurons. Prokaryotic K^+ channels are more easily expressed in *E. coli* than mammalian K^+ channels. Therefore, much of the structural information about voltage-dependent potassium ion channels is from the study of prokaryotic K^+ channels. The structure of a mammalian voltage-dependent *Shaker* Family K^+ channel was described recently (129). Mammalian Kv1.2 was overexpressed in the yeast *Pichia pastoris*, and purified using an 8-His tag. Kv1.2 expressed in yeast was solubilized with DDM, and purified by affinity chromatography followed by protease cleavage of the affinity tag (129). This approach is similar to that used to purify SERCA1a, where affinity purification was followed by proteolytic cleavage to obtain pure homogeneous protein (130). Also similar is the use of DDM to solubilize mammalian

membrane protein from yeast membranes. The study of Kv1.2 and SERCA1a serve as a model for the expression of mammalian membrane proteins in yeast, and subsequent purification that can lead to a high-resolution crystal structure of a mammalian membrane protein.

1.4 Purification and characterization of AE1

1.4.1 Protein expression in Saccharomyces cerevisiae

The major limiting step in membrane protein crystallization is the ability to generate sufficient amounts of purified protein. In the absence of an abundant native source of membrane protein, a heterologous expression system can be employed. Several eukaryotic expression systems have been used to express membrane proteins, including yeast (*Saccharomyces cerevisiae, Pichia pastoris,* and *Schizosaccharomyces pombe),* mammalian cells, and insect cells. While mammalian cell lines such as human embryonic kidney (HEK) 293 cells, and Chinese hamster ovary (CHO) cells are commonly use to examine mammalian membrane proteins for protein-protein interactions, functional, and structural studies, the cost and low-scale of protein production from these cell lines make them impractical for large scale membrane protein purification. Insect cell lines such as *Spodoptera frugiperda* (Sf9 and Sf21) cell lines are commonly used for the investigation of cell surface receptors. Membrane proteins heterologously expressed in insect cells are posttranslationally modified by glycosylation, palmitoylation, and phosphorylation. These posttranslational modifications may introduce heterogeneity that could inhibit protein crystallization.

Yeast expression of membrane proteins has many advantages. Yeast expression systems allow large-scale culture growth at low cost. *Saccharomyces cerevisiae* (Baker's yeast) is the best genetically characterized yeast. Yeast displays most features of higher eukaryotes including an endoplasmic reticulum. Molecular biology for yeast expression plasmids can still be carried out easily in *E. coli*. The doubling time of yeast is roughly 1.5 h in rich medium, and yeast is easy to grow on a large scale in a fermenter. Recombinant proteins, especially membrane proteins, are susceptible to proteolytic degradation during expression and purification (131). Protease-deficient strains of yeast are available, which limits the chance of proteolytic degradation of heterologously expressed membrane proteins. Expression in a eukaryotic system provides a membrane of suitable thickness for a mammalian membrane protein (30 Å) (132). In contrast, bacterial expression systems have a membrane of 25 Å thickness (133). Also, a yeast expression system allows recombinant proteins to be processed through the endoplasmic reticulum, which is essential for correct protein folding and membrane insertion.

In the case of AE1, an abundant source of native protein is available. Unfortunately, attempts to generate crystals of AE1 that diffract to a high resolution have been unsuccessful, and only low resolution structures are available for the majority of the protein (116, 117). Several reasons could explain this. AE1 in the erythrocyte is heterogeneous due to post-translational modification. Also, the full length protein has a flexible region separating the cytosolic N-terminal domain from the membrane domain, and this flexibility could impair crystal formation (116). *S. cerevisiae* provides an ideal system for expression of human AE1. AE1 has previously been expressed heterologously in

a yeast expression system under both an inducible and constitutive promoter (127, 134). A heterologous expression system for AE1 allows for reproducible and rapid purification of homogeneous protein, as well as the flexibility to examine AE1 mutants through molecular biology. For example, the membrane domain alone of AE1 can be expressed to reduce protein flexibility. While expression in a heterologous system may never achieve the level of native protein in the erythrocyte membrane, protein homogeneity is required for high quality crystals.

1.4.2 Subcellular localization

Since AE1 is a plasma membrane anion exchanger, the subcellular localization of heterologously expressed AE1 membrane domain is of interest. While AE1 is highly expressed at the erythrocyte cell surface, making up 50% of the total integral membrane protein, processing of AE1 to the plasma membrane in other cell systems is not as high. In HEK 293 cells transiently transfected with cDNA for AE1, roughly 30% of the total expressed AE1 protein is targeted to the cell surface. In a previously described galactose-inducible yeast expression system of AE1 membrane domain, only 5-10% of the total expressed AE1 protein was processed to the cell surface (127). Another study of AE1 expressed in *S. cerevisiae* examined processing of the protein to the cell surface using density gradient sedimentation analysis and found primarily intracellular localization of AE1 (134). Intracellular localization of AE1 does not appear to impair purification of the protein (134), but it is important to determine where the expressed AE1 is being targeted.

1.4.3 Glycosylation of AE1

One goal of membrane protein purification is the eventual expression of protein pure enough to crystallize. With this goal in mind, there are many factors to consider when planning a purification strategy. One of these factors is heterogeneity of the protein. AE1 is glycosylated and palmitoylated (10, 135-137). There is a well-characterized polylactosaminoglycan carbohydrate structure at Asn642 in the large fourth extracellular loop of AE1 (111, 135). AE2 and AE3 are glycosylated on extracellular loop 3, which is the largest extracellular loop in those anion exchangers (138, 139). The functional significance of palmitoylation of AE1 at Cys843 is unclear. While glycosylation is not required for protein function, it may aid in protein stability (99, 100). However, glycosylation can introduce heterogeneity that could potentially impair homogeneous protein crystallization.

Like erythrocyte AE1, AE1 expressed in HEK 293 cells is heterogeneously glycosylated, with up to 10 kDa of carbohydrate (113, 135). Mammalian proteins expressed heterologously in yeast, including AE1, have been reported to be non-glycosylated (134), and protein purified from a yeast system may therefore be more homogenous. The enzyme peptide-N-glycosidase F (PNGaseF) removes N-linked carbohydrate residues, and can be used to distinguish between glycosylated and non-glycosylated protein (140). Previous attempts at crystallization of the AE1 membrane domain from erythrocytes have reported that deglycosylation of AE1 is essential for 2D and 3D crystallization of the protein (117, 118). The importance of deglycosylation of a membrane protein for

crystallization is also described for the bovine erythrocyte water channel, AQP1 (141). For some mammalian membrane proteins, glycosylation is required for correct folding or protein function. For these proteins, expression in a yeast system could lead to non-glycosylated and potentially non-functional protein. Luckily, in the case of AE1, this feature of yeast is an advantage.

1.4.4 Detergent solubilization

One problem that arises when purifying membrane proteins is aggregation. Even in the presence of detergents, membrane proteins can form aggregates, which makes purification and crystallization difficult (117). It is therefore vital to select a detergent capable of solubilizing the protein, and maintaining it in a monodisperse state (142). A detergent must also be chosen that retains the membrane protein of interest in an active state, which is indicative of a native conformation and correct folding. The detergent chosen must also be compatible with subsequent purification steps. For example, a charged detergent would not be an ideal choice if the protein of interest were to be purified by ion exchange chromatography. Of particular importance for the purification of membrane proteins is selection of a detergent able to satisfy the hydrophobic requirements of a protein that spans the eukaryotic lipid bilayer (143).

AE1 is nearly completely solubilized from the erythrocyte membrane with the polyoxyethylene $C_{12}E_8$ (144). Dodecyl maltoside, a mild sugar detergent, has also been used to purify AE1 from erythrocytes (117). Since one major impediment to membrane protein crystallization is the ability to generate large amounts of protein, a suitable detergent must be chosen to maximally solubilize

AE1 from isolated membranes, and to maintain AE1 in an active state. AE1 has previously been purified from yeast using $C_{12}E_8$, but the extent of solubilization was only 38% (134). LPC has also been used in a yeast system to purify functional AE1, with solubilization of 93% (134). Cost is ultimately a factor when choosing a detergent, and while one may be capable of a high degree of solubilization, the cost may be too high to be practical for large-scale protein purification. A compromise must be sought between protein isolation and cost.

1.4.5 Affinity chromatography

Affinity chromatography is a popular method for purifying heterologously expressed proteins. N-terminal tags can improve protein yield by providing a reliable context for efficient initiation of translation (145). In some cases, the affinity tag can help increase solubility of the over-expressed protein. The choice of affinity tag depends on many factors such as the cost of affinity resin, the elution conditions, and the size of the tag. Popular tags for affinity purification include Maltose Binding Protein (MBP) (146), Calmodulin binding protein (CBP) (147), 6-His (148), and Glutathione S-transferase (GST) (149).

MBP is a 40 kDa tag that requires an inexpensive affinity resin. It enhances solubility of proteins to which it is fused, and requires mild elution conditions (145). CBP is a 4 kDa protein that binds calmodulin. CBP is highly specific but requires an expensive resin (145).

Metal chelate chromatography is a powerful method of affinity chromatography that has previously been used to purify membrane proteins, including AE1 (129, 134). The principle of immobilized metal affinity chromatography (IMAC) is that different proteins and amino acid compositions

have different affinity for immobilized metal ions (148, 150). By tagging a protein of interest with multiple consecutive histidine residues, usually six or 10, the protein will bind immobilized metals such as nickel, cobalt, zinc, or copper. The imidazole groups of the histidine residues interact to form a ligand binding site for the metal ions. The bound recombinant protein can be eluted with free imidazole, EDTA, or pH <5.0.

Glutathione S-transferase (GST) is a 26 kDa protein that offers mild elution conditions and an inexpensive affinity resin, immobilized glutathione resin (151).

Affinity tags have the potential to interfere with functional or structural protein studies. When the ultimate goal of protein purification is crystallization, optimal conditions allow for the removal of any affinity tags from the protein of interest prior to crystallization. The inclusion of a protease site to separate the tags from the protein not only increases the purification power of the system, but allows the purified protein to be homogeneous, and free of other moieties. One protease that is used for this purpose is PreScission Protease. PreScission Protease recognizes the sequence LEVLFQGP and is used in the pGEX line of GST fusion protein vectors (Amersham Biosciences).

An advantage to using a large protein tag such as GST is the ability to clearly identify purified protein following cleavage. The removal of the six residues of a 6-His tag would not be easily visually detected on Coomassie Blue-stained gel or immunoblot, but a loss of 26 kDa would be easily identified. The combination of both a 6-His and GST tag would allow a protein to be purified by a dual affinity chromatography system, and thereby increase the overall purity of the protein. Both tags require inexpensive affinity resins, and mild elution

conditions. Combined with a PreScission Protease cleavage site, a membrane protein could be specifically and inexpensively purified.

1.5 Thesis objectives

The goal of this project was to develop a novel expression and purification system for the membrane domain of the human erythrocyte anion exchanger AE1 (AE1MD). Specifically, the goal was to improve on previously described expressions, and lay the ground work for high resolution structural studies of the AE1 membrane domain. The AE1 membrane domain was expressed with a 6-His tag and a GST-tag. Expression was optimized and purification was achieved with affinity chromatography. While purification of AE1MD remains to be optimized, this project describes the expression and purification of a novel construct of the human AE1 membrane domain in a yeast system.

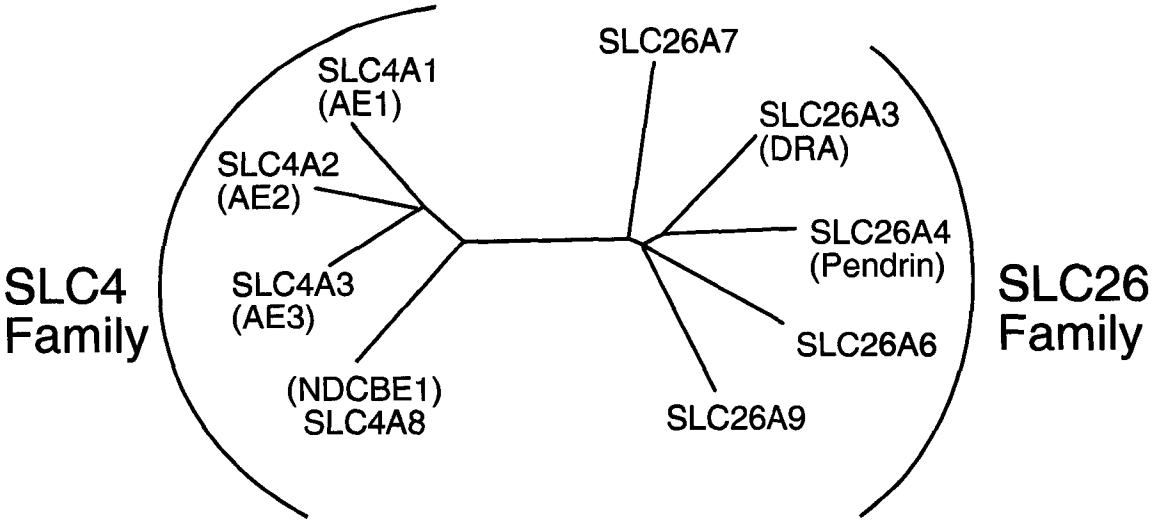

Figure 1.1. Phylogeny of mammalian Cl^-/HCO_3^- exchangers. The tree was generated through analysis of the similarity of amino acid sequences for the human Cl^-/HCO_3^- exchange proteins, using the program Phylip on the ClustalW website. The degree of sequence similarity is proportional to the length of the line between proteins. The bracketed names are commonly used names. The solid curves enclosing the transporters indicate different groups: the SLC4 family, which includes the Na^+-dependent SLC4A8, and the SLC26 family.

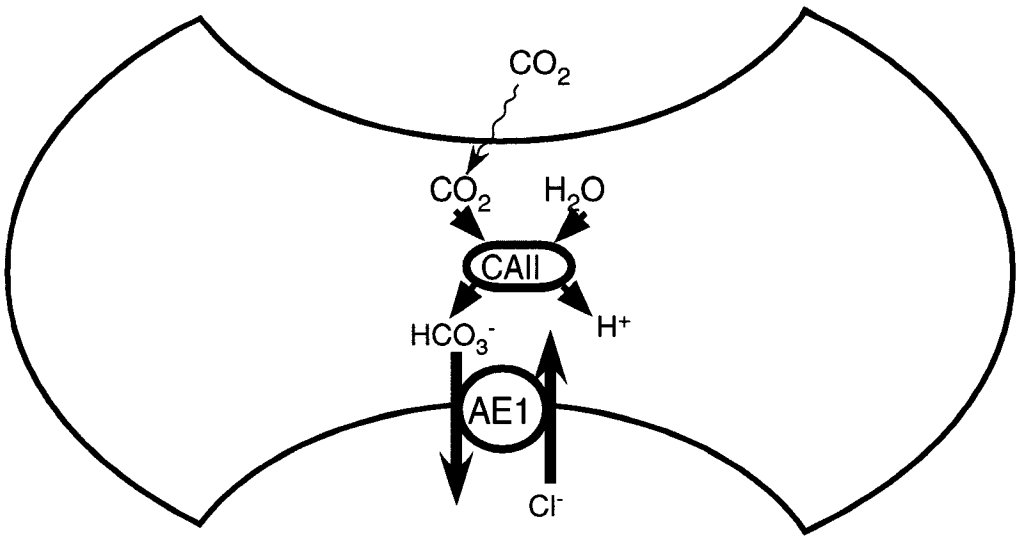

Figure 1.2. Cl^-/HCO_3^- exchange in the erythrocyte. As a waste product of metabolism, CO_2 accumulates. CO_2 diffuses across the erythrocyte membrane in peripheral capillaries where it is reversibly hydrated to HCO_3^- by the cytosolic enzyme carbonic anhydrase II (CAII). A proton is also produced in this process. The anion exchanger AE1 extrudes HCO_3^- in exchange for Cl^- to move HCO_3^- into the blood plasma. The process is reversed at the lung, and CO_2 diffuses into the alveoli and is exhaled.

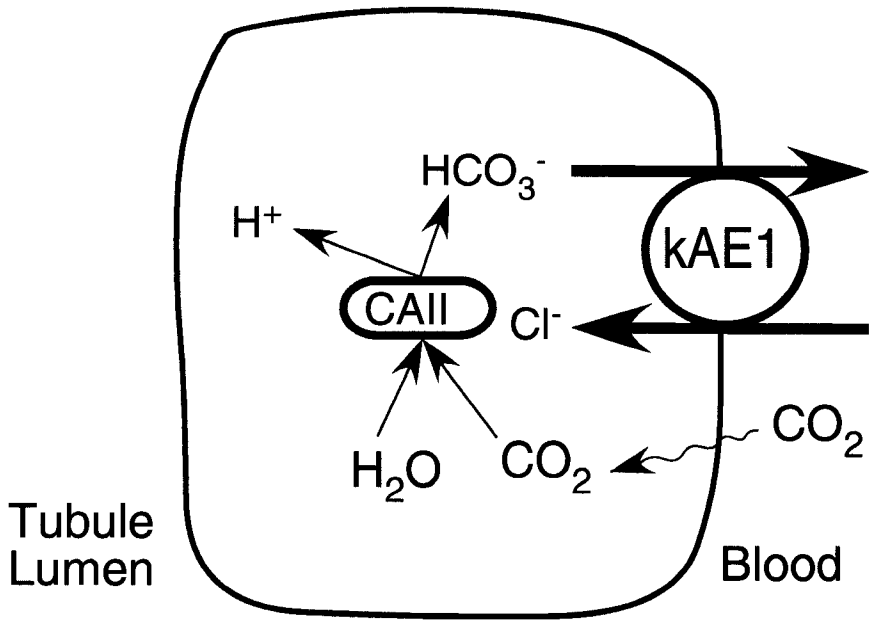

Figure 1.3. Cl^-/HCO_3^- exchange by kAE1 in the basolateral surface of renal α-intercalated cells. kAE1 is expressed at the basolateral membrane of α-intercalated cells of the distal renal tubule. These cells are acid secreting, and take up HCO_3^- into the blood in exchange for Cl^-, which allows a proton to be secreted into the tubule lumen by other membrane protein transporters at the apical surface. HCO_3^- for reabsorption is generated when CO_2 diffuses into the a-intercalated cell from the blood and is converted to HCO_3^- by the cytosolic enzyme carbonic anhydrase II (CAII).

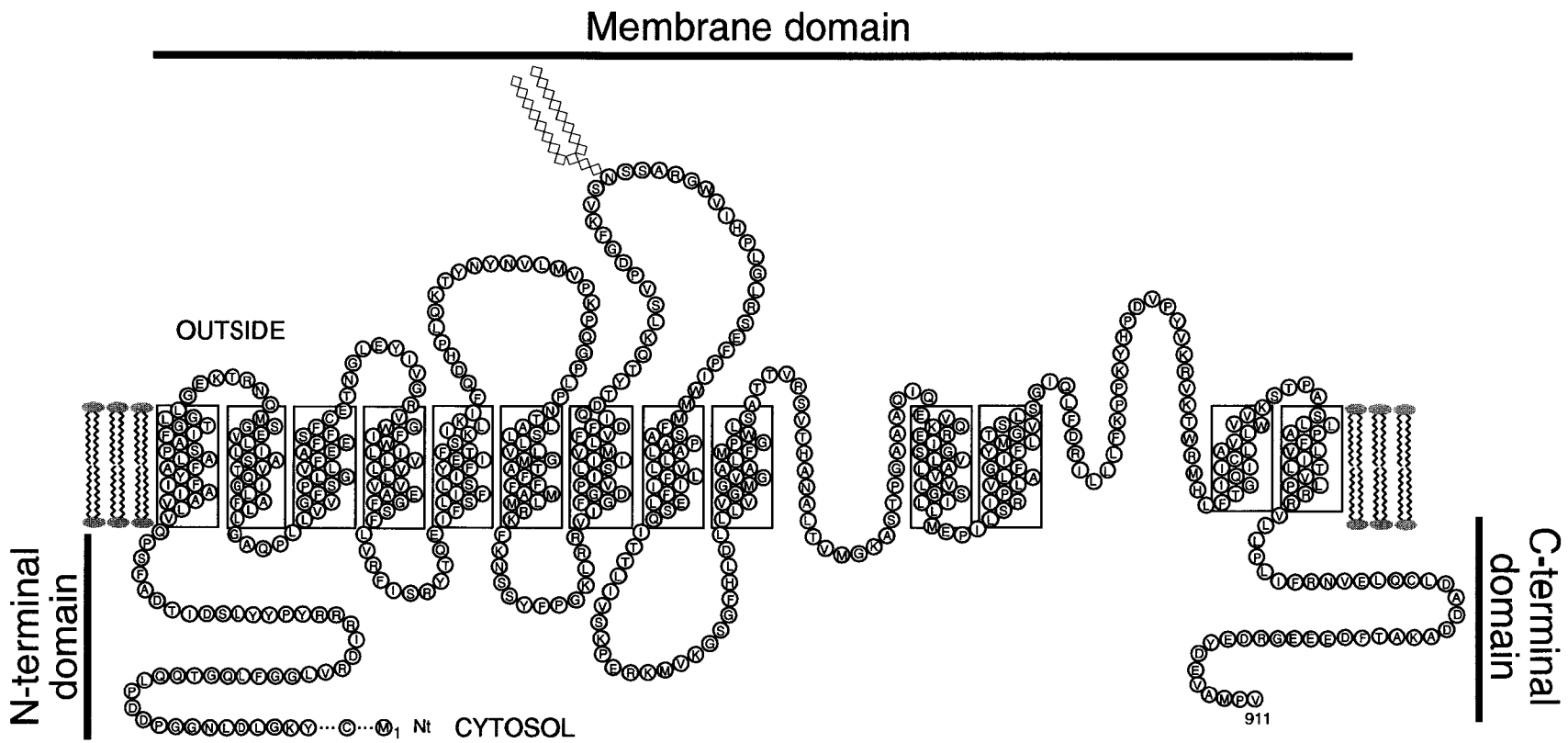

Figure 1.4. AE1 Protein topology. The N-terminal cytoplasmic domain of AE1 interacts with cytoskeletal components. A crystal structure of residues 1-379 has been solved. The membrane domain traverses the membrane 12-14 times, and is responsible for the anion exchange function of the transporter. Residues responsible for ion translocation have not been identified. The C-terminal cytoplasmic domain (residues 872-911) interacts with the enzyme Carbonic Anhydrase II. No high resolution structure exists for the membrane domain or the C-terminal domain of AE1. The region from 388-911 was overexpressed in this project. This model is based on previous topological determinations (27).

Chapter 2

Materials and Methods

2.1 Materials

Enzymes for molecular biology were obtained from New England Biolabs (New England Biolabs Inc., Pickering, Ontario) or Invitrogen (Invitrogen Canada Inc., Burlington, Ontario). Oligos for PCR were from Qiagen (pHJC1 and pHJC4 constructs) or Invitrogen (pGAL-AE1 construct). n-Dodecyl-β-D-Maltopyranoside (DDM), n-Octyl-β-D-Glycopyranoside (OG), and Fos-Choline-14 (FC) were from Anatrace. Soybean lysophosphatidylcholine (LPC) was from Avanti Polar Lipids (Alabaster, AL). $C_{12}E_8$ (octaethylene glycol monododecyl ether) was from Nikko Chemical Co. (Tokyo). Anti-AE1 antibody IVF12 was from Dr. Mike Jennings. Anti-PMA1 antibody was from Dr. Gary Eitzen (152). Anti-GST antibody Z-5, and donkey anti-rabbit HRP antibody were from Santa Cruz. ECL Anti-mouse HRP antibody was from Amersham Biosciences. Anti-mouse Cy2-conjugated antibody was a gift from Dr. Richard Rachubinski. Anti-rabbit AlexaFluor 488-conjugated antibody was from Molecular Probes. Qiagen Hi-Speed Maxi Prep kits and Gel Extraction Kits were from Qiagen Inc. TALON Metal Affinity resin was from BD Bioscience. GSH-Sepharose was from Amersham Biosciences. Materials for yeast transformation, imidazole, and fish gelatine were from Sigma. PNGase F was from New England Biolabs. PreScission Protease was from Amersham Biosciences. Compounds for culture media and solutions were from Sigma, Fisher, and BD Biosciences. CSM-Leu$^-$ amino acid dropout mixture was from Q-BioGene. Complete Mini Protease Inhibitor tablets were from Roche. Bradford protein assay reagent was from Bio-Rad. BCA protein assay reagent was from Pierce. ECL reagent was from Perkin-Elmer. IPTG was from Rose Scientific.

2.2 Strains and Media

Saccharomyces cerevisiae protease-deficient strain BJ1991 (α*leu2 trp1 ura3-52 prb1-1122 pep4-3 gal2*) was from the Yeast Genetic Stock Collection (153). *Saccharomyces cerevisiae* strain W303.1b (*a leu2 his3 trp1 ura3 ade2-1 can*^{r} *cir*$^{+}$) was a gift from Dr. Denis Pompon, Gif-sur-Yvette, France (154). Untransformed BJ1991 yeast cultures were grown in YPD medium (1% (w/v) Bacto-yeast extract, 2% (w/v) peptone, 2% (w/v) glucose, 2% (v/v) glycerol, pH 6.0). BJ1991 yeast cultures transformed with pMA91, pJRC16 or pHJC4 were grown in selective Leu^{-} medium (0.17% (w/v) yeast nitrogen base, 2% (w/v) glucose, 0.5% (w/v) ammonium sulfate, 0.07% (w/v) Leu^{-} amino acids, 0.0037% (w/v) adenine hemisulfate, pH 6.0), and YPD medium. Untransformed W303.1b yeast cultures were grown in YPDA medium (1% (w/v) Bacto-yeast extract, 2% (w/v) peptone, 2% glucose, 0.01% (w/v) adenine hemisulfate, pH 6.0). W303.1b yeast transformed with control plasmid pYeDP60 or pGAL-AE1 were first grown in selective SGI medium (0.67% (w/v) yeast nitrogen base, 2% (w/v) glucose, 0.003% (w/v) adenine hemisulfate, 0.1% Casamino acids, 0.004% (w/v) Trp, pH 6.0) then in YPGE medium (5% (w/v) glucose, 1% (w/v) yeast extract, 1% (w/v) peptone, 3% (v/v) ethanol, pH 6.0).

2.3 Plasmid DNA

2.3.1 PCR

Polymerase chain reaction (PCR) was used to generate both bacterial and yeast expression constructs of AE1. The yeast expression construct pHJC4 was assembled from the yeast AE1 expression vector pJRC16, the mammalian AE1

expression vector pJRC9 and the GST expression vector pGEX-5x-3. Two rounds of polymerase chain reaction (PCR) were used to insert a GST tag into the plasmid pJRC16 and truncate AE1. The first round 5′ primer sequence (5′) GGGGG**CCGCGG**ATCCAA*ATCCCCTATACTAGGTTATTGGAAAATTAAG* (3′) was complementary to GST cDNA (italics), with a SacII restriction site (bold). The first round 3′ primer sequence (5′) *GGTAATAGGGGTAGCGGCGACCACCACC***TGGACCTTGAAACAAAACTTC CAA**ACCACCACCatccgattttggaggatgga (3′) was complementary to codons 388-393 of AE1 (italics), with a PreScission Protease recognition site (bold) and the C-terminus of GST (lower case). The first round template was pGEX-5x-3. The 20 μl PCR reactions contained 0.4 mM dNTPs, 1x PCR buffer (Invitrogen), 2 mM $MgSO_4$, 2 μM forward primer, 2 μM reverse primer, 5 ng of pGEX-5x-3, 0.4 μl of Platinum Pfx (Invitrogen), and was made up to volume with ddH_2O.

The PCR protocol used is as follows:

1. 1 cycle of 95 °C for 5′
2. 30 cycles of 95 °C, 30″; 51 °C, 30″; 72 °C, 45″
3. 1 cycle of 72 °C for 10′

The second round 5′ primer was the product of the first round (megaprimer). The second round 3′ primer sequence (5′) AGGGCGGAGGCAAACATC (3′) was complementary to codons 662-668 of AE1 cDNA. The second round template was pJRC9 (155). The 30 μl PCR reactions contained 0.4 mM dNTPs, 1x PCR buffer (Invitrogen), 2 mM $MgSO_4$, 1 μM forward primer, 1 μM reverse primer, 160 ng of round 1 megaprimer, 0.4 ng of pJRC9, 0.4 μl of Platinum Pfx (Invitrogen), and was made up to volume with ddH_2O.

The PCR protocol used is as follows:

1. 1 cycle of 95 °C for 5′
2. 7 cycles of 95 °C, 30″; 51 °C, 1′; 72 °C, 1′35″
3. 26 cycles of 95 °C, 30″; 51 °C, 30″; 72 °C, 1′35″
4. 1 cycle of 72 °C for 10′

The resulting product was digested at the 5′ end at the SacII site, and at the 3′ end at the SmaI site and ligated into pJRC16 between the SacII site, downstream of the 6-His tag, and the SmaI site at codon 645 of AE1 to yield pHJC4 (Fig. 2.1). The construct was confirmed by DNA sequencing. The protein encoded by pHJC4 is named AE1MD (Fig. 2.1) (Table 3.1).

A galactose-inducible AE1 membrane domain plasmid was assembled from the yeast AE1 expression vector pHJC4, described above, and the yeast plasmid pYeDP60. The AE1 membrane domain with N-terminal 6-His and GST tags was amplified from pHJC4 using PCR. The forward primer sequence is (5′) GCGC**GAGCTC**ACCATGGAACATTTGGCCGGATCG (3′), which contains a SacI site (bold), and the reverse primer (5′) GCGC**GAATTC**CCGCCCCTCACACAGG (3′), which contains an EcoRI site (bold). The PCR product was cloned into the SacI and EcoRI sites of the yeast vector YeDP60. The resulting construct was designated pGAL-AE1 (Fig. 2.2) Correct construction was confirmed by sequencing. The protein encoded by pGAL-AE1 was named GAL-AE1MD (Fig. 2.2) (Table 3.1).

The AE1 C-terminal domain, comprising the last 40 amino acids of AE1 (codons 872-911) was amplified using PCR from the mammalian AE1 expression plasmid pJRC9. The forward and reverse primers used were 5′ CGCGGATCCGTCCTGCTGCCGCTCATCTTC 3′ and 5′ CGCGGATCCTCACACAGGCATGGCCACTTCGT 3′ respectively. The forward

primer introduced a new start codon, and the reverse primer introduced a new stop codon. The 50 μl PCR reactions contained 0.4 mM dNTPs, 1x PCR buffer (Invitrogen), 1 mM $MgSO_4$, 1 μM forward primer, 1 μM reverse primer, 1 ng of pJRC9, 1 μl of Platinum Pfx (Invitrogen), and was made up to volume with ddH_2O.

The PCR protocol used is as follows:

1. 1 cycle of 95 °C for 5′
4. 30 cycles of 95 °C, 30″; 56 °C, 45″; 72 °C, 10″
5. 1 cycle of 72 °C for 10′

pGEX-6p-1 and the AE1Ct PCR product were digested with BamHI and ligated together to yield pHJC1. pGEX-6p-1 was treated with CIP prior to ligation. The construct was confirmed with colony PCR, diagnostic restriction digest and sequencing. The plasmid pHJC1 encodes the protein GST-AE1Ct (Fig 2.3).

2.3.2 Plasmid DNA isolation

DH5α *E.coli* cells were transformed with plasmid DNA via electroporation with an Electroporator 2510 (Eppendorf). Electroporated cells were recovered in 600 μl SOC media (20 g/l Bacto Tryptone, 5 g/l Bacto yeast extract, 0.58 g/l NaCl, 0.186 g/l KCl in H_2O, pH 7.0) with shaking at 200 rpm at 37 °C for 1 h. Liquid culture (150 μl) was then plated on LB +Amp plates that had been pre-warmed to 37 °C. Plates were incubated at 37 °C overnight, and single colonies were isolated to inoculate 200 ml of LB medium supplemented with 100 μg/ml ampicillin. Liquid cultures (100 ml) were grown overnight at 37 °C with shaking at 200 rpm. Liquid cultures were harvested by centrifugation at 6 500 x g and

plasmid DNA was isolated with Qiagen Hi-Speed Maxi Prep kit (Qiagen Inc., Mississauga, Canada). Plasmid DNA identity was verified by restriction digest analysis.

2.3.3 Restriction Digests

Restriction digests of plasmid DNA were used both for ligations and for diagnostic analysis of newly constructed plasmids. DNA was digested with restriction enzyme as follows: 13 U BamHI/μg DNA, 5 U SmaI/μg DNA, 5 U SacII/μg DNA. The total volume of the restriction digest was adjusted to ensure a glycerol concentration of less than 5%, and the minimum total volume was used to maximize efficiency of digestion. BSA (1x) was included in the restriction digest mixture when required for the enzyme. Restriction digest mixture was incubated at the appropriate temperature for the enzyme being used for 1 h. Agarose gel loading dye (Fermentas) was added to terminate the reaction. For plasmid DNA to be used as the vector in the ligation reaction, 10 U Calf intestinal phosphatase (CIP) was added and the mixture was incubated at 37 °C for an additional 45 min prior to termination of reaction by addition of agarose gel loading dye. For digests with two restriction enzymes, digestion was first performed with the enzyme requiring the lower temperature for 1 h at that temperature, and then the second enzyme was added and the temperature raised to that appropriate for the second enzyme for 1 h. Following addition of agarose gel loading dye, DNA was resolved on a 0.7-1.5% agarose gel, depending on the size of the digested DNA, to determine correct DNA banding pattern in the case of diagnostic digests, or to isolate the appropriate band via agarose gel DNA extraction in the case of bands to be used for ligation.

2.3.4 DNA purification from agarose gels

Gel purification from agarose gels was performed using Qiagen's Gel Extraction Kit.

2.3.5 Ligation

Vector plasmid DNA and insert PCR product DNA were digested using the appropriate enzymes as described (see section 2.3.3). CIP-treated digested vector and digested insert (see section 2.3.3) were incubated at a ratio of 50 ng vector: 200 ng insert. The ligation mixture for construction of pHJC1 was incubated at room temperature for 2 h. The ligation mixture for construction of pHJC4 and pGAL-AE1 were incubated in a thermal cycler using the following program:

1. 70 cycles of 12 °C for 30", 18 °C for 1', 12 °C for 30", 18 °C for 1'
2. 70 cycles of 13 °C for 30", 18 °C for 1', 13 °C for 30", 18 °C for 1'
3. 70 cycles of 14 °C for 30", 21 °C for 1', 14 °C for 30", 21 °C for 1''

Following incubation, ligation mixtures were transformed into XL10 chemically competent *E. coli* cells using chemical competent transformation.

2.3.6 Chemically Competent Bacterial Transformation

XL-10 chemically competent *E. coli* cells (100 μl) were incubated in ice for 30 min with 2 μl of ligated DNA mixture. Cells were heat pulsed at 42 °C for 30 s, and 0.9 ml of warmed LB^+ broth (25 g/l LB broth base, 12 mM $MgCl_2$, 12 mM

$MgSO_4$, 0.4% glucose(w/v)) was added. Cells were incubated 37 °C for 1 h with shaking, then plated on LB-amp agar plates and incubated overnight at 37 °C.

2.3.7 Colony PCR

Colony PCR was used as a diagnostic method to select successful clones for both pHJC1 and pHJC4 plasmids. A single colony of transformed bacteria was selected with a P20 tip and pipetted into 25 μl of sterile water in a PCR tube. 3 μl of 10X PCR buffer was added to the tube and the mixture was heated 5 min at 96 °C in a thermal cycler to lyse cells. Tubes were centrifuged 30 s at 16 800 x g in a benchtop centrifuge and 5 μl of supernatant was used as template in a standard PCR reaction.

2.3.8 Miniprep Analysis

Single *E. coli* colonies were isolated to inoculate 2 ml of LB media supplemented with 100 μg/ml ampicillin. Liquid cultures (2 ml) were grown overnight at 37 °C with shaking at 200 rpm and then harvested by centrifugation. Each pellet was resuspended in 100 μl of lysozyme solution (50 mg/ml lysozyme, 50 mM glucose, 10 mM EDTA, 25 mM Tris, pH 8.0). Alakaline SDS solution (200 μl) (0.2 M NaOH, 1% SDS) was then added and samples were inverted until clear. Next, 150 μl of 3 M sodium acetate pH 4.8 was added, and the cell suspension was centrifuged at 16 800 x g for 5 min. Supernatants were transferred to new microfuge tubes, and 1 ml cold 95% ethanol added. Following centrifugation, pellets were resuspended in 100 μl H_2O and 200 μl cold 95% ethanol added. Following centrifugation, supernatants were discarded, and

pellets left to air dry for 10 min. Dried pellets were resuspended in 50 μl TE (1 mM EDTA, 10 mM Tris, pH 7.5) supplemented with 20 μg/ml RNAse A. To confirm sequence of isolated plasmid DNA, colony PCR, restriction digest analysis and sequencing analysis was performed to confirm the sequence of all constructs.

2.3.9 DNA sequencing

DNA sequencing confirmed the insertion of the desired sequence into the plasmids. Plasmid DNA was purified with a Qiagen Maxiprep kit, and resuspended in ddH_2O. Sequencing was performed by the DNA Core Service lab, Department of Biochemistry, University of Alberta.

2.4 Yeast Transformation

Transformation of yeast was achieved using lithium acetate and polyethylene glycol as described previously (156-158). Overnight cultures of BJ1991 or W303.1b yeast grown at 30 °C with shaking were used to inoculate 50 ml of YPD (BJ1991) or YPDA (W303.1b) media to $5x10^6$ cells/ml. Following 4 h of growth, cultures were centrifuged 5 min at 850 x g in a Beckman GH 3.8 rotor, and washed with 25 ml sterile ddH_2O. Cells were resuspended to $2x10^9$ cells/ml in ddH_2O. Cells ($2x10^8$) cells were transferred to a microfuge tube, and incubated with transformation mix for 40 min at 42 °C. Transformation mixture consisted of PEG 3500, LiAc, boiled salmon sperm carrier DNA, and plasmid DNA. pMA91, pJRC16, or pHJC4 cDNA (10 μg) were used to transform BJ1991 yeast, and 1 μg of cDNA was used to transform W303.1b yeast (Table 3.1).

Transformed cells were pelleted 5 min at 1 500 x g, resuspended in H_2O to 1 ml and 600 µl spread on Leu$^-$ (BJ1991) or Ura$^-$ (W303.1b) selective media plates. Colonies appeared within 5-7 days.

2.5 Inducible Expression

SGI medium (6.7 g/l yeast nitrogen base without amino acids, 20 g/l glucose, 30 mg/l Adenine hemisulfate, 1 g/l Casamino acids, 40 mg/l Tryptophan, pH 6.0) (50 ml) was inoculated with a single colony of W303.1b *S. cerevisiae* transformed with pGAL-AE1 (Table 3.1). Pre-cultures were grown overnight at 30 °C with shaking at 200 rpm to an A_{600} of 4.8. YPGE medium (5 g/l glucose, 10 g/l yeast extract, 10 g/l peptone, 3% (v/v) ethanol, pH 6.0) (200 ml) was inoculated with pre-culture to an A_{600} of 0.040, and incubated at 30 °C with shaking at 200 rpm. Cultures (4 x 200 ml) were inoculated with pre-culture, and grown for 24, 28, 32, and 36 h prior to induction. Expression of GAL-AE1MD was induced with addition of 20% (w/v) galactose to a final concentration of 2%. Following induction, cultures were grown for a further 14 h at 30 °C with shaking at 200 rpm. At 12 h, 13 h, and 14 h post-induction, samples were harvested from each culture for analysis. A_{600} for each culture was assessed prior to induction, and also at 12 h, 13 h, and 14 h post-induction. Culture samples (3 ml) were pelleted at 1 500 x g in a benchtop microcentrifuge for 5 min. Pellets were then resuspended in 500 µl TEK buffer (0.1 M KCl, 1 mM EDTA, 10 mM Tris-HCl, pH 7.5) and incubated at room temperature for 5 min. Samples were centrifuged 16 800 x g for 1 min in a benchtop microcentrifuge, and the supernatant was discarded. Pellets were resuspended in 50 µl TES B buffer (0.6

M sorbitol, 1 mM EDTA, 10 mM Tris-HCl, pH 7.5) and glass beads were added until skimming the top of the cell suspension. Samples were disrupted by vortexing for 30 seconds. A hole was poked in the bottom of the tube with a 30G1/2 needle and cell lysate spun into a new microfuge tube 16 800 x g for 5 s. Liquid was transferred from the bottom tube into a new microfuge tube. TES B (50 μl) was added to wash the glass beads, and the sample was again centrifuged and the supernatant pooled with the first supernatant. SDS-PAGE sample buffer (100 μl) was added to the pooled supernatant and the samples were heated at 65 °C for 4 min. SDS-PAGE and immunoblotting was then performed. All samples were analyzed by 10% SDS PAGE. Expression level of AE1MD (μg/l AE1MD) was determined using densitometry with a GST-AE1Ct standard. Expression of AE1MD per cell was determined using the following calculation, where at A_{600} = 1, there are 1 x 10^7 yeast cells/ml:

$$\mu g \text{ AE1MD/cell} = (\mu g/\text{ml AE1MD}) \times (1/A_{600}) \times (1/1 \times 10^7 \text{ cells}).$$

2.6 Isolation of Yeast Membranes

Membranes were isolated from competent BJ1991 yeast transformed with pHJC4 grown in both Leu$^-$ and YPD media. Cultures grown in Leu$^-$ medium were harvested between A_{600} of 0.6-1.0. Cultures grown in YPD medium were harvested between A_{600} of 3 and 6. YPD medium (3 l) was inoculated from a pre-culture grown from several independent colonies for 3 days in Leu$^-$ media at 30 °C with shaking at 200 rpm. Cultures were harvested at 6 500 x g for 10 min in a JLA 8.1000 rotor in a JA-20 Beckman centrifuge. Cells were resuspended in 30% glycerol and stored at –20 °C prior to membrane isolation. After thawing, cells

were centrifuged at 6 500 x g for 10 min in a Beckman JA-14 rotor. Cells were resuspended in cold lysis buffer (1 mM EDTA, 10% glycerol, 1 mM DTT, 1 mM PMSF, Complete Mini protease inhibitor, 10 mM sodium phosphate, pH 7.5) to a volume of 0.5 g cells/ml buffer. Resuspended cells were disrupted by passage 7 times through an EmulsiFlex-C3 homogenizer (Avestin, Ottawa, Canada). Broken cells were spun twice at 6 500 x g to remove unbroken cells and cell debris in a Beckman JA-14 rotor. Cell homogenates were spun in a Ti70 rotor at 100 000 x g for 1 h. Supernatants were discarded, and the resulting pellets were combined and homogenized using a 21 1/2 G needle and 3 ml syringe to 1 ml membrane: 1 ml resuspension buffer (68 mM NaCl, 10% glycerol, 58 mM Na_2HPO_4, 17 mM NaH_2PO_4, pH 7.5). Homogenized membranes were stored at –20 °C in 1 ml aliquots.

2.7 Protein Characterization

2.7.1 Deglycosylation

HEK 293 cells grown in a 100 mm culture dish were transiently transfected with the AE1 expression vector pJRC9. Two days post-transfection, cells here harvested in IPB buffer (5 mM EDTA, 1% NP40, 150 mM NaCl, 0.5% sodium deoxycholate, 1 mM PMSF, and CompleteMini protease inhibitor tablets, 10 mM Tris-HCl, pH 7.5). Cell lysate (15 μl) was made up to 100 μl in H_2O and heated at 50 °C for 10 min. PNGase F was added to a final concentration of 10 U/ml and samples incubated for 1 h at 37 °C. An equal volume of sample buffer was added and 56 μl loaded onto a polyacrylamide gel. Alternatively, isolated yeast membranes were solubilized in 0.1% DDM and 100 μl of solubilized

membrane was heated 50 °C for 10 min, then incubated with 10 U/ml of PNGase F for 1 h at 37 °C. An equal volume of sample buffer was added and 20 μl loaded onto a 7.5% polyacrylamide gel.

2.7.2 Immunocytochemsitry

BJ1991 yeast transformed with plasmid DNA was grown overnight to A_{600} = 0.8. Formaldehyde (37%) was added directly to cell culture to a final concentration of 3.7%. Cells were fixed by incubation at 30 °C with shaking for 10 min. Cells were collected by centrifugation 16 800 x g for 30 s and resuspended in 1.5 ml PBS (140 mM NaCl, 3 mM KCl, 6.5 mM Na_2HPO_4, 1.5 mM KH_2PO_4, pH 7.4). Resuspended cells were incubated with 0.15 ml 37% formaldehyde at 30 °C for 1 h with shaking. Cells were pelleted and washed twice with 1 ml PBS and twice with 1 ml solution B (1.2 M sorbitol, 19 mM KH_2PO_4, 80 mM K_2HPO_4, pH 7.5). Cells were resuspended in 1 ml solution B, and transferred to a 13 x 100 mm glass tube. 2-mercaptoethanol (3 μl), and 40 μl of zymolyase solution (10 mg/ml zymolyase 100T in H_2O) were added. Cells were incubated with shaking 30 °C for 30-60 min. Cells were washed twice in solution B and resuspended in 500 μl solution B. Slides were prepared by spotting with 100 μl of poly-L-lysine (100 μg/ml) and air dried. Spheroplasted cells (50 μl) were spotted onto the coated slide and removed again. Spotted cells were washed once with solution B. Slides were air dried, immersed in 100% -20 °C methanol for 6 min and 100% -20 °C acetone for 30 s, and air dried again. Mounted cells were washed twice with 100 μl PBS/glycine (0.75% glycine (w/v), 140 mM NaCl, 3 mM KCl, 6.5 mM Na_2HPO_4, 1.5 mM KH_2PO_4, pH 7.4) for 5 min.

Slides were blocked by treatment twice for 15 min with PBG (0.5% BSA (w/v), 0.5% fish gelatine (v/v) 140 mM NaCl, 3 mM KCl, 6.5 mM Na_2HPO_4, 1.5 mM KH_2PO_4, pH 7.4) and incubated overnight at 4°C with 1:250 mouse monoclonal 1° antibody in PBG (either anti-AE1 antibody IVF12 from Dr. Mike Jennings, or anti-PMA1 antibody from Dr. Gary Eitzen). Following six 5 min washes with PBG, slides were incubated with 1:250 anti mouse Cy2-conjugated secondary antibody in PBG room temperature for 1 h. Slides were washed 6 x 5 min with PBG and 6 x 5 min with PBS before a drop of mounting media was placed on each spot of cells. Coverslips were sealed on slide with nail polish and left to dry overnight at 4 °C in a dark box. Fixed cells were imaged with a Zeiss LSM 510 laser scanning confocal imaging system and images collected using a 40x oil immersion objective at a resolution of 0.9 μm field depth.

2.8 Protein purification

2.8.1 Purification of GST-AE1Ct

GST-AE1Ct expression plasmid, pHJC1, was transformed into BL21 codon plus *E. coli* cells using electroporation. A single colony was isolated and used to inoculate 50 ml of LB medium, and growth occurred overnight at 37 °C with shaking. Liquid culture was used to inoculate 200 ml of LB medium. Cultures were grown at 37 °C with shaking until A_{600} reached 0.6-0.8. Protein expression was induced by the addition of Isopropylthiogalactoside (IPTG) to 1 mM and growth continued for 3 h at 37 °C with shaking. Cells were harvested by centrifugation at 7 500 x g for 10 min, 4 °C and the pellet resuspended in cold PBS buffer (140 mM NaCl, 3 mM KCl, 6.5 mM Na_2HPO_4, 1.5 mM KH_2PO_4, pH

7.4) containing Complete Mini Protease Inhibitor Cocktail (1 tablet/10 ml buffer). Cells were disrupted by sonication (4 x 60 s, power level 9.5, with model W185 probe sonifier (Heat systems-Ultrasonic Inc., Plainview, N.Y.)), and stirred slowly for 30 min following addition of Triton X-100 (1% (v/v)). Following centrifugation (2 000 x g, 10 min, 4 °C) the supernatant was incubated with 1.2 ml GSH-Sepharose 4B (50% slurry washed with 5 ml PBS) at room temperature with gentle rocking for 1-2 h. The sample was centrifuged 2 000 x g 5 min and the resin washed six times with PBS until the A_{280} approached zero.

GST-AE1Ct was eluted from the GSH-Sepharose resin with 3 x 100 μl glutathione elution buffer (10 mM reduced glutathione, 50 mM Tris-HCl, pH 8). Total protein concentration was determined using the Bradford protein assay (159). Protein purity was assessed using SDS-PAGE.

2.8.2 Detergent Selection

Re-homogenized frozen membrane aliquots (50 μl), containing 25 μl of yeast membranes and roughly 5 μg AE1, were incubated in a total volume of 500 μl 1% detergent solution in resuspension buffer (68 mM NaCl, 10% glycerol, 58 mM Na_2HPO_4, 17 mM NaH_2PO_4, pH 7.5). Membranes were incubated on ice for 30 min and then centrifuged 100 000 x g in a TLA100.3 rotor in a TL100 centrifuge. Detergents tested were sodium dodecyl sulfate (SDS), octyl glucoside (OG), dodecyl maltoside (DDM), $C_{12}E_8$, lysophosphatidylcholine (LPC) and Fos-choline (FC). A control sample was also performed in the absence of any detergent. Following centrifugation, 10 μl of SDS-PAGE sample buffer was added to 10 μl solubilized membrane supernatant and 2 μl was run in each lane of a 10% SDS polyacrylamide gel and immunoblots performed. Immunoblots

were probed with anti-AE1 antibody, IVF12. Percent solubilization was normalized to solubilization with 1% SDS.

2.8.3 Protein Solubilization

Frozen yeast membrane aliquots (0.5 ml membrane/ml total) were thawed and re-homogenized with a 21G1/2 needle and 1 ml syringe. Membranes were resuspended to a volume of 1x pellet volume to 10 x 1% DDM in resuspension buffer. Membranes were incubated on ice 30 min and then centrifuged 30 min 100 000 x g in a Beckman Ti70 rotor. Supernatants were used for protein purification and the pellet was discarded.

2.8.4 Affinity Purification of AE1MD

Isolated membranes equivalent to 7 l of culture were re-homogenized and solubilized in resuspension buffer with 1% DDM for 30 min on ice and centrifuged 100 000 x g 30 min in a 70Ti rotor. The supernatant, containing approximately 500 μg AE1MD, was supplemented with 1 M imidazole to a final concentration of 5 mM imidazole was bound to pre-washed metal resin (200 μl bed volume) overnight at 4 °C with rotation. Resin was washed 3 times with 10 bed volumes of metal wash (300 mM NaCl, 10% glycerol, 0.1% DDM, 50 mM sodium phosphate, pH 7.0) and transferred to a 2 ml microfuge tube. Resin was incubated 10 min with agitation with 1 ml (5 bed volumes) metal elution buffer (300 mM NaCl, 1% DDM, 10% glycerol, 250 mM imidazole, 50 mM sodium phosphate, pH 7.0) and the supernatant applied to 75 μl bed volume of pre-washed GSH resin. Protein was bound to the resin overnight at 4 °C with

rotation. Resin was centrifuged at 2 000 rpm for 5 min and the unbound fraction discarded. Resin was washed 4 times with 10 bed volumes of GSH wash buffer (140 mM NaCl, 3 mM KCl, 0.1% DDM, 6.5 mM Na_2HPO_4, 1.5 mM KH_2PO_4, pH 7.5). PreScission protease (10 U) in cleavage buffer (10% glycerol, 1% DDM, 150 mM NaCl, 1 mM EDTA, 1 mM dithiothreitol, 50 mM Tris-HCl, pH 7.0), was added to the resin and allowed to incubate 48 h at 4 °C with rotation. Supernatants were collected and analyzed on a 10% polyacrylamide gel. Immunoblots were performed to determine protein concentration with the GST-AE1Ct standard. BCA protein assays were performed to determine protein concentration (160). Poly-acrylamide gels were stained with Coomassie Blue stain to examine protein purity.

2.9 Protein Characterization and Quantification

2.9.1 SDS-PAGE

Protein samples were prepared by addition of an equal volume of 2 x SDS sample buffer (20% (v/v) glycerol, 2% (v/v) 2-mercaptoethanol, 4% (w/v) SDS, 1 % (w/v) bromophenol blue, 150 mM Tris, pH 6.8) containing CompleteMini Protease Inhibitor Cocktail (Roche). Samples were heated at 65 °C for 4 min and then centrifuged at 16 800 x g for 10 min prior to gel loading. Samples were loaded on 1.5 mm 7.5% or 10% (w/v) polyacrylamide gels prepared in Bio-Rad Mini-PROTEAN II electrophoresis cell. Gels were electrophoresed at 90 mA/gel until the dye front ran off the gels. Expression level of AE1MD (μg/l AE1MD) was determined using densitometry with a GST-AE1Ct standard. Expression of

AE1MD per cell was determined using the following calculation where at A_{600} = 1, there are 1 x 10^7 yeast cells/ml:

$$\mu g \text{ AE1MD/cell} = (\mu g/ml \text{ AE1MD}) \times (1/A_{600}) \times (1/1 \times 10^7 \text{ cells}).$$

2.9.2 Coomassie Blue staining of SDS-PAGE gels

Following SDS-PAGE, gels were removed from the electrophoresis cell and stained with Coomassie Blue stain (0.05% Coomassie Blue R-250, 25% isopropanol, 10% acetic acid) for 1 h with rocking at room temperature. Gels were destained with 5% methanol, 10% acetic acid overnight at room temperature with rocking. Gel images were collected on a Kodak Image Station 440CF.

2.9.3 Immunoblotting

Following SDS-PAGE, proteins were transferred to PVDF membrane (Millipore) at 100 V for 1 h at room temperature in transfer buffer (20% (v/v) methanol, 192 mM glycine, 25 mM Tris). PVDF membranes were blocked in 5% TBST-M (TBST (0.1% (v/v) Tween-20, 127 mM NaCl, 20 mM Tris, pH 7.5), supplemented with 5% (w/v) nonfat dry milk) for 30 min and then incubated overnight with rocking at 4 °C with primary antibody in 5% TBST-M. Membranes were washed 3 x 10 min with 10 ml TBST and then incubated with secondary antibody in 5% TBST-M at room temperature for 1 h with rocking. Membranes were washed 3 x 10 min with 10 ml TBST and then exposed using ECL reagent (Perkin Elmer). Membrane images were collected with a Kodak

Image Station 440CF and protein bands were quantified with Kodak ID software (Eastman Kodak Company).

2.9.4 Microtitre-dish protein quantification assay

The Bradford Protein assay was performed as described previously (159). A microtitre-dish version of the Bradford assay was performed using a Multiskan Ascent 100-120 V plate reader (Thermo Electron Corporation). In the microtitre-dish assay, BSA standards (0.625 μg to 5 μg) and samples were loaded into wells of a 96 well plate to a total volume of 10 μl. Bio-Rad dye diluted four fold with water (200 μl) was added to each well and mixed by pipetting. Plates were shaken 30 s at 890 rpm in the Multiskan Ascent plate reader, and absorbance was measured at 595 nm. Protein assay data was collected using Ascent Software version 2.6 (Thermo Electron Corporation) and analysed using Microsoft Excel.

The BCA protein assay was performed as described previously (160). A microtitre-dish version of the BCA assay was performed using a Multiskan Ascent 100-120 V plate reader (Thermo Electron Corporation). BSA standards (0.625 μg to 5 μg) and samples (10 μl) were loaded into wells of a 96 well plate. BCA reagent (200 μl) was added to each well and mixed by pipetting. Plates were shaken 30 s at 890 rpm in the Multiskan Ascent plate reader, and absorbance was measured at 620 nm. Protein assay data was collected using Ascent Software version 2.6 (Thermo Electron Corporation) and analysed using Microsoft Excel.

2.10 Statistics

All errors and error bars represent the standard error of the mean (SEM). Statistical significance was defined as $p \leq 0.05$ as determined by paired t-test. Statistical analysis was performed using KaleidaGraph software. Each experiment where error was calculated was repeated at least three times, although n values vary.

A

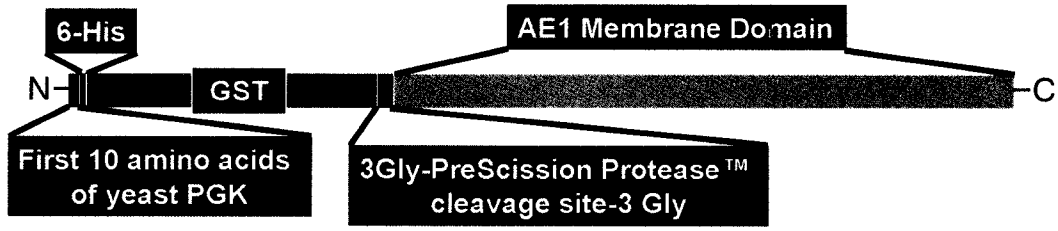

B

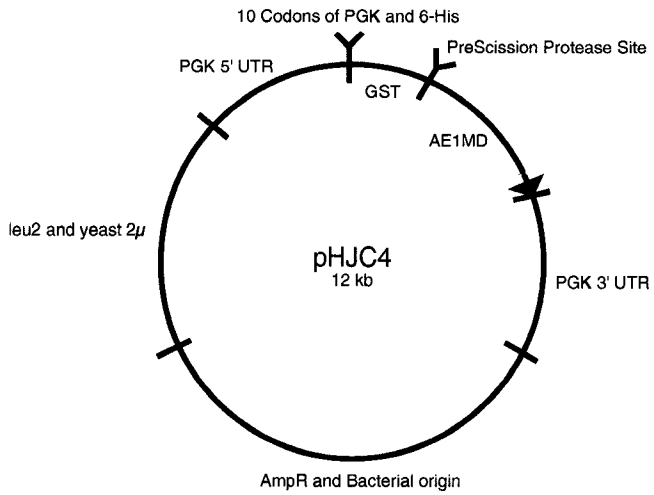

Figure 2.1. Constitutive AE1 membrane domain expression construct, pHJC4. (A) Recombinant protein shown to scale. The first 10 amino acids of the yeast protein phosphoglycerate kinase (PGK) promote a high expression level. The 10 PGK amino acids are followed by a 6-His tag, which binds to metal affinity resin in purification steps. The 6-His tag is followed by a glutathione-S-transferase (GST) tag, which binds to glutathione resin. A PreScission Protease™ cleavage site follows the two tags. Cleavage at this site allows for removal of the tags from the AE1 membrane domain. A spacer comprised of 3 Gly codons flanks the cleavage site to allow access to the site and facilitate efficient cleavage. Expressed tagged protein (AE1MD) consists of amino acids 388-911 of human AE1, which includes the last 17 amino acids of the N-terminal domain, the entire membrane domain, and the C-terminal domain. (B) The expression plasmid for AE1MD is called pHJC4. AmpR indicates the ampicillin reistance gene, and the Bacterial origin is the region required for propogation in bacteria. Leu2 is a selective marker that allows for growth in the absence of leucine. 2 μ is the yeast origin of replication. UTR designates the untranslated region of PGK. Protein expression is driven by the constitutive *PGK* promoter. The construct is 12 kilobases (kb) in size.

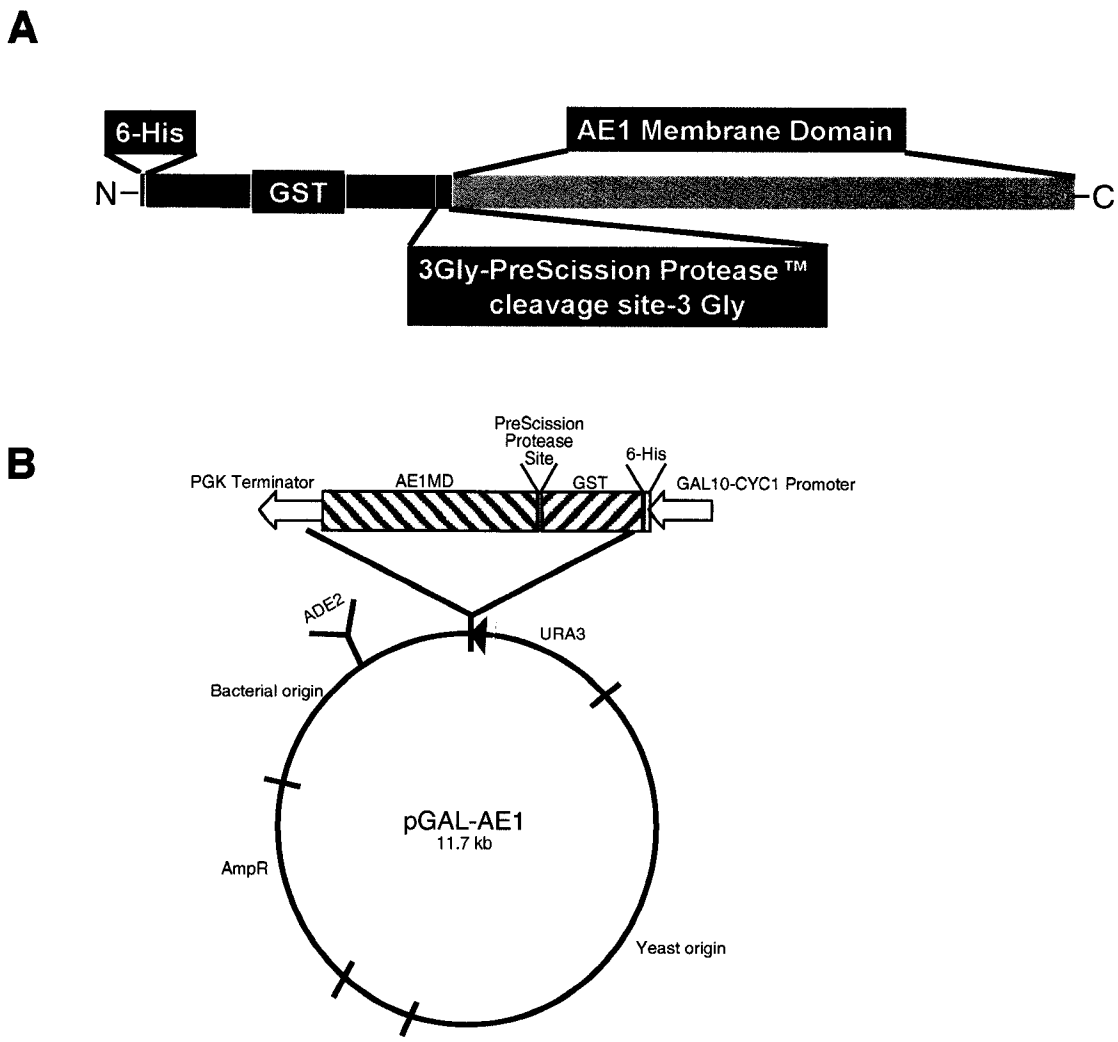

Figure 2.2. Inducible AE1 membrane domain expression construct, pGAL-AE1. (A) Recombinant protein shown to scale. A 6-His tag, which binds to metal affinity resin in purification steps is followed by a glutathione-S-transferase (GST) tag, which binds to glutathione resin. A PreScission Protease™ cleavage site follows the two tags. Cleavage at this site allows for removal of the tags from the AE1 membrane domain. A spacer comprised of 3 Gly codons flanks the cleavage site to allow access to the site and facilitate efficient cleavage. Expressed tagged protein (AE1MD) consists of amino acids 388-911 of human AE1, which includes the last 17 amino acids of the N-terminal domain, the entire membrane domain, and the C-terminal domain. (B) The inducible expression plasmid for AE1MD is called pGAL-AE1. Bacterial origin is the region required for bacterial propogation. Yeast origin is the region required for yeast propogation. *ADE2* and *URA3* are selective markers that allow for growth in the absence of adenine and uracil respectively. Protein expression is driven by the galactose-inducible *GAL10-CYC1* promoter. The construct is 11.7 kilobases (kb) in size.

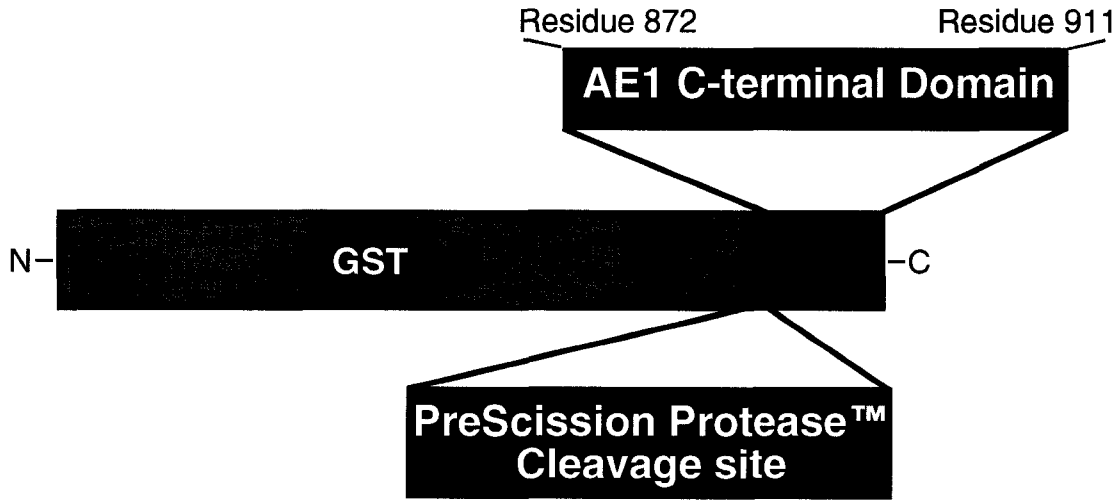

Figure 2.3. AE1 C-terminal GST-fusion protein construct, pHJC1. A glutathione-S-transferase (GST) tag, which binds to glutathione resin, is followed by a PreScission Protease™ cleavage site and the 40 residue C-terminal cytoplasmic domain of AE1. Cleavage at the PreScission Protease site allows for removal of the GST tag from the AE1 C-terminal domain.

Chapter 3

Expression of AE1MD in Yeast

3.1 Results

3.1.1 Purification of GST-AE1Ct

To quantify AE1MD expressed in yeast, a standard was constructed. The C-terminal tail of AE1 is recognized by the monoclonal antibody IVF12. A GST-fusion protein of the C-terminal tail of AE1, GST-AE1Ct, was made. Since AE1MD also contains the C-terminus of AE1 and is detected by IVF12, GST-AE1Ct can be used as a protein standard to detect expression of AE1MD. pHJC1 plasmid DNA was transformed into BL21 codon plus *E. coli* cells. Expression of GST-AE1Ct by pHJC1 was induced using IPTG. Cells were lysed in two ways to release expressed, soluble GST-AE1Ct. The first method was sonication, to disrupt the cell wall. The second was incubation with the non-ionic detergent, Triton-X-100, to solubilize the plasma membrane. Cell lysate was collected following the two solubilization steps, and applied to glutathione Sepharose resin pre-equilibrated with PBS. GST-AE1Ct was eluted using GSH-elution buffer, and the protein concentration was assessed (Fig. 3.1). GST-AE1Ct is detected on a Coomassie Blue-stained gel (Fig. 3.1 A). In blots probed with anti-AE1 antibody, both AE1MD and GST-AE1Ct are detected (Fig. 3.1 B). Bands were quantified with densitometry using a Kodak Image station, which is linear over a range of four orders of magnitude, according to the manufacturer.

3.1.2 Expression of Human AE1MD in S. cerevisiae

Expression and purification of human AE1 expressed in the yeast *S. cerevisiae* has previously been described with the expression construct pJRC16, which encodes the protein yAE1 (Table 3.1) (134). The primary goal of this study

was to improve upon the expression and purification level found with the earlier yeast expression system. Another goal was generate a construct that would allow for expression of purified AE1 membrane domain alone. pJRC16 was modified to introduce a glutathione S-transferase (GST) tag between the 6-His tag and AE1. AE1 coding sequence was truncated to remove the majority of the N-terminal cytoplasmic domain. A PreScission protease cleavage site was introduced between the tags to facilitate tag removal during purification. The resulting construct, pHJC4 (Fig. 2.1) (Table 3.1), retains the 5′- and 3′-untranslated regions of the highly expressed yeast protein, phosphoglycerate kinase (PGK), as well as the first 10 codons of that gene. The final construct consists of: the first 10 amino acids of PGK, a 6-His tag, a GST tag, a PreScission protease cleavage site, and codons 388-911 of human AE1. Protein expression is driven by the strong, constitutive promoter for PGK. The selective marker is *leu2* allowing for selection on the basis of growth in media lacking leucine. The membrane domain of AE1, codons 388-911, is sufficient for anion transport activity (161, 162), and therefore truncation of AE1 in the construct to include only these residues should not disrupt anion exchange activity of the expressed protein, AE1MD (Table 3.1).

Expression of AE1 was characterized in both a constitutive and inducible system. In the inducible system, human AE1 was inserted into the yeast galactose-inducible expression vector pYeDP60 (154), to generate the plasmid pGAL-AE1 (Table 3.1). The AE1 membrane domain with a 6-His and GST tag were amplified from pHJC4 and ligated into pYeDP60. The protein encoded by pGAL-AE1, GAL-AE1, is identical to the protein expressed from pHJC4, as described above, except that the 10 codons of yeast PGK have been deleted (Fig.

2.2) (Table 3.1). AE1 expression in pGAL-AE1 is driven by the inducible galactose promoter *GAL10-CYC1* of pYeDP60. The selective markers are *ade2* and *URA3*, allowing selection on the basis of growth in media lacking adenine and uracil.

Expression levels of AE1MD in the constitutive expression system were examined under various conditions. A major concern in this project was to ensure that each colony chosen for inoculation consistently exhibited a high level of AE1MD expression. Sekler *et al.* described variability of yAE1 expression in yeast cells transformed with pJRC16 (134). Colonies had variable morphology, growing in large and small colonies. Smaller colonies had higher yAE1 expression per ml of culture (134). The first step to identifying highly expressing colonies was to develop a technique for screening AE1MD expression on a small scale before inoculating large cultures. Two methods were tested to examine AE1MD expression (mg/ml culture) of individual colonies. Cultures inoculated from individual yeast colonies transformed with pHJC4 were grown in selective media lacking leucine. The first method tested was mechanical disruption with glass beads followed by addition of sample buffer, and the second method was addition of sample buffer alone. With mechanical disruption, cells were disrupted by vortexing in the presence of glass beads. With sample buffer extraction, cells were resuspended in sample buffer and vortexed briefly in the absence of glass beads. An equivalent lysate fraction from each was loaded on a 10% SDS polyacrylamide gel and analyzed by immunoblotting. For all colonies analyzed, protein extraction was greatly increased with mechanical disruption as compared to incubation with sample buffer alone (Fig. 3.2). When extraction with mechanical disruption was normalized to 100%, only 7% of total AE1MD

was extracted with sample buffer (Fig. 3.2). The duration of glass bead disruption was optimized. Protein extraction was optimally achieved with 300 s of vortexing (Fig. 3.3).

With a method established for screening individual colonies for high expression, the variability of AE1MD expression (mg/ml culture) between individual colonies was analyzed (Fig. 3.4). Individual colonies grown in Leu^- medium were disrupted by mechanical disruption and protein content analyzed by immunoblotting. Only small colonies were chosen to examine expression, since small colonies have been shown to exhibit the highest expression of yAE1 per ml culture (134). A GST-AE1Ct standard was included on the immunoblot for quantification (Fig. 3.4 lane S). Expression of AE1MD from different colonies was on average 1.7 μg/cell x 10^{-8} in selective medium using the calculation, where at $A_{600} = 1$, there are 1×10^7 yeast cells/ml:

$$\mu g/\text{cell AE1MD} = (\mu g/\text{ml AE1MD}) \times (1/A_{600}) \times (1/1 \times 10^7 \text{ cells}).$$

In an effort to ensure that maximal protein expression was achieved, we tested protein expression when media was inoculated with single or multiple pHJC4 colonies (Fig. 3.5). Average expression with single colony inoculation was 0.19 mg/l culture, and with multiple colony inoculation was 0.23 mg/l culture. Using a paired t-test to compare the two methods, p=0.7, and therefore there is no statistically significant difference between them. When multiple colonies were used for inoculation as compared to single colonies, there was, however, a slight average in AE1MD expression per ml culture. Using multiple colonies may negate any variability between cultures, and therefore individual colonies did not need to be screened prior to inoculation of large cultures in further experiments. In large cultures of yeast, up to 18 l of yeast culture per

membrane preparation, yields of 50-100 g wet yeast cell were found. With such a large amount of material to disrupt, the use of glass beads is not a practical option. Equipment exists, such as the Bead Beater (BioSpec Products Inc., Bartlesville, OK), to disrupt cells with glass beads. However, cell disruption can be variable with the Bead Beater and cell lysates can become warm during disruption, causing protein aggregation and degradation. We decided to use an Emulsiflex high pressure homogenizer, which disrupts a large mass of cells at high pressure. Cell lysates are also kept cold using the Emulsiflex, which can help decrease protein degradation and aggregation.

The yeast AE1MD expression construct pHJC4 was designed with the hopes of increasing expression over that previously seen with AE1 from pJRC16. AE1MD protein expression in pHJC4 was compared to yAE1 expression in the parent vector pJRC16 and the empty vector pMA91 (Table 3.1). BJ1991 yeast transformed with each plasmid was grown in selective Leu^- medium overnight. Cells were disrupted by vortexing with glass beads, and samples were run on 10% SDS-PAGE and analyzed by immunoblots probed with the anti-AE1 antibody IVF12. There was no immunoreactive material detected when the samples harvested from pMA91-transformed yeast were probed with anti-AE1 antibody IVF12 (Fig. 3.6 A). yAE1 expressed by pJRC16 migrated on SDS-PAGE at approximately the same electrophoretic mobility as AE1MD, a molecular weight close to 75 kDa. The predicted molecular weight for yAE1 is 84 kDa and AE1MD is predicted to be 89 kDa. Thus, the predicted molecular weights are in good agreement with the molecular masses seen on the blot (Fig. 3.6). yAE1 expression (mg/litre culture) using pJRC16 was less than AE1MD expression (mg/litre culture) using pHJC4 as determined by densiometric comparison of the

bands on the immunoblots (Table 3.1). When the average expression of AE1 from pJRC16 (mg/ml culture) is normalized to 100%, the expression of AE1MD from pHJC4 is 159% (Fig. 3.6 C). There is no apparent difference between the cell lysates of the three samples when examined on Coomassie-blue stained SDS-PAGE when equivalent volumes of cell lysate were loaded (Fig. 3.6 B).

For protein purification, it is essential to generate non-aggregated, properly folded protein. We wanted to determine if any additives could be included in the culture medium that would aid in protein folding and/or enhance protein expression per litre of culture. Ethanol and glycerol can act as non-fermentable carbon sources for yeast, and may also act as molecular chaperones to assist protein folding (163). Therefore, we investigated the effect of addition of ethanol and glycerol on AE1MD protein expression per litre of culture. AE1MD expression (mg/ml culture) when grown with no additive was normalized to 100%. AE1MD expression with 2% ethanol in the medium decreased to 55% ± 27%. With 2% glycerol in the medium, expression decreased to 93% ± 4%. There is no statistically significant difference between cultures grown in the presence of 2% ethanol or 2% glycerol as compared to cells grown with no additive (Fig. 3.7). When both 2% ethanol and 2% glycerol were included in the medium, expression dropped to 38% ± 20% compared to no additive, which is significantly different than with no additive. Since glycerol may play a chaperone role in expression of AE1MD, and did not significantly decrease AE1MD expression (mg/l culture), we decided to include glycerol in the culture medium.

The doubling time of yeast in Leu$^-$ selective media is 6 h, while the doubling time in rich YPD media is 1.5 h. We wanted to determine if yeast

transformed with pHJC4 could be first grown in selective media and then AE1MD expression maintained by growth in rich media. The concern in this situation is that a lack of selective pressure would cause the yeast cells to expel the pHJC4 plasmid and cease to express AE1MD. If the plasmid could be maintained in rich media, the time for large-scale growth of AE1MD-expressing yeast could be reduced significantly. As determined using mechanical disruption and immunoblotting, there was an increase of 45% in the expression of AE1MD in cells grown in non-selective YPD, over those grown in selective Leu$^-$ synthetic media, although the difference was not statistically significant (Fig. 3.8). Protein expression per cell in non-selective YPD medium is lower than in Leu$^-$ medium, but since a higher cell density can be reached in rich medium, the overall result in an increase in expression per litre of culture. 1 litre of yeast grown to A_{600} = 3.0 in YPD media yields approximately 57 mg membrane protein, as determined by Bradford protein assay following high pressure cell disruption with an Emulsiflex homogenizer. Quantification of AE1MD in resuspended membranes from immunoblots shows that AE1MD makes up roughly 0.4% of the total membrane protein in yeast. Expression of AE1MD in YPD medium is 0.5-0.8 mg of AE1MD/liter of culture (Fig. 3.9). Since AE1MD expression per litre of culture is increased with growth in YPD medium and membranes can be isolated after a shorter growth period, large-scale growth of AE1MD was carried out in YPD medium.

Tanner's group previously expressed the AE1 membrane domain, B3mem, in a yeast system using a galactose inducible promoter (Table 3.1) (127). To compare expression of the AE1 membrane domain in the constitutive and inducible system, a new construct of AE1 membrane domain under an inducible

promoter, pGAL-AE1, was prepared as described above (Table 3.1). Cultures were grown for 24, 28, 32, and 36 h prior to induction by addition of galactose to a final concentration of 2%. At 11, 12 h, 13 h, and 14 h post-induction, samples were harvested from each culture for analysis by immunoblotting (Fig. 3.10 A). Maximal expression was achieved with 12 h of induction after 28 h of growth (Fig. 3.10 B). For comparison of GAL-AE1MD and AE1MD protein expression on immunoblots, 20x the total number of cells from the inducible system was required to see expression of GAL-AE1MD as compared to the number of cells needed to see a band in the constitutive system (Fig. 3.11). In Figure 3.10, $5x10^7$ cells were loaded per lane. In Figure 3.11, $2.5x10^6$ cells were loaded for both the constitutive and inducible system. With $2.5x10^6$ cells loaded, no GAL-AE1MD was detected, although AE1MD was. This indicates a much lower expression per cell of GAL-AE1MD as compared to AE1MD.

3.1.3 Glycosylation of AE1MD

To determine the glycosylation state of AE1MD, membranes expressing the protein were solubilized with 1% DDM and treated with PNGase F, which removes N-linked carbohydrate by cleavage at the asparagine site of linkage (140). Erythrocyte AE1 is heterogeneously glycosylated, as is AE1 expressed in HEK 293 cells (113, 135). Glycosylation increases the molecular weight of AE1 by up to 10 kDa (135). Carbohydrate modification is not required for AE1 to carry out anion-exchange function (100). yAE1 expressed in yeast has previously been reported to be not glycosylated (134), as have other mammalian membrane proteins (164, 165), suggesting that AE1MD will not be glycosylated when expressed in yeast. AE1 expressed in HEK 293 cells treated with PNGase F

shows an increase in electrophoretic mobility on SDS-PAGE compared to samples not treated with PNGase F, indicating deglycosylation by PNGase F in treated cells. (Fig. 3.12). AE1MD electrophoretic mobility was not altered upon treatment with PNGase F, indicating that AE1MD expressed in yeast is not glycosylated.

3.1.3 Subcellular localization of AE1MD

yAE1 expressed in yeast was previously found to localize primarily to sites in membranes other than the plasma membrane, such as the endoplasmic reticulum (134). Localization of AE1MD expressed in yeast was analyzed by confocal microscopy (Fig. 3.13). Monoclonal anti-AE1 antibody IVF12 was used as the primary antibody. As a positive control for plasma membrane localization, spheroplasted yeast cells were incubated with rabbit anti-PMA1 antibody (Fig. 3.13, panel B). PMA1 is the plasma membrane yeast H^+-ATPase. Negative controls included incubation with secondary antibody alone (Fig. 3.13, Panel C), and transformation with empty vector, pMA91 (Fig. 3.13, panel D). PMA1 localization is clearly at the plasma membrane on the basis of pericellular localization (Fig. 3.13, panel B). AE1MD localization appears to be primarily non-plasma membrane, rather in intracellular membranes such as endosomes, or endoplasmic reticulum, as evidenced by the clear difference in localization between AE1MD and PMA1. Increased staining in circular intracellular bodies suggests that AE1MD may be localized to the vacuole (Fig. 3.13, panel A). No immunofluorescence was seen for cells treated with secondary antibody alone, or yeast transformed with empty vector (Fig. 3.13, panel C and D respectively).

3.1.5 Solubilization of AE1MD

To choose an appropriate detergent for protein purification, AE1MD was solubilized from isolated yeast membranes with six different detergents at a concentration of 1% (Fig. 3.14). AE1MD was maximally solubilized with LPC and FC at 97% and 87% relative to the amount solubilized by SDS, respectively. LPC has previously been used to solubilize yAE1 expressed from yeast (134). DDM solubilized a large amount of AE1MD, 68% of the amount solubilized by SDS. Rabbit SERCA1a Ca^{2+}-ATPase has been successfully expressed in *S. cerevisiae* and solubilized using DDM (125). DDM has also been used in the purification and crystallization of the K^+ channel Kv1.2 expressed in *Pichia pastoris*. $C_{12}E_8$ has been shown to solubilize AE1 completely from erythrocyte membranes (144), but only solubilizes 38% of AE1MD expressed in *S. cerevisiae*. This value is in excellent agreement with previously reported values (134). Because DDM is relatively inexpensive and has been effective in structural studies of membrane proteins, 1% DDM was chosen to solubilize AE1MD for purification.

3.1.6 Purification of AE1MD

Yeast membranes (Fig. 3.15, lane 1) were solubilized with 1% DDM, (Fig. 3.15, lane 2) bound to TALON metal affinity resin, which binds 6-His tags, and eluted with 250 mM imidazole and 1% DDM (Fig. 3.15, lane 4). Eluted protein was then bound to glutathione Sepharose affinity resin, which binds glutathione S-transferase, and eluted by cleavage with PreScission protease (Fig. 3.15, lane 6 and 7). Cleaved AE1MD (cAE1MD) has an electrophoretic mobility of 46 kDa.

The membrane domain of erythrocyte AE1 is 55 kDa, which includes up to 10 kDa from glycosylation (135). Enzymatic deglycosylation of the isolated erythrocyte AE1 membrane domain from causes a shift in 55 kDa to 46 kDa (100). Since AE1MD is not glycosylated, an electrophoretic mobility of 46 kDa is expected for cAE1MD. On the basis of the immunoblot and densiometric analysis of the bands using the GST-AE1Ct standard, of the total solubilized protein incubated with the resin, only 18% bound to the metal resin. Of that, 8%, or 5.6 μg was eluted successfully and the majority (5.2 μg) was bound to the GSH resin. Cleaved protein, 2.4 μg, was finally eluted from the GSH resin.

Uncleaved protein was retained on the GSH resin, which amounted to 0.8 μg, or 20% of the total protein subjected to cleavage. A portion of the cleaved protein appears in dimer form on the immunoblot (100 kDa) both in the eluted fraction and associated with the resin, amounting to 2% of the eluted fraction and 20% of the fraction associated with the resin. The Coomassie-Blue stained SDS-polyacrylamide gel (Fig. 3.15, A, lane 6) indicates that eluted AE1MD is highly pure, constituting roughly 68% of the total protein (Table 3.2). On the immunoblot, there is a higher weight molecular species likely corresponding to dimeric AE1MD at 150 kDa, and a molecular weight species corresponding to dimeric cAE1MD near 100 kDa (Fig. 3.15, B). Immunoblotting with an anti-GST antibody revealed the presence of PreScission Protease in the eluted fraction (Fig. 3.16), and this finding was confirmed with in-gel digestion and mass spectrometry. The amount of PreScission Protease in the eluted fraction is roughly 0.8 ng/μl, for a total in the lane of 64 ng, as determined by densitometry (Fig. 3.16), which is too low to be detected with Coomassie Stain.

Table 3.1. Constructs to Express AE1 in yeast.

Name of Protein	Description of protein	Yeast vector used and properties	Citation
AE1MD	PGK N-terminal 10 residues-6-His tag-GST tag-AE1 residues 388-911	pHJC4; leucine selection, constitutive expression	This thesis
yAE1	PGK N-terminal 10 residues-6-His tag-AE1 residues 183-911	pJRC16; leucine selection, constitutive expression	(134)
GAL-AE1	6-His tag-GST tag-AE1 residues 388-911	pGAL-AE1; adenine and uracil selection, inducible expression	This thesis
B3mem	AE1 residues 361-911	pYeDP.b3mem; uracil selection	(127)

Table 3.2. Purification of AE1MD.

Fraction	Total protein (mg)	AE1MD (μg)	AE1MD/total (%)	Yield (%)
Isolated membranes	190	325	0.17	100
Solubilized membranes	150	317	0.20	98
Final elution	7.5	2.18	29	0.70

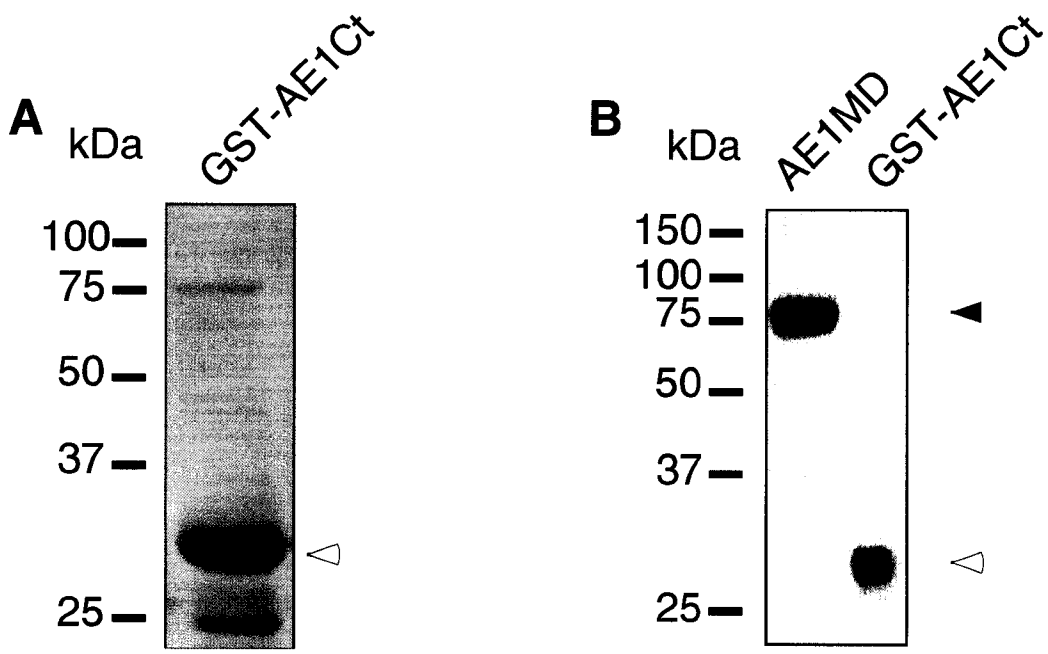

Figure 3.1. Purification of GST-AE1Ct. (A) Protein expressed in *E. coli* was affinity purified on glutathione Sepharose resin and then loaded on a 12.5% SDS-polycrylamide gel and stained with Coomassie dye. Open arrowhead indicates GST-AE1Ct, with a molecular weight of 31 kDa. (B) Yeast cells transformed with pHJC4 were disrupted with glass beads and run on SDS-PAGE (AE1MD) with 0.04 μg GST-AE1Ct standard (GST-AE1Ct). Closed arrowhead indicates AE1MD, open arrowhead indicates GST-AE1Ct.

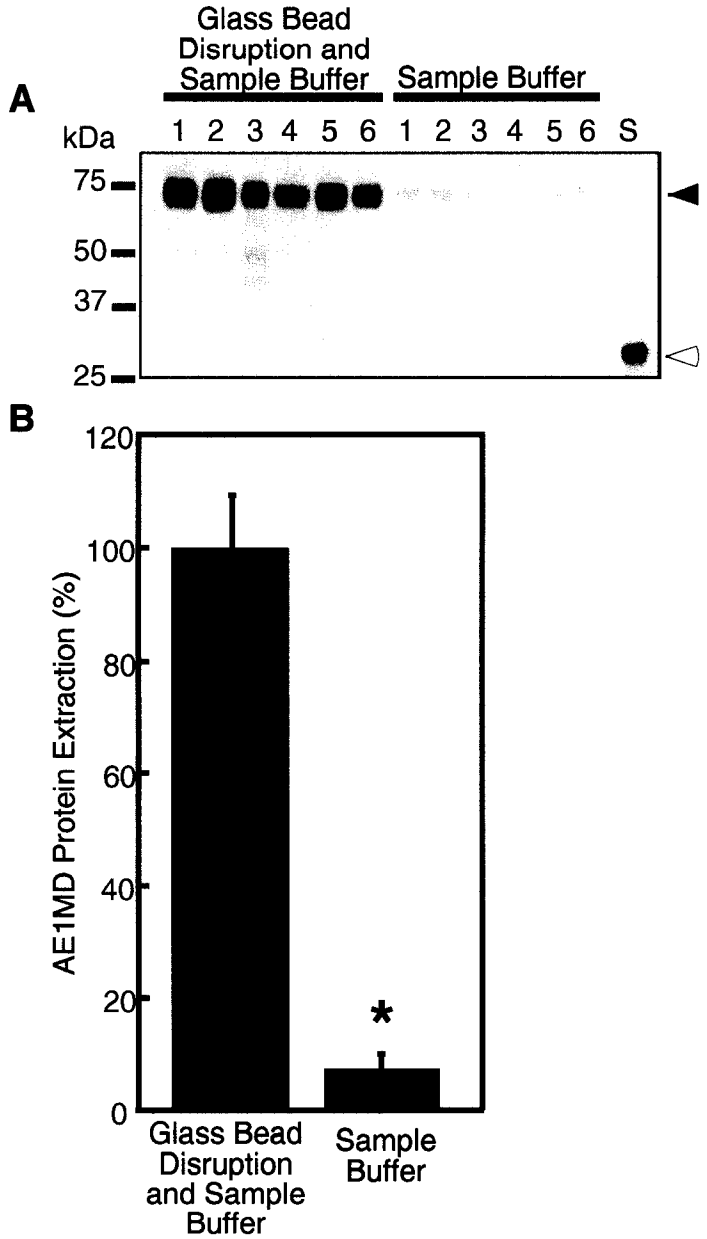

Figure 3.2. Selection of cell disruption method for analysis of AE1MD expression in yeast cultures. (A) Six independent colonies (lanes 1-6) were used to inoculate separate 25 ml of selective medium. Following 93 h of growth, 9 ml of each culture was processed using mechanical disruption, and 9 ml of each culture was centrifuged and the pellets incubated with 100 μl of sample buffer alone. The equivalent of 1.125 ml culture was loaded onto each lane of a 10% SDS polyacrylamide gel and an immunoblot performed using anti-AE1 antibody IVF12. Lane S contains 0.125 μg of GST-AE1Ct standard. (B) The average protein extraction was calculated for both the mechanical disruption method and the sample buffer method. The amount of extraction achieved with mechanical disruption was set to 100%. Data represent the mean of 6 independent experiments ± S.E. Asterisk, $p<0.05$ vs. Mechanical Disruption.

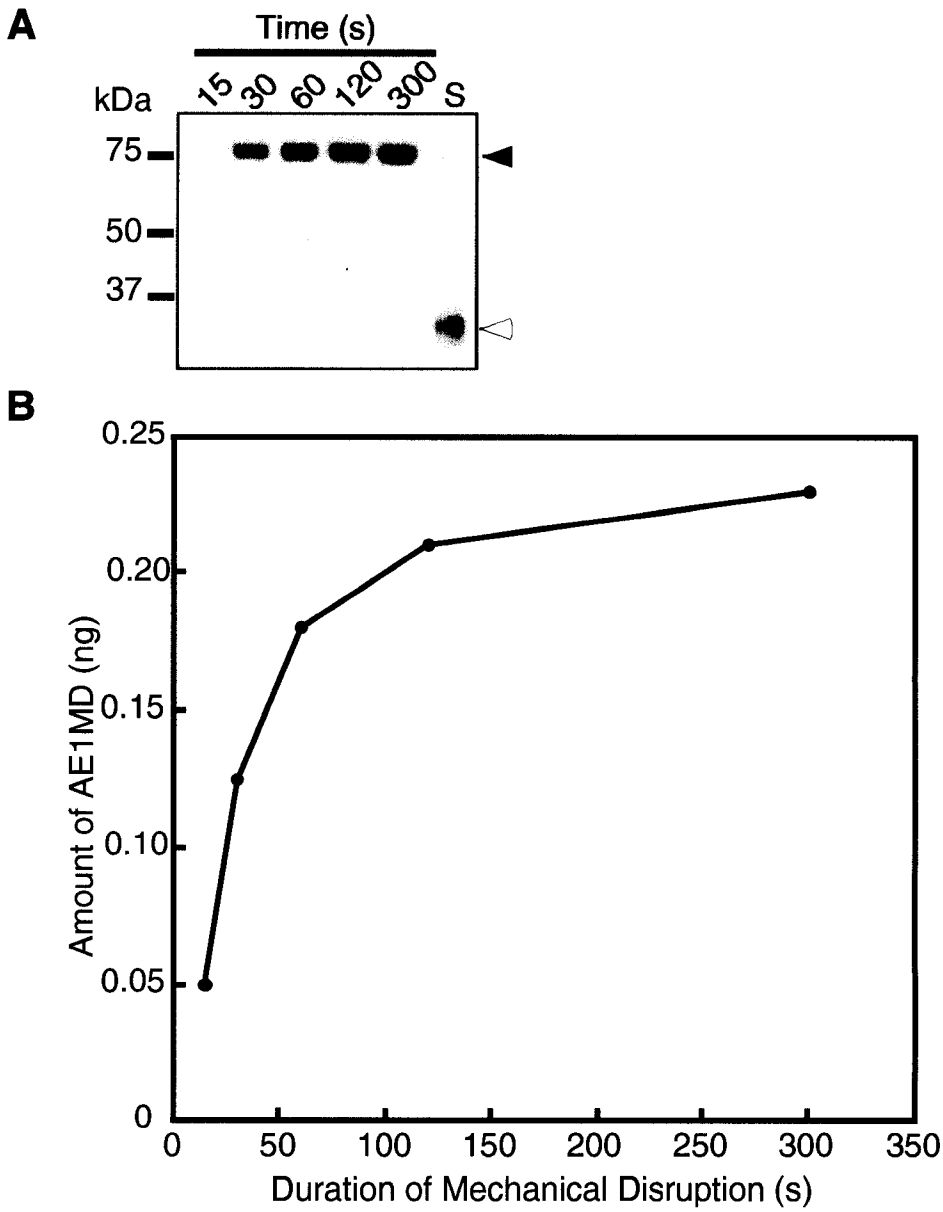

Figure 3.3. Optimization of cell disruption to optimize AE1MD isolation. Selective medium (9 ml) was inoculated with a single BJ1991 colony transformed with pHJC4. The culture was divided into 5 samples, and each was processed using mechanical disruption, with vortexing in the presence of glass beads for an increasing length of time. SDS-PAGE was run with an equivalent volume of culture being loaded for each sample. An immunoblot was performed using anti-AE1 antibody IVF12. (A) Lane S was loaded with 0.04 μg of GST-AE1Ct standard. Closed arrowhead indicates AE1MD, open arrowhead indicates GST-AE1Ct. (B) Graphical representation of densiometric analysis of bands.

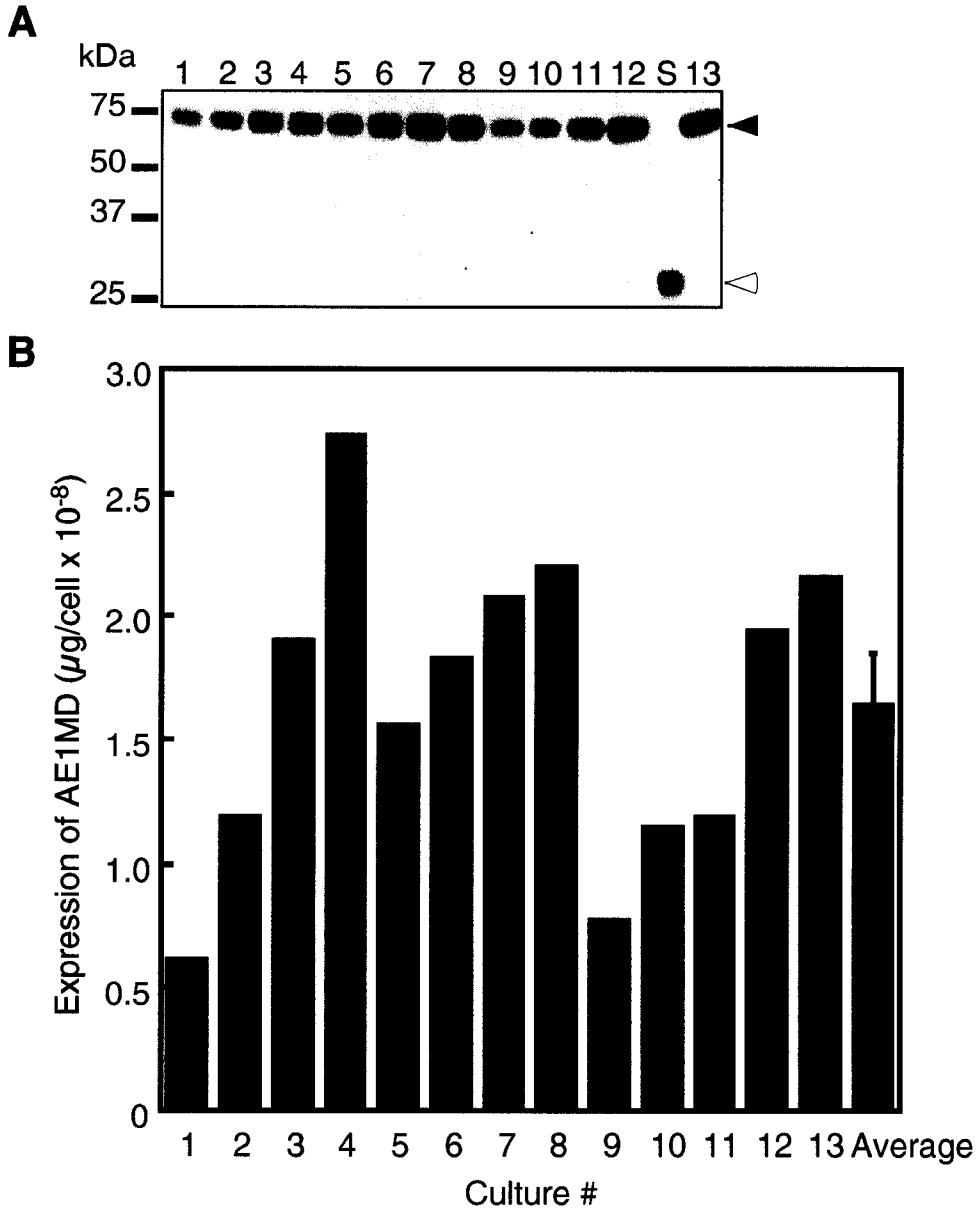

Figure 3.4. AE1MD expression variability. 13 cultures (9 ml) were inoculated with individual BJ1991 colonies transformed with pHJC4. Samples (4 ml) were harvested after 69 h of growth at 30 °C, and analyzed for cell density by measuring A600. (A) To determine protein expression levels, whole cell lysates prepared from these cultures using mechanical disruption were analyzed on immunoblots probed with anti-AE1 antibody IVF12. Lanes 1-12 and 14 are individual cultures. Lane 13 contains 0.04 μg GST-AE1Ct standard. Closed arrowhead indicates AE1MD, open arrowhead indicates GST-AE1Ct. (B) Cellular expression levels were calculated as amount of AE1/l culture (determined by densitometry) / cell density (A_{600}). Average represents the mean of 13 independent experiments ± S.E.

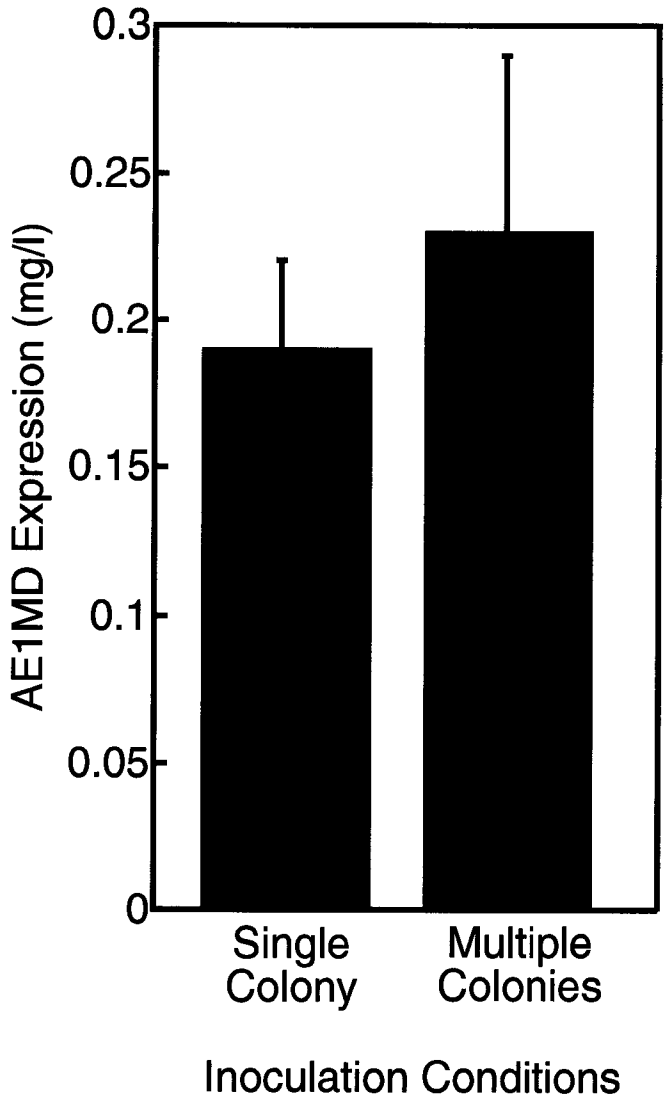

Figure 3.5. Single colony versus multiple colony inoculation. Cultures (7.5 ml) inoculated either with individual or multiple BJ1991 colonies transformed with pHJC4 were grown for 50 h and harvested using mechanical disruption. An equivalent volume of sample was loaded for each on a 10% SDS polyacrylamide gel and an immunoblot was performed using anti-AE1 antibody IVF12. Protein expression levels were quantified using GST-AE1Ct standard. Data represent the mean of 3-4 independent experiments ± S.E.

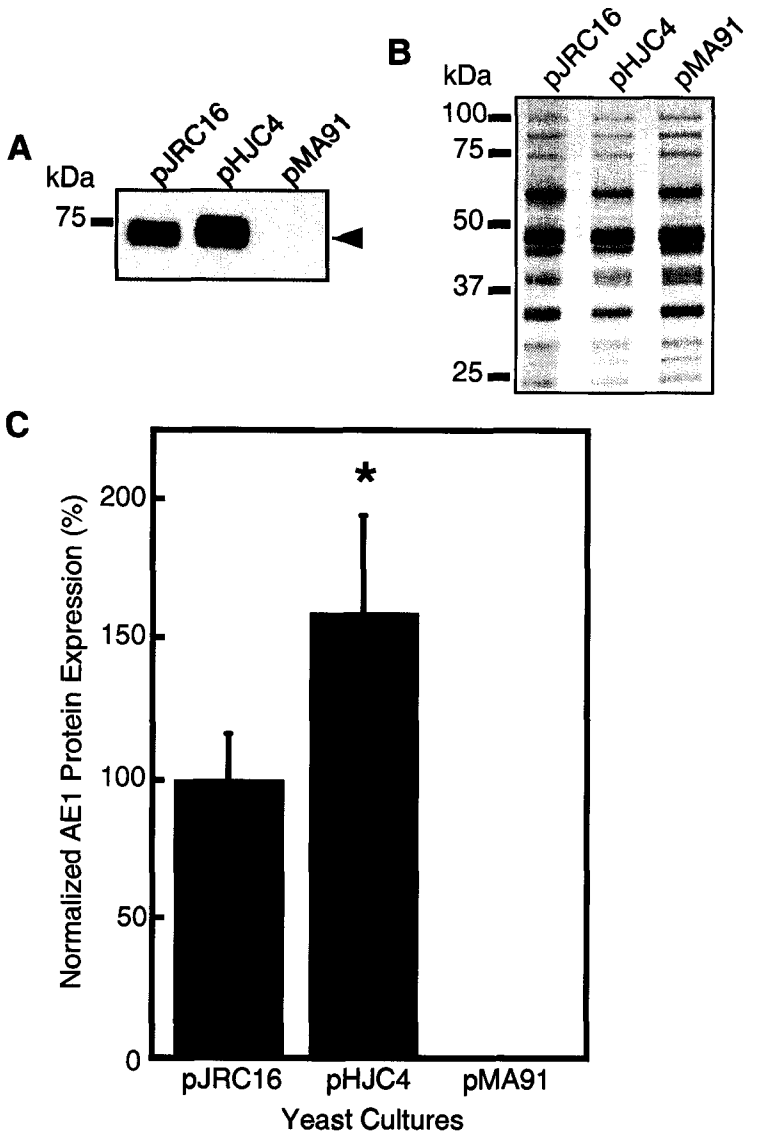

Figure 3.6. Comparison of AE1 expression by pJRC16, pHJC4 and pMA91. Selective medium (7.5 ml) was inoculated with BJ1991 colonies transformed with pJRC16, AE1MD, or pMA91. Cultures were grown for 1-2 days and harvested using mechanical disruption, then equivalent fractions of lysate were run in duplicate on 10% SDS polyacrylamide gel and the gel cut. (A) Protein expression was assessed on immunoblots using anti-AE1 antibody IVF12. Closed arrowhead indicates yAE1 and AE1MD. (B) Gels were stained with Coomassie Blue dye. (C) The expression of AE1 protein in pJRC16 cultures was normalized to 100%. Average AE1 protein expression in AE1MD and pMA91 cultures were calculated as a percentage of expression in pJRC16 cultures. Data represent the mean of 4-16 independent experiments ± S.E. Asterisk, $p<0.05$ vs. pJRC16.

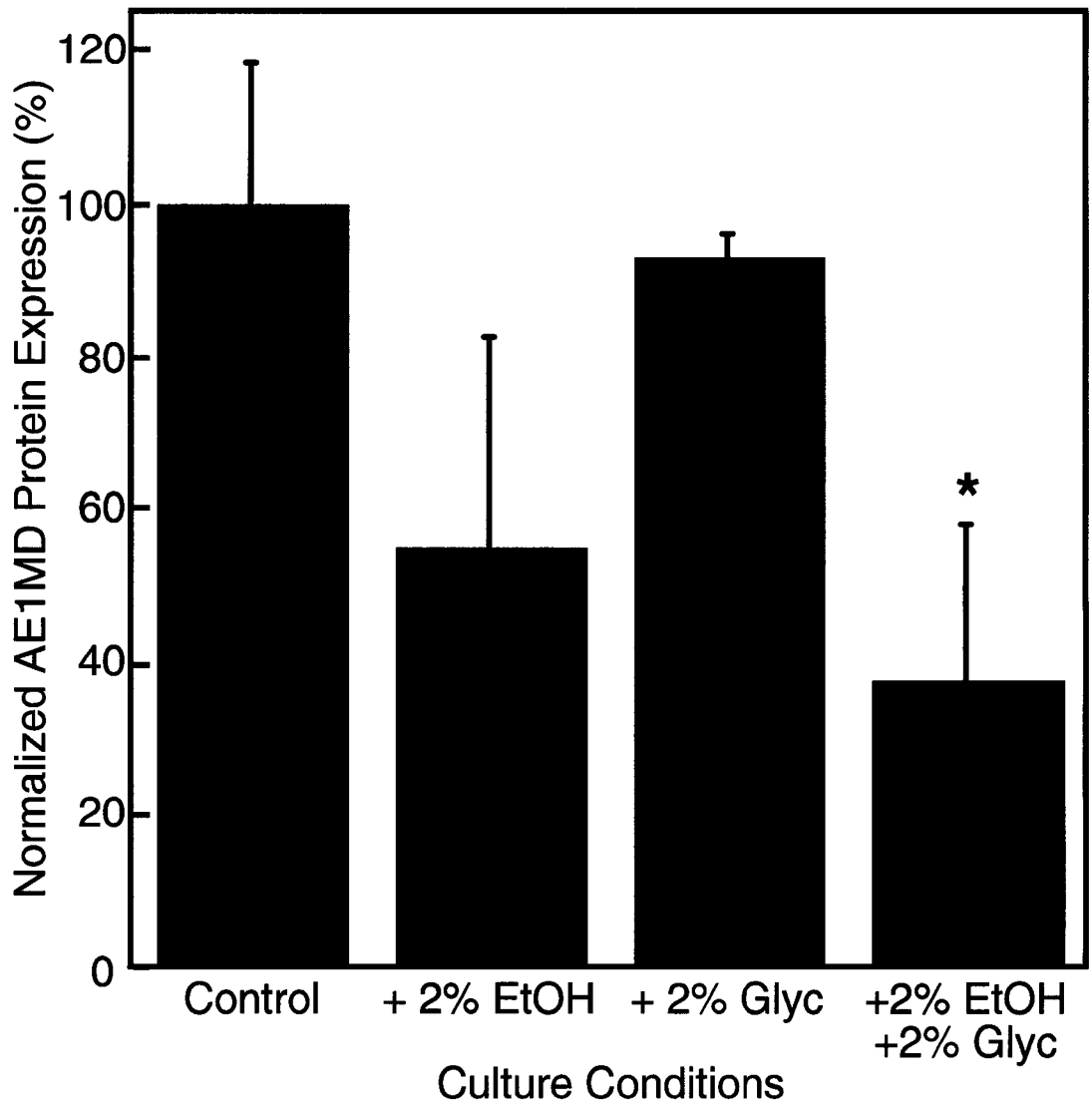

Figure 3.7. AE1MD expression with media additives. Selective medium was inoculated with BJ1991 colonies transformed with pHJC4. Selective cultures were used to further inoculate selective medium that contained 2% ethanol, 2% glycerol, 2%ethanol plus 2% glycerol or no additive as indicated. Samples were harvested from the cultures between A_{600} of 0.3 and 2. Samples were run on 10% acrylamide SDS-PAGE and protein expression was quantified from an immunoblot using anti-AE1 antibody IVF12. Protein expression in medium with additives was calculated as a percent of expression with no additive, which was normalized to 100%. Data represent the mean of 3-14 independent experiments ± S.E.

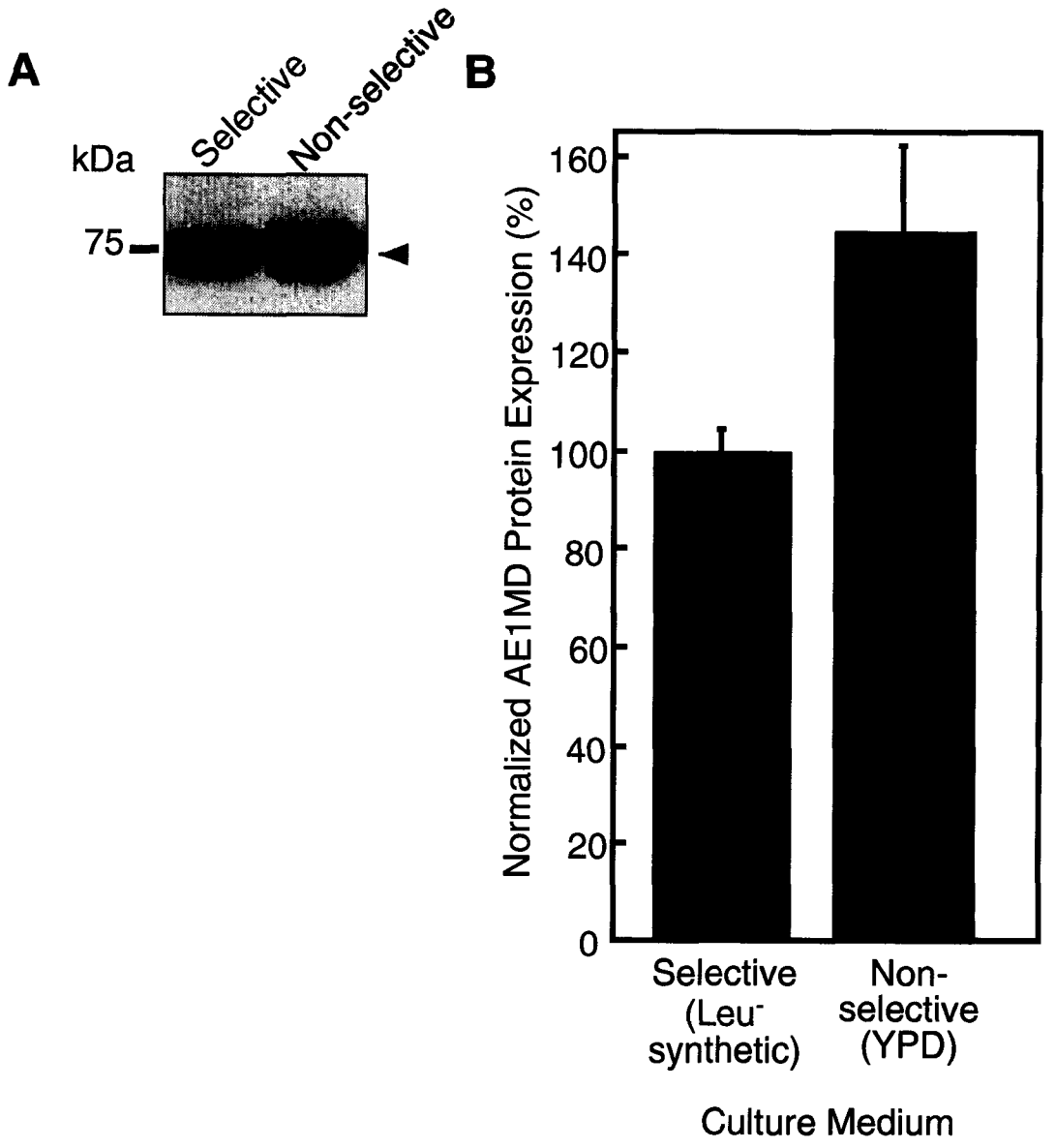

Figure 3.8. AE1MD Expression in selective versus rich media. Selective medium was inoculated with BJ1991 colonies transformed with pHJC4. Cultures were used to further inoculate 25 ml of selective and rich media (YPD). Samples were harvested from the cultures between A_{600} of 0.3 and 3. (A) Samples were run on 10% SDS-PAGE and protein expression was assessed from an immunoblot using anti-AE1 antibody IVF12. Both samples on the immunoblot were harvested at A_{600} of 1. Closed arrowhead indicates AE1MD. (B) Average AE1MD protein expression per ml culture medium in selective medium was normalized to 100%. Average AE1MD protein expression was calculated as a percentage of expression per ml culture in selective medium. Data represent the mean of 3 independent experiments ± S.E.

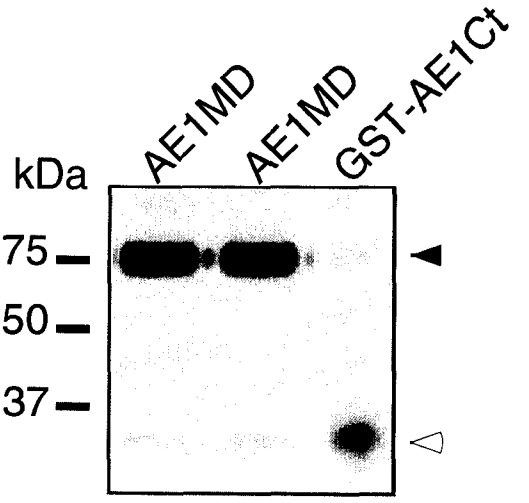

Figure 3.9. Expression of AE1MD in a constitutive system. Two separate yeast cultures transformed with pHJC4 were disrupted with glass beads and the equivalent of 0.25 ml culture run on SDS-PAGE (AE1MD) with 0.04 μg GST-AE1Ct standard (GST-AE1Ct). Closed arrowhead indicates AE1MD, open arrowhead indicates GST-AE1Ct.

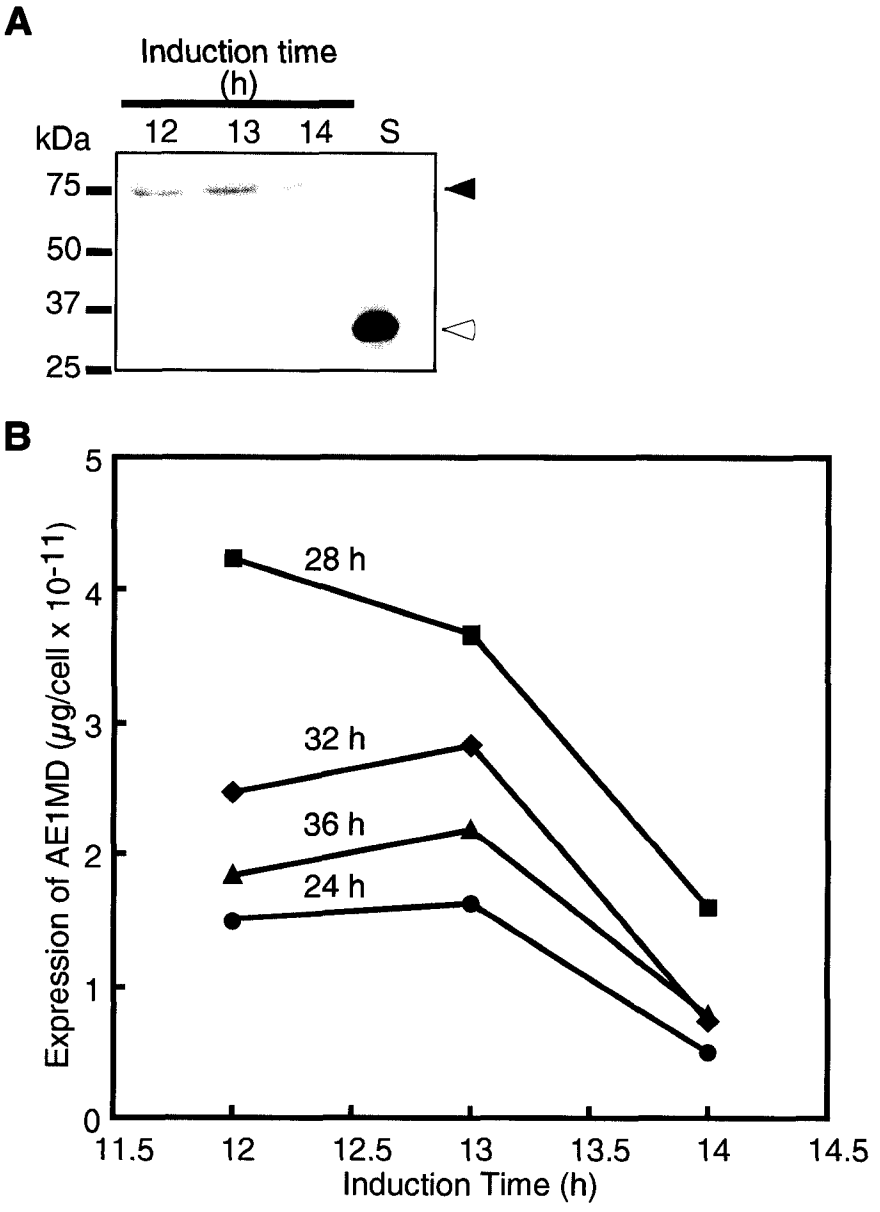

Figure 3.10. GAL-AE1MD expression in an inducible system. W303.1b yeast transformed with pGAL-AE1 were grown in rich medium for 24, 26, 28, or 32 h before protein expression was induced by the addition of galactose to a final concentration of 2%. Samples were harvested at 12, 13, and 14 h post-induction from each culture. Cells were harvested using mechanical disruption with vortexing for 30 s. (A) And equivalent number of cells (5 x 10^7 cells) from each sample induced at 28 h were loaded on to 10% SDS polyacrylamide gel and an immunoblot was performed using anti-AE1 antibody. S is 0.04 μg GST-AE1Ct standard. Closed arrowhead indicates GAL-AE1MD, open arrowhead indicates GST-AE1Ct. (B) Protein expression for each sample was determined using GST-AE1Ct as a standard. Expression of AE1 was calculated as μg/cell by dividing the total μg AE1 by the number of cells (as determined by measuring culture absorbance), and represented graphically.

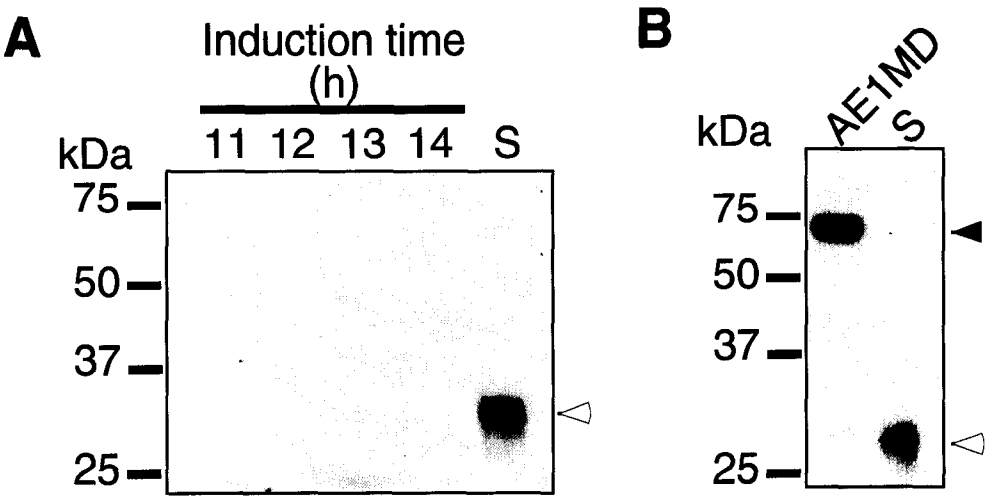

Figure 3.11. Comparison of AE1MD expression in an inducible versus a constitutive system. W303.1b yeast transformed with pGAL-AE1 were grown in rich medium for 28 h before protein expression was induced by the addition of galactose to a final concentration of 2%. Samples were harvested at 11, 12, 13 and 14 h post-induction. Cells were harvested using mechanical disruption with vortexing for 300 s. (A) An equivalent number of cells from each sample was loaded on to 10% SDS polyacrylamide gel and an immunoblot was performed using anti-AE1 antibody IVF12. Lane S is loaded with 0.04 μg GST-AE1Ct standard. Closed arrowhead indicates GAL-AE1MD, open arrowhead indicates GST-AE1Ct. (B) A representative blot of AE1MD expressed in the constitutive system harvested using the same mechanical disruption method as for the inducible system. Lane S is 0.04 μg GST-AE1Ct. Closed arrowhead indicates AE1, open arrowhead indicates GST-AE1Ct. An equivalent number of cells (2.5 x 10^6 cells) were loaded for both constitutive and inducible samples (lanes 11-14 panel A and AE1MD panel B).

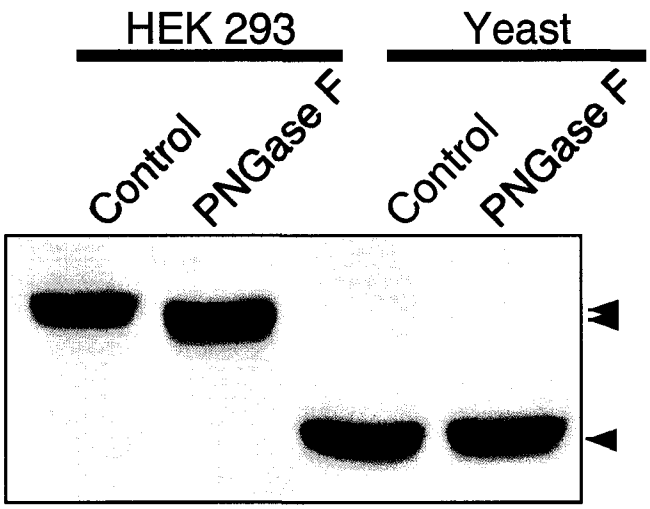

Figure 3.12. Glycosylation state of AE1MD expressed in *S. cerevisiae*. HEK 293 cells transfected with AE1 cDNA were harvested in IPB buffer and incubated without or with PNGase F as indicated. BJ1991 yeast transformed with pHJC4 were solubilized with 0.1% DDM and incubated without or with PNGase F as indicated. Samples were run on 7.5% SDS polyacrylamide gel and transferred to PVDF membrane. AE1 and AE1MD were detected with IVF12 antibody. Double arrowhead indicates Glycosylated (top) and de-glycosylated (bottom) AE1 expressed in HEK 293 cells. Single arrowhead indicates AE1MD expressed in yeast.

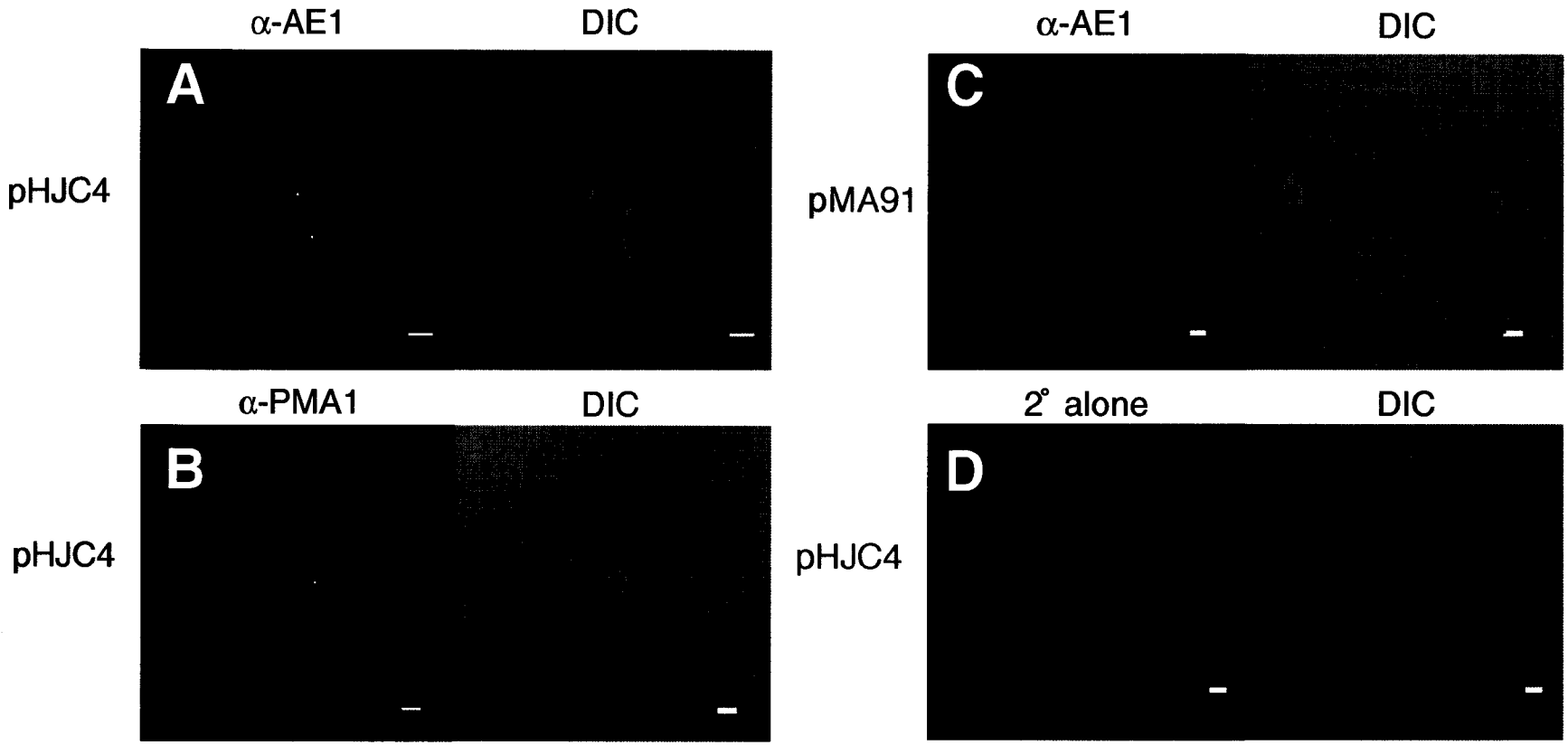

Figure 3.13. Localization of AE1MD expressed in *S. cerevisiae*. BJ1991 yeast transformed with either pHJC4 or pMA91 were grown overnight in YPD medium and spheroplasted. Spheroplasted yeast were fixed with 3.7% formaldehyde on glass slides and incubated with mouse monoclonal anti-AE1 antibody IVF12 or mouse monoclonal anti-PMA1 antibody. A Cy-2-conjugated anti-mouse secondary antibody was used to visualize labelled cells. Images were collected with a Zeiss LSM 510 laser-scanning confocal microscope using a 40x oil immersion objective. (A) pHJC4-transformed cells, probed with anti-AE1 antibody IVF12. (B) pHJC4-transformed cells, probed with anti-PMA1 antibody (C) pMA91-transformed cells, probed with anti-AE1 antibody IVF12. (D) pHJC4-transformed cells, probed with secondary antibody alone. Scale bar = 2 μm, DIC = differential interference contrast.

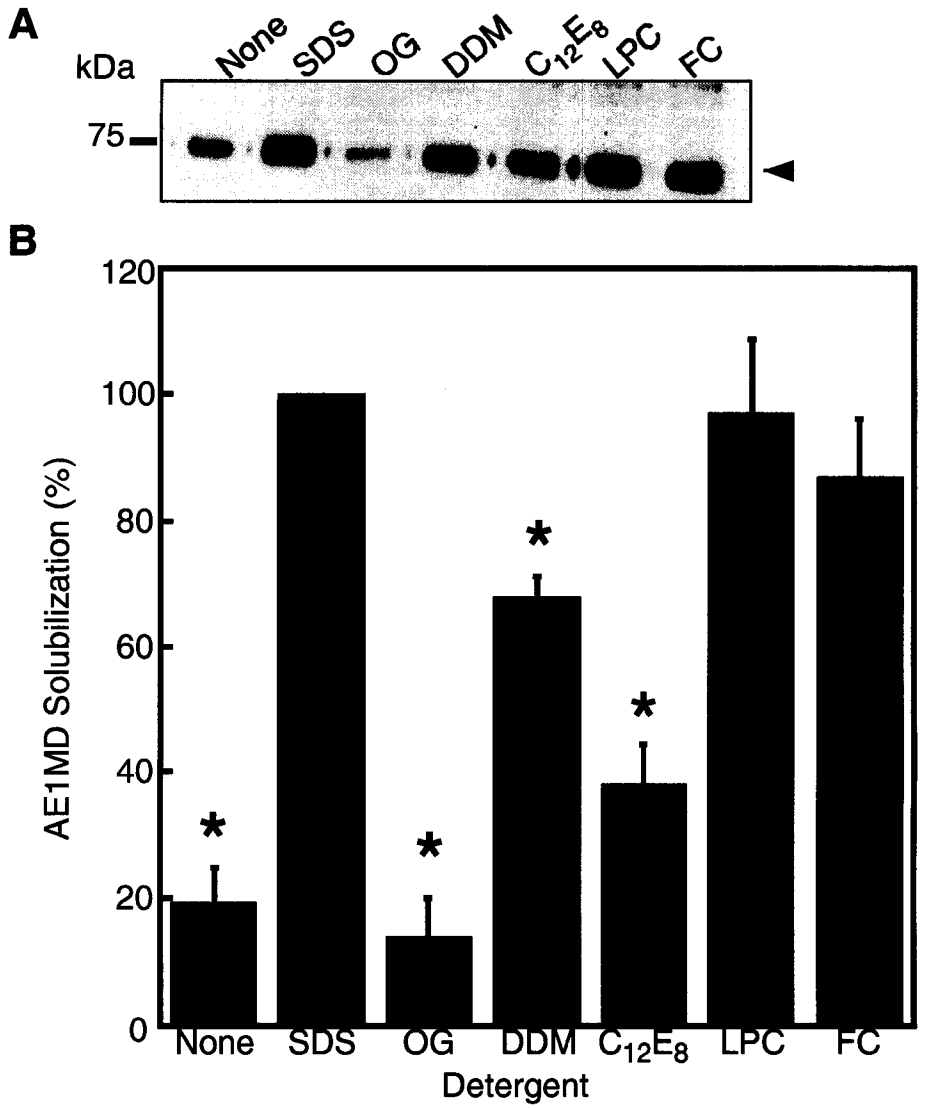

Figure 3.14. Solubilization of AE1MD from isolated yeast membranes. Membranes were isolated from cultures expressing AE1MD. Isolated yeast membranes were incubated with different detergents at 1% on ice for 30 min and centrifuged for 30 min at 100 000 x g. Supernatant from each sample was collected, and electrophoresed on a 10% acrylamide gel. The gel was blotted to PVDF membrane and an immunoblot was performed with anti-AE1 antibody IVF12. (A) Detergents used are as indicated. All detergents used at 1%. Closed arrowhead indicates AE1MD. (B) AE1MD solubilization in 1% SDS was set to 100%. Solubilization of AE1MD in all other samples was calculated as a percentage of solubilization in 1% SDS and represented graphically. Data represent the mean of 3 independent experiments ± S.E. Asterisk, $p<0.05$ versus SDS.

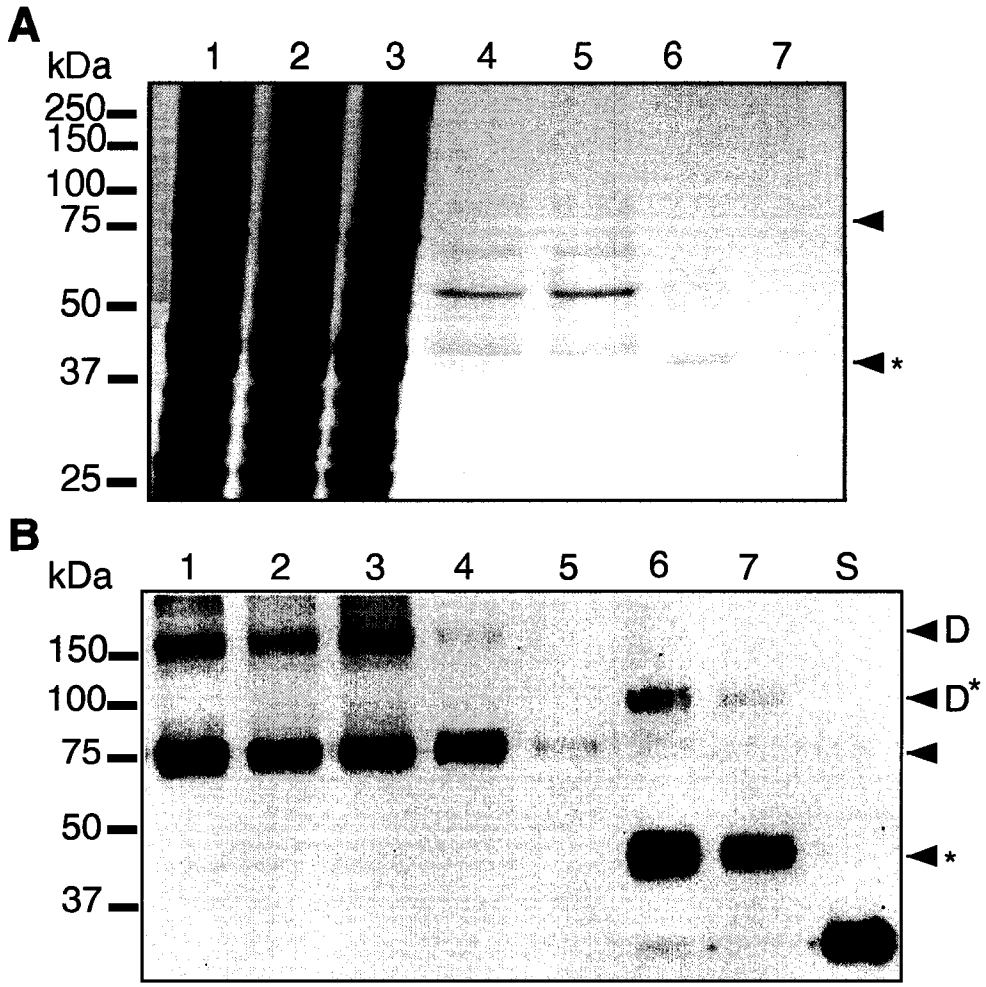

Figure 3.15. Purification of AE1MD expressed in *S. cerevisiae.* AE1MD was purified as in the methods section Samples were run on two 10% SDS polyacrylamide gels. One gel was stained with Coomassie Blue dye and the other was transferred to PVDF membrane and an immunoblot was performed with anti-AE1 antibody IVF12. (A) Coomassie Blue-stained gel. Percentages indicate the fraction of the total volume that was loaded on the gel. 1, isolated membranes (0.02%); 2, solubilized membranes (0.02%); 3, unbound fraction from Co^{2+} resin (0.02%); 4, elution from Co^{2+} resin (4%); 5, unbound fraction from GSH resin (4%); 6, first elution from GSH resin (32%); lane 7, second elution from GSH resin (32%). Closed arrowhead indicates AE1MD, closed arrowhead with star indicates cleaved AE1MD (cAE1MD). (B) Immunoblot. Percentages indicate the fraction of the total volume that was loaded on the gel. 1, isolated membranes (0.005%); 2, solubilized membranes (0.005%); 3, unbound fraction from Co^{2+} resin (0.005%); 4, elution from Co^{2+} resin (0.25%); 5, unbound fraction from GSH resin (0.25%); 6, first elution from GSH resin (2%); lane 7, second elution from GSH resin (2%). Lane 8 is 0.04 μg GST-AE1Ct standard. Closed arrowhead indicates AE1MD, closed arrowhead with star indicates cleaved AE1MD (cAE1MD). D indicates AE1MD dimer, and D with star indicates cAE1MD dimer.

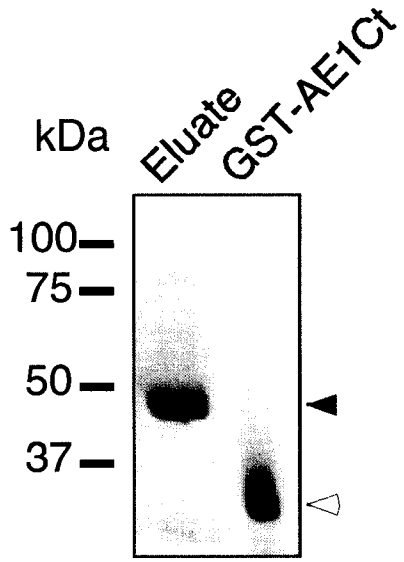

Figure 3.16. PreScission Protease in cAE1MD eluate. Eluate from purification of AE1MD (60 μl), and 0.04 μg GST-AE1Ct were run on 10% SDS-PAGE, transferred to PVDF membrane, and probed with anti-GST antibody. Closed arrowhead indicates PreScission Protease, open arrowhead indicates GST-AE1Ct.

3.2 Discussion

The greatest barrier to the crystallization of membrane proteins is the ability to obtain sufficient amounts of pure protein. The goal of this study was to improve expression and purification over previously described systems (127, 134). In this study, the expression and purification of the human erythrocyte anion exchanger, AE1, in a constitutive yeast expression system has been optimized.

Several issues were explored to optimize expression. We found that expression of AE1MD per ml culture varies between colonies, but by inoculating cultures with multiple colonies instead of single ones, the variability in expression is negated. The addition of glycerol to culture medium did not alter expression of AE1MD per ml culture, but as it may act as a molecular chaperone, glycerol was included in culture media. Expression of AE1MD from pHJC4-transformed cells is higher per ml culture than yAE1 from pJRC16-transformed cells, and therefore the protein expression level is increased over previously described systems (134). Once AE1MD culture conditions were optimized, characteristics of the protein were explored. AE1MD was not glycosylated when expressed in yeast, and exhibited non-plasma membrane localization. AE1MD is 70% solubilized from yeast membranes by DDM, and dimeric AE1MD is detected on immunoblots, indicating that AE1MD is not mis-folded. Preliminary attempts at purification of the membrane domain of AE1 resulted in the cleavage of the GST and 6-His tags from the membrane domain of AE1MD, and purification of 2.2-2.4 μg of cAE1MD, at 30-70% purity.

A novel expression construct for AE1 is described, to express only the membrane domain of AE1 with both a 6-His and a GST purification tag. The expression vector retains several features of the parent plasmid, pJRC16, that was previously used to express AE1 in *S. cerevisiae* (134). AE1MD protein expression is under the strong PGK promoter, and the first 10 codons of yeast PGK are included at the N-terminus of the protein to encourage expression of recombinant AE1MD. Since PGK is highly expressed in yeast, the strong constitutive promoter and first 10 codons should drive high level expression of AE1MD. The first 10 amino acids of PGK are followed by a 6-His tag. A GST-tag and PreScission protease cleavage site was introduced between the 6-His tag and AE1 membrane domain to increase the purification power of the construct. *S. cerevisiae* express proteins that can bind to metal resins, and therefore a second purification tag was required to increase purity. GST, a 26 kDa soluble protein, was chosen as the second tag. Since GST is so large, cleavage of the tags from the membrane domain of AE1 by PreScission Protease can be readily confirmed by a significant shift in electrophoretic mobility, which would not be seen with a small tag such as 6-His alone.

With the inclusion of a protease cleavage site between with GST tag and AE1 membrane domain, the construct essentially has three purification tags instead of the single tag of the parent construct. Three glycine residues were introduced on either side of the PreScission protease site to increase accessibility of the tag, and ensure maximal cleavage. The ability to cleave the affinity tags from the protein ensures purification of homogeneous AE1MD alone. Purification of an un-tagged protein is preferable to purification of a protein with

tags, since the ultimate goal of AE1 purification is x-ray crystallization, and higher quality crystals may be generated with untagged protein.

The region of AE1 included in the expression construct was chosen carefully. The N-terminal cytoplasmic domain of AE1 is proposed to be flexible, separated from the membrane domain by a hinge region (97). Since heterogeneity and flexibility can inhibit crystal formation, the AE1MD construct includes only residues 388-911, and not the flexible N-terminus. Also, the crystal structure of the N-terminal cytoplasmic domain has already been determined (115). A structure of AE1MD from pHJC4 would begin where the cytoplasmic domain structure left off. Also, there is an endogenous proteolytic cleavage site in the AE1 N-terminus at residue 360, suggesting a natural division of domains (166). The membrane domain of AE1 alone is required for transport function, and deletion of the N-terminus does not decrease AE1 transport activity. The C-terminus of AE1 (residues 871-911) was retained in the construct, since the C-terminus is required for plasma membrane processing of the transporter (101), and therefore may be required for proper folding and activity of the protein. Although removal of the N-terminal cytoplasmic domain may help reduce flexibility of the protein and aid in crystal formation, the low-resolution 2D structure of AE1 suggests flexibility in the membrane domain as well. For crystallization trials, an inhibitor such as DIDS that can lock AE1 into one conformation may be required to ensure high quality crystal formation.

In the absence of a protein standard, it can be difficult to estimate a protein expression level until final purification is achieved, and a sufficient amount of material can be seen on a Coomassie Blue-stained gel. In order to quantify AE1MD expression from yeast cultures, a protein standard recognized

by a common antibody was generated. The standard is a GST-fusion protein of the C-terminus of AE1, GST-AE1Ct. The monoclonal anti-AE1 antibody, IVF12, recognizes the C-terminal region of AE1. Since the proteins AE1MD and GST-AE1Ct both include the C-terminal region of AE1, they are both detected by IVF12. Quantified GST-AE1Ct was thus used as a standard for the quantification of expressed and purified AE1MD. The GST-AE1Ct standard allowed expression to be optimized efficiently at the earliest stages of protein expression, and allowed for consistent and quantitative analysis of each membrane preparation and purification trial.

The expression level of AE1MD in a constitutive expression system is higher than the level in an inducible system, found in both this study, and compared with previously reported results for yAE1 and B3mem (Table 3.1) (127, 134). In the inducible system, GAL-AE1MD expression is under the glucose-repressed galactose-inducible *GAL10-CYC1* promoter. Protein expression is delayed until the end of growth phase to favour high copy numbers and higher protein expression. This system can be especially useful in cases where the over-expressed protein is toxic to the cell. This is not the case with AE1, as the protein can be maintained in a constitutive expression system without apparent deleterious effects on the yeast. B3mem was reported to be expressed to 0.13 x 10^{-8} μg/cell in the inducible system (127). Tanner's group reported the expression level of B3mem in pmol/A_{600}, and the molecular weight of their expressed protein is 41.7 kDa (127). Expression was determined using the following calculation:

μg B3mem/cell = (pmol/A_{600}) x (41.7 μg AE1/1 nmol) x (1 nmole/1 000 pmol) x (A_{600} of 1/1 x 10^7 cells/ml).

Here, GAL-AE1MD in the inducible system was expressed at 0.0042 x 10^{-8} μg/cell, as opposed to 5 x 10^{-8} μg/cell for AE1MD in the constitutive system (Table 3.1). AE1MD expression was seen between 0.5-0.8 mg/l yeast culture in the constitutive system, which is in good agreement with previous reported results (134). AE1MD expression is therefore higher in the constitutive system. Although the inducible system has been successful for purification of other membrane proteins, such as SERCA1a Ca^{+}-ATPase, in the case of AE1 it appears that an inducible system will not lead to high-level expression and purification of the protein.

There is no clear reason why expression of GAL-AE1MD in the inducible system is 30 times lower than described for B3mem. There are, however, several differences between the two studies. We expressed residues 388-911 of AE1, while Tanner's group expressed residues 361-911. The truncation of 27 residues is not likely to cause such a large decrease in protein expression. We were careful to maintain the Kozak consensus sequence, required for efficient translation, spanning the start codon in the pGAL-AE1MD construct (167). The difference may be explained by differences in the vectors and strains used. Tanner's group used the vector pYeDP1/8-10 for the expression construct, while we used pYeDP60. pYeDP1/8-10 uses the *ADH1* terminator, as opposed to the *PGK* terminator of pYeDP60. Also, pYeDP1/8-10 has only a *URA3* selective marker, while pYeDP60 has both a *URA3* and a *ADE2* selective marker. These subtle differences don't clearly point to a reason for a decrease in expression. Possibly the most significant difference was Tanner's use of a protease deficient yeast strain, FKY282, while we used the strain W303.1b, which is not protease deficient. A possible reason for a higher expression level achieved by Tanner's

group may be a decrease in protein degradation with the protease deficient strain.

A yeast expression system for AE1 has several advantages over other expression systems. The protein level expressed in a mammalian cell system is much lower than that of the constitutive yeast system. The estimated protein expression level in HEK 293 cells is only 6.8 $\mu g/100$ cm^2 tissue culture dish surface (134) so that over 1 m^2 of culture dish surface would be required to reach the level of expression achieved with 1 l of yeast culture. Use of HEK cells for expression and purification of AE1 is thus impractical. The yeast *S. cerevisiae* offers a low-cost, large-scale option for over-expression of heterologous proteins. Also, a eukaryotic system provides a membrane of suitable thickness for a mammalian membrane protein (30 Å) (132) as opposed to bacterial expression systems where the membrane is 25 Å thick (133). A yeast expression system allows recombinant proteins to be processed through the endoplasmic reticulum, which is essential for correct protein folding and membrane insertion. While AE1 is abundant in erythrocyte membranes, the heterogeneity of the protein due to posttranslational modifications may impede crystallization that will lead to a high-resolution structure.

Although erythrocyte AE1 has been crystallized previously, only low-resolution structures were described. These studies expressed the need for higher quality crystals for a high resolution structure (117, 118). By decreasing protein heterogeneity in the recombinant yeast expression system, perhaps higher quality crystallization can be achieved. An additional advantage of expression in a yeast system as opposed to purification from the erythrocyte is that the power of molecular biology allows mutant proteins to be examined in the yeast system,

and structural changes between wild type and mutant AE1 can be assessed. There is no endogenous source of mutant protein.

Expression of AE1MD was optimized in the constitutive yeast expression system by exploring media additives and media composition. Maximal expression was found with yeast growth in non-selective YPD media following initial growth in selective media (Fig. 3.8), indicating that constant selective pressure is not required for maintenance of the expression plasmid. Growth in rich media is more rapid than growth in selective media. In rich media, the doubling time of transformed BJ1191 cells was 1.5 h, while in selective media the doubling time was greater than 6 h. Rich media therefore not only offers an increase in protein expression, but also a decrease in the amount of time required to express the protein.

Disrupting cells with an Emulsiflex high pressure homogenizer allowed for rapid and efficient cell lysis, as little AE1MD was associated with unbroken cells and cell debris following lysis. Disruption with glass beads is an adequate method to screen small culture samples, but on a large scale cell lysates become warm, and cell lysis can be lower. With a high-pressure disruption system such as the EmulsiFlex, cell lysates are kept chilled during lysis, which can prevent protein degradation, and high-pressure ensures maximal cell disruption. The report of yAE1 expression from pJRC16 identified heterogeneity between individual colonies (134). The use of mechanical disruption as a screening method for individual colonies allowed us to determine that variability of expression between small colonies is not that great, and can be overcome by inoculating media with multiple colonies.

Glycerol added to culture medium has previously been shown to act as a molecular chaperone (163), and can potentially assist in membrane protein folding and stabilization. There is also evidence that glycerol has no effect on protein folding when included as a media additive (128). Since the addition of glycerol did not significantly decrease the expression of AE1MD, and since it may act as molecular chaperone, it was included as a media additive.

While the functional activity of AE1MD has not been tested, other factors indicate that AE1MD is correctly folded. The presence of dimeric AE1MD and dimeric cAE1MD during purification indicates that AE1MD and cAE1MD may exist primarily in dimeric form in the absence of a denaturant such as SDS. Erythrocyte AE1 is dimeric, and the membrane domain alone is capable of forming dimers (104). yAE1 expressed in yeast also appears to have a dimeric structure (134). Retention of the ability to form dimers indicates that AE1MD is correctly folded throughout the purification process, and thus likely active. Additionally, solubilization of AE1MD in the non-ionic detergent DDM indicates that the expressed protein is not aggregated, and therefore likely properly folded. yAE1 expressed from pJRC16 was active and properly folded, and was also solubilized to a high level by DDM. These two lines of evidence together suggest that AE1MD is not grossly mis-folded.

The subcellular localization of AE1MD was determined to be primarily in intracellular membranes. An antibody against the yeast plasma membrane H^+-ATPase, PMA1, stained spheroplasted yeast with a strong pericellular pattern, consistent with plasma membrane localization. When stained with IVF12, a monoclonal antibody against AE1, the pattern was distinctly different. Since the staining of AE1MD differed from that of PMA1, non-plasma membrane

localization is suggested. Since AE1MD can be isolated from membranes and not the cytosolic fraction of transformed yeast, the staining must be indicative of localization in intracellular membranes. Indeed, the staining of AE1MD is suggestive of vaculolar localization. Since yeast proteases are found in the vacuole, overexpressed proteins may be targeted to the vacuole for degradation. The use of the protease-deficient yeast strain BJ1991 may prevent degradation of proteins targeted to the vacuole.

Some AE1MD displays plasma membrane localization. While native AE1 is expressed at the plasma membrane of erythrocytes, the intracellular localization of AE1MD does not inhibit purification. AE1MD is found only in the membrane fraction of transformed yeast, which includes both plasma and intracellular membranes (data not shown). Intracellular membrane localization for yAE1 expressed in yeast has been previously seen, and that yAE1 was found to be active in transport assays and therefore correctly folded (134). AE1 is not endogenously expressed in yeast, and overexpression of AE1MD may overwhelm cellular protein expression and targeting machinery. It is therefore not surprising that over-production of the protein would result in retention of the protein in intracellular membranes and targeting to the vacuole. Only 10% or less of cells exhibited no AE1 staining, which may have been due to incomplete spheroplasting, which prevents antibodies from binding to proteins on the plasma membrane due to the presence of the cell wall. SERCA1a expressed heterologously in *S. cerevisiae* localized to the plasma membrane, mitochondria, ER, and secretory vesicles, as determined by membrane fractionation. Importantly, the proportion of SERCA1a that was most active was found in the ER and secretory vesicles (130).

Yeast-expressed AE1MD was not glycosylated. Erythrocyte AE1 is heterogeneously N-glycosylated at Asn^{642} in the fourth extracellular loop (168-170) with up to 10 kDa of sugar per AE1 molecule (135). AE1 expressed in HEK 293 cells is also glycosylated (113). Glycosylation introduces heterogeneity, and deglycosylation of erythrocyte AE1 has previously been reported to be essential for formation of 2D and 3D crystals of the membrane domain (117, 118). Neither recombinantly expressed yeast AE1 homologue (YNL275w), nor recombinantly expressed yAE1 are glycosylated when expressed in yeast (44, 134). The yeast expression system is preferable over purification of protein from erythrocytes, where glycosylation and protein degradation result in protein heterogeneity or from expression in HEK 293 cells, where the protein is heterogeneously glycosylated.

Conditions used to solubilize AE1MD were consistent with previously reported results of AE1 solubilized from yeast membranes (134). While AE1 can be almost completely solubilized from erythrocytes with $C_{12}E_8$ (144), AE1 expressed in yeast from pJRC16 is only 38% solubilized from yeast membranes (134), as is AE1MD (Fig. 3.13). LPC and Fos-choline were able to almost completely solubilize AE1MD from yeast membranes (Fig. 3.13) and LPC has previously been used to purify AE1 from yeast membranes (134). Although it was able to solubilize AE1MD to a lesser extent than LPC or Fos-choline, DDM was chosen as the detergent for protein purification in this study. DDM produces the best diffracting 3D crystals of AE1 membrane domain purified from erythrocytes when compared to a battery of detergents and maintains AE1 in a monodisperse state (117, 143). DDM is also a mild detergent, and other mammalian membrane proteins have been solubilized from yeast membrane for

crystallization using DDM (125, 129). Proteins purified in mild sugar detergents such as DDM are more likely to be active. In fact, the Ca^{2+}-ATPase SERCA1a expressed in yeast was more active when purified using DDM than when purified with LPC (128).

Preliminary purification of AE1MD was achieved using both the 6-His tag and the GST-tag for affinity purification, followed by PreScission Protease cleavage to remove the tags. While purification still needs to be optimized, the preliminary results are encouraging. The first step was binding of solubilized AE1MD to a Co^{2+} resin. Only a small fraction of the protein bound to the metal resin, which indicates the need to optimize resin binding. Another possibility is that AE1MD is misfolded and can't bind to the resin, although as discussed above, AE1MD is probably folded correctly. In one purification trial, the unbound fraction from the metal resin was applied to a second metal resin, and AE1MD binding occurred. This suggests that the protein is folded correctly, but there was not enough resin to bind all of the protein. Saturation of the resin does increase the specificity of protein binding, since non-specific binding is less likely to occur, but the majority of the protein incubated with the resin should be bound to improve overall protein yield.

Of the protein bound to the metal resin, only a small fraction eluted with 250 mM imidazole (8%). Elution of AE1MD from metal resin, thus, remains a problem. Possible solutions to increase elution include increasing the imidazole concentration in elution buffer, adding EDTA to the elution buffer, and eluting with low pH. Increasing the imidazole concentration increases the number of moieties competing for resin binding. Adding EDTA results in chelation of the

cobalt ions, thereby releasing cobalt-bound AE1MD from the resin. Eluting with low pH decreases the interaction between His-residues and the cobalt ions.

Efficient binding to the GSH resin was seen as well as a high level of cleavage from the resin, although elution of the cleaved protein from the resin remains a problem. Roughly 25% of AE1MD left on the resin is not cleaved, and 75% of AE1MD left on the resin is cAE1MD. PreScission Protease contains a GST moiety, which binds to GSH resin. In order to achieve complete cleavage of a PreScission Protease tag, free PreScission Protease must be available. If an excess of resin is present, PreScission Protease will bind to the resin rather than be available to cleave substrate. The choice to cleave the tags from AE1MD off of GSH resin may not be ideal, since the protease will bind the resin, reducing its efficacy. In preliminary purification trials, PreScission Protease co-eluted with cAE1MD. PreScission Protease was identified using in-gel digestion and mass spectrometry, and immunoblotting with an anti-GST antibody. One possible solution for this contamination is to pass the eluate over glutathione resin a second time, to bind any free PreScission Protease.

A possible reason for inefficient elution from either the GSH resin or the metal resin could be protein aggregation. When AE1MD is solubilized, 1% DDM was sufficient to solubilize 70% of the protein. Once on the resin, AE1MD becomes concentrated, and without sufficient detergent, AE1MD may aggregate. In this study, 0.1% DDM was used in each resin wash buffer, and 1% DDM was used in each elution. Perhaps 1% DDM is required in the wash buffers to maintain AE1MD in a monodisperse state, and perhaps a higher concentration of DDM is needed during elution from both resins (143).

PreScission protease has a molecular weight of 46 kDa, and unfortunately runs at approximately the same level on polyacrylamide gels as cleaved AE1MD (cAE1MD). It would therefore be difficult to distinguish cAE1MD from PreScission Protease on a Coomassie Blue-stained gel. The amount of protease present in the elution sample is small (only 64 ng/80 μl loaded) and therefore not enough to be detected strongly on a Coomassie Blue-stained poly-acrylamide gel (Fig. 3.16). The minimum detection limit for Coomassie-stained gel is roughly 0.1 μg, and less than 0.1 μg of PreScission Protease would have been loaded onto the Coomassie-stained gel. In contrast, the amount of AE1 loaded is roughly 0.6 μg, which would present a much stronger band (Fig. 3.15). Since only one band is clearly visible on the Coomassie-stained gel, the likelihood is that the band can be attributed to cleaved AE1MD. In-gel digestion and mass spectrometry identified the presence of PreScission Protease in the eluate and AE1 was not identified. Detergent, however, was not included in the buffers used for digestion and mass spectrometry, and AE1MD, being a hydrophobic membrane protein, may have aggregated and come out of solution. AE1MD likely constitutes the majority of the eluted band (Fig. 3.15, A, lane 6), but was not detected due to the conditions used for in-gel digestion. The detection of AE1MD on the immunoblot (Fig. 3.15, B, lane 6) and quantification using GST-AE1Ct standard support this. Because of this, the purity of cAE1MD can still be assessed. The maximal protein purity achieved with the expression construct pHJC4 was ~68% (Fig. 3.14) as determined by densitometric analysis of the Coomassie-stained poly-acrylamide gel. This is an improvement over previously published purification of AE1 from yeast membranes, which was 35% (134). The purity level reported in Table 3.2, 29%, is one example of a purification trial, and

is similar to previously reported levels of purification for AE1 expressed in yeast (134).

While this purification is not optimal and leads to a purification of only a small fraction of the total protein, is serves as a proof of principle that AE1MD can be purified with these affinity tags and protease cleavage. Optimization of the purification will explore the advantages and disadvantages of using a single tag for affinity purification followed by PreScission protease cleavage, as well as resin binding optimization and all purification conditions (time, buffer composition, amount of protease). To carry out crystallization trials with a robot, 480 conditions can be tested at 10 μg pure protein per well. That means that 5 mg pure protein is necessary for one round of crystallization trials. With the currently described conditions, just over 0.3 μg of cAE1MD can be purified from one litre of yeast culture. We routinely isolate membranes from 18 l of culture, at a level of 0.5 mg/l crude AE1MD. At this expression level, assuming 25% yield following purification, 20 mg of crude AE1MD needs to be expressed. Only 40 l of culture would therefore be required, which would be achieved with 2.5 of our routine membrane isolations. If resin binding and elution were improved, the current purification level could be increased substantially. While there is much more progress to be made, initial strides have been taken here to establish a protocol for high-level purification of the membrane domain of AE1.

3.3 Conclusion

In conclusion, the dual tag protein expression system described in this paper allows for purification of the membrane domain of human AE1 when expressed in *S. cerevisiae*. With efficient protein purification will come the ability to crystallize the protein, and gain further insight into the structural mechanism of the protein and other anion exchange proteins.

Chapter 4

Summary and Future Directions

4.1 Summary

The expression of the human erythrocyte anion exchanger AE1 in previous yeast systems (127, 134) has been modified and improved in this study. AE1MD, the membrane domain construct of AE1 includes a 6-His and a GST purification tag, separated from the membrane domain of AE1 by a PreScission Protease site. This multi-tag affinity chromatography purification system results in the ability to purify the membrane domain of AE1 alone. Under a constitutive promoter, in a protease-deficient yeast strain, the expression of AE1MD has been optimized to 0.5-0.8 mg/l culture medium. The expression of AE1MD in a constitutive system was 10^4 times greater than expression in a galactose-inducible system. Expression of AE1MD is increased by growing transformed yeast in rich media, following initial selection in selective media. While glycerol may or may not act as a molecular chaperone its inclusion in the culture media did not decrease the expression of AE1MD significantly, and therefore the potential benefits of its inclusion outweigh the costs.

Many characteristics of AE1MD expressed in yeast were examined during this study. Two lines of evidence indicate that AE1MD may be correctly folded. The persistence of dimeric AE1MD and dimeric cAE1MD, even in the presence of the strong denaturant SDS indicates that AE1MD is capable of forming dimers, as AE1 does in the native erythrocyte membrane. The ability to dimerize may indicate correct protein folding, and potentially that the protein is active. AE1MD was solubilized to 70% by dodecyl maltoside, a detergent that has previously been used to form the 3D crystals with the highest resolution of AE1 from erythrocytes. Solubilization of AE1MD in non-ionic detergents to a high

level (70%) suggests that AE1MD does not form insoluble aggregates when expressed in yeast. Solubilization in various detergents is consistent with previously reported values for AE1 expressed in yeast. Similarly to yAE1 previously expressed in yeast, AE1MD is found primarily in yeast intracellular membranes. Non-plasma membrane localization does not inhibit protein isolation or purification. AE1MD is not glycosylated in yeast, and the lack of post-translational modification may aid in protein crystal formation by reducing protein heterogeneity.

Purification of AE1MD was similar to previously reported values for AE1 expressed in yeast, although the total yield of protein was low. Although AE1MD was eluted along with PreScission Protease, this purification system is a proof-of-principle that a dual tag affinity purification combined with protease cleavage allows for purification of AE1MD heterologously expressed in yeast.

4.2 Future Directions

This study confirms that the membrane domain of AE1 can be expressed in yeast. Two lines of evidence indicate that AE1MD is folded correctly, and behaves similarly to previously expressed active AE1 in yeast. However, this study has not address the functional activity of AE1MD, nor confirmed that the protein is correctly folded. Several approaches can be taken to assess these features. Resin-immobilized inhibitor has been used to assess correct folding of anion exchangers. SITS-Affi gel is a resin with a SITS moiety covalently attached. SITS is a disulfonic stilbene inhibitor of anion exchangers that binds to the membrane domain of AE1 (171). Binding of purified AE1MD to SITS-Affi gel would suggest appropriate folding of the inhibitor binding site. Also, correct

folding will result in the formation of AE1MD dimers. The presence of dimers can be determined by size exclusion chromatography. If the protein is correctly folded, it should also be capable of anion exchange activity. Exchange activity can be examined in a variety of ways. Previous studies have assessed activity using $^{36}Cl^-$ influx assays that are inhibitable by DIDS, and efflux of $[^{35}S]SO_4^{2-}$ in exchange for SO_4^{2-} by AE1 in reconstituted liposomes (134).

Flexibility of proteins can hinder the formation of well-ordered crystals. Membrane transporters in particular can have a problem of flexibility due to the dynamic nature of transport. Since AE1 has a very high transport rate, the protein is likely very flexible and undergoes rapid conformational changes during transport. In order to generate well-ordered crystals, it may be necessary to lock AE1 in a particular conformation. This can be achieved through the use of inhibitors. The covalent inhibitor DIDS, and the non-covalent inhibitor niflumic acid both lock AE1 in an outward facing conformation and prevent transport activity (172). An alternative to transport inhibition is to express functionally inactive AE1 mutants that are still folded correctly, but are transport incompetent.

The yield of protein using this purification system is very low. For crystallization experiments, close to 5 mg of purified protein are required, and the level achieved in this study is far below that. One option is to simply scale up purification. If the current purification scheme were optimized to even 25% yield from crude isolated membrane, only 40 l of culture would be required. We routinely isolate membranes from 18 l of culture. The optimal amount of resin required to bind solubilized AE1MD can be determined, thereby ensuring minimal protein loss during purification. Affinity purification using only the

GST-tag and GSH resin alone may be sufficient for protein purification followed by protease cleavage of the tags. Since each purification step results in a loss of material, removing the initial step of binding to metal resin could help minimize protein loss. Alternately, the order of affinity purification steps could be reversed, with binding to GSH resin first, then binding to Co^{2+} resin, and cleavage by PreScission Protease. The protease could then be removed from the elution fraction by passing the eluate over an additional GSH resin. This current study uses batch purification, and next steps would be to purify the protein using columns to concentrate the final eluted protein and obtain more efficient washing. The long-term goal is to obtain a high-resolution crystal structure of AE1. By carefully optimizing this purification scheme, eventually sufficient amounts of pure protein will be generated to begin crystallization trials.

The *S. cerevisiae* homologue of AE1, YNL275w, has been overexpressed and characterized (44). YNL275w, which is 26% identical and 47% similar to AE1 in amino acid sequence, binds the anion exchanger inhibitor DIDS, indicating a similar structure to AE1 in the membrane domain (44). It is not glycosylated, and potential substrates include HCO_3^-, I^-, Br^-, NO_3^-, and Cl^- (44). Since the yeast homologue shares some similarities with AE1, it may be valuable to investigate the structure of YNL275w. It has previously been over-expressed in a yeast system, and could be used for crystallographic studies. Comparing the functional and structural profiles of AE1 and the yeast homologue would provide insight into transport capabilities and function.

Human erythrocytes lacking glycophorin A (M^kM^k) cells, exhibit a 40% decrease in AE1 transport activity, a difference that could be attributed to slight structural differences that occur during folding of AE1 in the absence of

glycophorin A (87). There is evidence that glycophorin A and AE1 interact during biosynthesis, and glycophorin A could potentially act as a chaperone molecule during the folding and processing of AE1 to the plasma membrane. In the absence of glycophorin A, the structure of AE1 may be slightly different. It would be interesting to co-express glycophorin A and AE1 in crystallographic studies to identify structural differences in AE1 when expressed in the presence and absence of glycophorin A. The differences could help clarify the role of glycophorin A in the processing of AE1. Glycophorin A can be co-expressed with AE1MD in yeast using a vector with different selective markers.

Once pure AE1 is obtained, crystallization of the protein is not the only avenue to be explored to gain structural information. Circular dichroism spectroscopy is a method of light absorption spectroscopy that is used to determine the secondary structure of proteins in solution. Circular dichroism can give an estimation of the percentage of AE1 that is α-helical, β-sheet, or random coil in structure. Cryo-electron microscopy, which uses electron diffraction of 2D protein arrays at extremely low temperature to determine structure, can also be used to help determine helix packing of the protein. Cryo-EM is often a faster technique than x-ray crystallography. Cryo-EM has previously been used to determine a 20 Å structure of the AE1 membrane domain (118), and information garnered from an EM structure, and circular dichroism spectroscopy, along with other biochemical data, can complement structural data from x-ray crystallographic studies to generate a detailed, high-resolution structure of AE1.

Chapter 5

References

1. http://www.hugo-international.org, *The Human Genome Organization.* 2004.
2. Kopito, R.R., *Molecular biology of the anion exchanger gene family.* Int. Rev. Cytol., 1990. **123**: 177-199.
3. Alper, S.L., *The Band 3-related anion exchanger family.* Annu. Rev. Physiol., 1991. **53**: 549-564.
4. Richards, S.M., Jaconi, M.E., Vassort, G., and Puceat, M., *A spliced variant of AE1 gene encodes a truncated form of Band 3 in heart: the predominant anion exchanger in ventricular myocytes.* J Cell Sci, 1999. **112**: 1519-1528.
5. Alvarez, B.V., Fujinaga, J., and Casey, J.R., *Molecular Basis for angiotensin II-induced increase of chloride/bicarbonate exchange in the myocardium.* Circ. Research, 2001. **89**: 1246-1253.
6. Fairbanks, G., T.L. Steck, and Wallach., D.F.H., *Electrophoretic analysis of the major polypeptides of the human erythrocyte membrane.* Biochemistry, 1971. **10**: 2606-2617.
7. Steck, T.L., *The band 3 protein of the human red cell membrane: a review.* J Supramol Struct, 1978. **8**: 311-324.
8. Sterling, D. and Casey, J.R., *Bicarbonate Transport Proteins.* Biochem. Cell Biol., 2002. **80**: 483-497.
9. Brown, D., Zhu, X.L., and Sly, W.S., *Localization of membrane-associated carbonic anhydrase type IV in kidney epithelial cells.* Proc Natl Acad Sci U S A, 1990. **87**(19): 7457-7461.
10. Kopito, R.R. and Lodish, H.F., *Structure of the murine anion exchange protein.* J. Cell. Biochem., 1985. **29**: 1-17.
11. Brahm, J., *The red cell anion-transport system: kinetics and physiological implications.* Soc Gen Physiol Ser, 1988. **43**: 141-150.
12. Bennett, V. and Stenbuck, P.J., *Association between ankyrin and the cytoplasmic domain of Band 3 isolated from the human erythrocyte membrane.* J. Biol. Chem., 1980. **255**: 6424-6432.
13. Rybicki, A.C., Qui, J.J.H., Musto, S., Rosen, N.L., Nagel, R.L., and Schwartz, R.S., *Human erythrocyte protein 4.2 deficiency associates with hemolytic anemia and a homozygous^{40} glutamic acid∅ lysine substitution in the cytoplasmic domain of band 3 (band 3^{montefiore}).* Blood, 1993. **181**: 2155-2165.
14. Pasternack, G.R., Anderson, R.A., Leto, T.L., and Marchesi, V.T., *Interactions between protein 4.1 and Band 3 an alternative binding site for an element of the membrane cytoskeleton.* J. Biol. Chem., 1985. **260**(6): 3676-3683.
15. Rogalski, A.A., Steck, T.L., and Waseem, A., *Association of glyceraldehyde-3-phosphate dehydrogenase with the plasma membrane of the intact human red blood cell.* J. Biol. Chem., 1989. **264**(11): 6438-6446.
16. Jenkins, J.D., Madden, D.P., and Steck, T.L., *Association of phosphofructokinase and aldolase with the membrane of the intact erythrocyte.* J. Biol. Chem., 1984. **259**(15): 9374-9378.
17. Walder, J.A., Chatterjee, R., Steck, T.L., Low, P.S., Musso, G.F., Kaiser, E.T., Rogers, P.H., and Arnone, A., *The interaction of hemoglobin with the cytoplasmic domain of Band 3 of the human erythrocyte membrane.* J. Biol. Chem., 1984. **259**: 10238-10246.

18. Harrison, M.L., Isaacson, C.C., Burg, D.L., Geahlen, R.L., and Low, P.S., *Phosphorylation of human erythrocyte band 3 by endogenous P72^{syk}*. J. Biol. Chem., 1994. **269**: 955-959.
19. Low, P.S., Willardson, B.M., Mohandas, N., Rossi, M., and Shohet, S., *Contribution of the band 3-ankyrin interaction to erythrocyte membrane mechanical stability*. Blood, 1991. **77**(7): 1581-1586.
20. Low, P.S., Rathinavelu, P., and Harrison, M.L., *Regulation of glycolysis via reversible enzyme binding to the membrane protein, band 3*. J. Biol. Chem., 1993. **268**(20): 14627-14631.
21. Kay, M.M.B., Bosman, G.J.C.G.M., and Lawrence, C., *Functional topography of Band 3: specific structural alteration linked to functional aberrations in human erythrocytes*. Proc. Natl. Acad. Sci., 1988. **85**: 492-496.
22. Low, P.S., Waugh, S.M., and Drenckhahn, D., *The role of hemoglobin denaturation and Band 3 clustering in red cell aging*. Science, 1985. **227**: 531-533.
23. Kay, M.M.B., *Localization of senescent cell antigen on Band 3*. Proc. Natl. Acad. Sci., 1984. **81**: 5753-5757.
24. Turrini, F., Arese, P., Yuan, J., and Low, P.S., *Clustering of integral membrane proteins of the human erythrocyte membrane stimulates autologous IgG binding, complement deposition, and phagocytosis*. J. Biol. Chem., 1991. **266**(35): 23611-23617.
25. Niv, Y. and Fraser, G.M., *The alkaline tide phenomenon*. J Clin Gastroenterol, 2002. **35**(1): 5-8.
26. Goel, V.K., Li, X., Chen, H., Liu, S.C., Chishti, A.H., and Oh, S.S., *Band 3 is a host receptor binding merozoite surface protein 1 during the Plasmodium falciparum invasion of erythrocytes*. Proc Natl Acad Sci U S A, 2003. **100**(9): 5164-5169.
27. Blumenfeld, O.O., and Patnaik, S.K., *Allelic genes of blood group antigens: a source of human mutations and cSNPs documented in the Blood Group Antigen Gene Mutation Database*. Human Mutation, 2004. **23**: 8-16.
28. Bruce, L.J., Ring, S.M., Anstee, D.J., Reid, M.E., Wilkinson, S., and Tanner, M.J., *Changes in the blood group Wright antigens are associated with a mutation at amino acid 658 in human erythrocyte band 3: a site of interaction between band 3 and glycophorin A under certain conditions*. Blood, 1995. **85**(2): 541-547.
29. Bruce, L.J., Pan, R.J., Cope, D.L., Uchikawa, M., Gunn, R.B., Cherry, R.J., and Tanner, M.J., *Altered structure and anion transport properties of band 3 (AE1, SLC4A1) in human red cells lacking glycophorin A*. J. Biol. Chem., 2004. **279**(4): 2414-2420.
30. Young, M.T., Beckmann, R., Toye, A.M., and Tanner, M.J., *Red-cell glycophorin A-band 3 interactions associated with the movement of band 3 to the cell surface*. Biochem J, 2000. **350**(Pt 1): 53-60.
31. Young, M.T. and Tanner, M.J., *Distinct regions of human glycophorin A enhance human red cell anion exchanger (band 3; AE1) transport function and surface trafficking*. J. Biol. Chem., 2003. **278**(35): 32954-32961.
32. Alpern, R.J., Stone D. K., Rector F. C. Jr., *Renal acidification mechanisms*, in *The Kidney*, B.M. Brenner, and Rector, F. C. Jr., Editor. 1991, Saunders: Philadelphia. 318-379.

33. Abuladze, N., Lee, I., Newman, D., Hwang, J., Boorer, K., Pushkin, A., and Kurtz, I., *Molecular cloning, chromosomal localization, tissue distribution, and functional expression of the human pancreatic sodium bicarbonate cotransporter.* J. Biol. Chem., 1998. **273**(28): 17689-17695.
34. Romero, M.F., Hediger, M.A., Boulpaep, E.L., and Boron, W.F., *Expression cloning and characterization of a renal electrogenic Na^+/HCO_3^- cotransporter.* Nature, 1997. **387**(6631): 409-413.
35. Burnham, C.E., Amlal, H., Wang, Z., Shull, G.E., and Soleimani, M., *Cloning and functional expression of a human kidney $Na^+:HCO_3^-$ cotransporter.* J. Biol. Chem., 1997. **272**(31): 19111-19114.
36. Gross, E. and Kurtz, I., *Structural determinants and significance of regulation of electrogenic Na^+-HCO_3^- cotransporter stoichiometry.* Am J Physiol Renal Physiol, 2002. **283**(5): F876-887.
37. Madsen, K.M., Verlander, J.W., Kim, J., and Tisher, C.C., *Morphological adaptation of the collecting duct to acid-base disturbances.* Kidney Int Suppl, 1991. **33**: S57-63.
38. Schuster, V.L., *Function and regulation of collecting duct intercalated cells.* Annu Rev Physiol, 1993. **55**: 267-288.
39. Tisher, C.C., Madsen, K.M., and Verlander, J.W., *Structural adaptation of the collecting duct to acid-base disturbances.* Contrib Nephrol, 1991. **95**: 168-177.
40. Verlander, J.W., Madsen, K.M., Cannon, J.K., and Tisher, C.C., *Activation of acid-secreting intercalated cells in rabbit collecting duct with ammonium chloride loading.* Am J Physiol, 1994. **266**(4 Pt 2): F633-645.
41. Verlander, J.W., Madsen, K.M., and Tisher, C.C., *Structural and functional features of proton and bicarbonate transport in the rat collecting duct.* Semin Nephrol, 1991. **11**(4): 465-477.
42. Verlander, J.W., Madsen, K.M., Low, P.S., Allen, D.P., and Tisher, C.C., *Immunocytochemical localization of band 3 protein in the rat collecting duct.* Am J Physiol, 1988. **255**(1 Pt 2): F115-125.
43. O'Callaghan, C., and Brenner, B. M., *The Kidney at a Glance.* 2000, Malden: Blackwell Science.
44. Zhao, R. and Reithmeier, R.A., *Expression and characterization of the anion transporter homologue YNL275w in Saccharomyces cerevisiae.* Am J Physiol Cell Physiol, 2001. **281**(1): C33-45.
45. Takano, J., Noguchi, K., Yasumori, M., Kobayashi, M., Gajdos, Z., Miwa, K., Hayashi, H., Yoneyama, T., and Fujiwara, T., *Arabidopsis boron transporter for xylem loading.* Nature, 2002. **420**(6913): 337-340.
46. http://www.ncbi.nlm.nih.gov/entrez/query.fcgi?db=OMIM. 2007.
47. Peters, L.L., Shivdasani, R.A., Liu, S.C., Hanspal, M., John, K.M., Gonzalez, J.M., Brugnara, C., Gwynn, B., Mohandas, N., Alper, S.L., Orkin, S.H., and Lux, S.E., *Anion exchanger 1 (band 3) is required to prevent erythrocyte membrane surface loss but not to form the membrane skeleton.* Cell, 1996. **86**(6): 917-927.
48. Southgate, C.D., Chishti, A.H., Mitchell, B., Yi, S.J., and Palek, J., *Targeted disruption of the murine erythroid band 3 gene results in spherocytosis and severe haemolytic anaemia despite a normal membrane skeleton.* Nat. Genet., 1996. **14**(2): 227-230.

49. Liu, S.-C., Zhai, S., Palek, J., Golan, D.E., Amato, D., Hassan, K., Nurse, G.T., Babano, D., Coetzer, T., Jarolim, P., Zaik, M., and Borwein, S., *Molecular defect of the Band 3 protein in southeast Asian ovalocytosis.* New Engl. J. Med., 1990. **323**: 1530-1538.
50. Schofield, A.E., Reardon, D.M., and Tanner, M.J.A., *Defective anion transport activity of the abnormal Band 3 in hereditary ovalocytic blood cells.* Nature, 1992. **355**: 836-838.
51. Dahl, N.K., Jiang, L., Chernova, M.N., Stuart-Tilley, A.K., Shmukler, B.E., and Alper, S.L., *Deficient HCO_3^- transport in an AE1 mutant with normal Cl^- transport can be rescued by carbonic anhydrase II presented on an adjacent AE1 protomer.* J. Biol. Chem., 2003. **21**: 21.
52. Sarabia, V.E., Casey, J.R., and Reithmeier, R.A., *Molecular characterization of the band 3 protein from Southeast Asian ovalocytes.* J. Biol. Chem., 1993. **268**(14): 10676-10680.
53. Genton, B., al-Yaman, F., Mgone, C.S., Alexander, N., Paniu, M.M., Alpers, M.P., and Mokela, D., *Ovalocytosis and cerebral malaria.* Nature, 1995. **378**(6557): 564-565.
54. Allen, S.J., O'Donnell, A., Alexander, N.D., Mgone, C.S., Peto, T.E., Clegg, J.B., Alpers, M.P., and Weatherall, D.J., *Prevention of cerebral malaria in children in Papua New Guinea by southeast Asian ovalocytosis band 3.* Am J Trop Med Hyg, 1999. **60**(6): 1056-1060.
55. Tse, W.T. and Lux, S.E., *Red blood cell membrane disorders.* Br J Haematol, 1999. **104**(1): 2-13.
56. Lux, S.E., and Palek, J., *Disorders of the red cell membrane*, in *Blood: Principles and Practice of Hematology*, R.I. Handin, Lux, S. E., and Stossel, T. P., Editor. 1995, Lippincott Co.: Philadelphia.
57. Bustos, S.P. and Reithmeier, R.A., *Structure and stability of hereditary spherocytosis mutants of the cytosolic domain of the erythrocyte anion exchanger 1 protein.* Biochemistry, 2006. **45**(3): 1026-1034.
58. Dhermy, D., Burnier, O., Bourgeois, M., and Grandchamp, B., *The red blood cell band 3 variant (band 3Biceetrel:R490C) associated with dominant hereditary spherocytosis causes defective membrane targeting of the molecule and a dominant negative effect.* Mol Membr Biol, 1999. **16**(4): 305-312.
59. Quilty, J.A. and Reithmeier, R.A., *Trafficking and folding defects in hereditary spherocytosis mutants of the human red cell anion exchanger.* Traffic, 2000. **1**(12): 987-998.
60. Jarolim, P., Rubin, H.L., Brabec, V., Chrobak, L., Zolotarev, A.S., Alper, S.L., Brugnara, C., Wichterle, H., and Palek, J., *Mutations of conserved arginines in the membrane domain of erythroid band 3 lead to a decrease in membrane-associated band 3 and to the phenotype of hereditary spherocytosis.* Blood, 1995. **85**: 634-640.
61. Han, J.S., Kim, G.H., Kim, J., Jeon, U.S., Joo, K.W., Na, K.Y., Ahn, C., Kim, S., Lee, S.E., and Lee, J.S., *Secretory-defect distal renal tubular acidosis is associated with transporter defect in H^+-ATPase and anion exchanger-1.* J Am Soc Nephrol, 2002. **13**(6): 1425-1432.

62. Morris, R.C., and Ives, H. E., *Inherited disorders of the renal tubule*, in *The Kidney*, B.M. Brenner, Editor. 1996, W. B. Saunders: Philadelphia, PA. 1764-1827.
63. Jarolim, P., Shayakul, C., Prabakaran, D., Jiang, L., Stuart-Tilley, A., Rubin, H.L., Simova, S., Zavadil, J., Herrin, J.T., Brouillette, J., Somers, M.J., Seemanova, E., Brugnara, C., Guay-Woodford, L.M., and Alper, S.L., *Autosomal dominant distal renal tubular acidosis is associated in three families with heterozygosity for the R589H mutation in the AE1 (band 3) Cl^-/HCO_3^- exchanger*. J. Biol. Chem., 1998. **273**(11): 6380-6388.
64. Kittanakom, S., Cordat, E., Akkarapatumwong, V., Yenchitsomanus, P.T., and Reithmeier, R.A., *Trafficking defects of a novel autosomal recessive distal renal tubular acidosis mutant (S773P) of the human kidney anion exchanger (kAE1)*. J. Biol. Chem., 2004. **279**(39): 40960-40971.
65. Devonald, M.A., Smith, A.N., Poon, J.P., Ihrke, G., and Karet, F.E., *Non-polarized targeting of AE1 causes autosomal dominant distal renal tubular acidosis*. Nat. Genet., 2003. **21**: 21.
66. Toye, A.M., Banting, G., and Tanner, M.J., *Regions of human kidney anion exchanger 1 (kAE1) required for basolateral targeting of kAE1 in polarised kidney cells: mis-targeting explains dominant renal tubular acidosis (dRTA)*. J Cell Sci, 2004. **2**.
67. Tanphaichitr, V.S., Sumboonnanonda, A., Ideguchi, H., Shayakul, C., Brugnara, C., Takao, M., Veerakul, G., and Alper, S.L., *Novel AE1 mutations in recessive distal renal tubular acidosis. Loss-of- function is rescued by glycophorin A*. J Clin Invest, 1998. **102**(12): 2173-2179.
68. Bruce, L.J., Wrong, O., Toye, A.M., Young, M.T., Ogle, G., Ismail, Z., Sinha, A.K., McMaster, P., Hwaihwanje, I., Nash, G.B., Hart, S., Lavu, E., Palmer, R., Othman, A., Unwin, R.J., and Tanner, M.J., *Band 3 mutations, renal tubular acidosis and South-East Asian ovalocytosis in Malaysia and Papua New Guinea: loss of up to 95% band 3 transport in red cells*. Biochem J, 2000. **350 Pt 1**: 41-51.
69. Yusoff, N.M., Van Rostenberghe, H., Shiakawa, T., Nishiyama, K., Amin, N., Darus, Z., Zainal, N., Isa, N., Nozu, H., and Matsuo, M., *High prevalence of Southeast Asian ovalocytosis in Malays with distal renal tubular acidosis*. J Hum Genet, 2003. **48**: 650-653.
70. Yenchitsomanus, P.T., Vasuvattakul, S., Kirdpon, S., Wasanawatana, S., Susaengrat, W., Sreethiphayawan, S., Chuawatana D., Mingkum, S., Sawasdee, N., Thuwajit, P., Wilairat, P., Malasit, P., and Nimmannit, S., *Autosomal recessive distal renal tubular acidosis caused by G710D mutation of anion exchanger 1 gene*. Am J Kidney Dis, 2002. **40**: 21-29.
71. Jennings, M.L., *Structure and function of the red blood cell anion transport protein*. Annu. Rev. Biophys. Biophys. Chem., 1989. **18**: 397-430.
72. Gunn, R.B. and Frohlich, O., *Asymmetry in the mechanism for anion exchange in human red blood cell membranes. Evidence for reciprocating sites that react with one transported anion at a time*. J Gen Physiol, 1979. **74**(3): 351-374.
73. Furuya, W., Tarshis, T., Law, F.Y., and Knauf, P.A., *Transmembrane effects of intracellular chloride on the inhibitory potency of extracellular H_2DIDS. Evidence for two conformations of the transport site of the human erythrocyte anion exchange protein*. J Gen Physiol, 1984. **83**(5): 657-681.

74. Passow, H., *Molecular aspects of Band 3-mediated anion transport across the red blood cell membrane.* Rev. Physiol. Biochem. Pharmacol., 1986. **103**: 61-223.
75. Frohlich, O. and Gunn, R.B., *Erythrocyte anion transport: the kinetics of a single-site obligatory exchange system.* Biochim Biophys Acta, 1986. **864**(2): 169-194.
76. Jennings, M.L., *Evidence for an access channel leading to the outward-facing substrate site in human red blood cell Band 3*, in *Anion Transport Protein of the Red Blood Cell Membrane*, N. Hamasaki and M.L. Jennings, Editors. 1989, Elsevier: Amsterdam. 59-72.
77. Ko, S.B., Shcheynikov, N., Choi, J.Y., Luo, X., Ishibashi, K., Thomas, P.J., Kim, J.Y., Kim, K.H., Lee, M.G., Naruse, S., and Muallem, S., *A molecular mechanism for aberrant CFTR-dependent HCO_3^- transport in cystic fibrosis.* EMBO J, 2002. **21**(21): 5662-5672.
78. Knauf, P.A., Breuer, W., McCulloch, L., and Rothstein, A., *N-(4-azido-2-nitrophenyl)-2-aminoethylsulfonate (NAP-taurine) as a photoaffinity probe for identifying membrane components containing the modifier site of the human red blood cell anion exchange system.* J Gen Physiol, 1978. **72**(5): 631-649.
79. Kopito, R.R., Lee, B.S., Simmons, D.M., Lindsey, A.E., Morgans, C.W., and Schneider, K., *Regulation of intracellular pH by a neuronal homolog of the erythrocyte anion exchanger.* Cell, 1989. **59**: 927-937.
80. Zhu, Q. and Casey, J.R., *The substrate anion selectivity filter in the human erythrocyte Cl^-/HCO_3^- exchange protein, AE1.* J. Biol. Chem., 2004. **279**: 23565-23573.
81. Zhu, Q., Lee, D.W.K., and Casey, J.R., *Novel Topology in C-terminal Region of the Human Plasma membrane anion exchanger, AE1.* J. Biol. Chem., 2003. **278**: 3112-3120.
82. Jennings, M.L. and Anderson, M.P., *Chemical modification and labelling of glutamate residues at the stilbenedisulonate site of human red cell Band 3 protein.* J. Biol. Chem., 1987. **262**(4): 1691-1697.
83. Jennings, M.L. and Smith, J.S., *Anion-proton cotransport through the human red blood cell band 3 protein. Role of glutamate 681.* J. Biol. Chem., 1992. **267**: 13964-13971.
84. Jennings, M.L., *Proton fluxes associated with erythrocyte membrane anion exchange.* J. Membr. Biol., 1976. **28**: 187-205.
85. Milanick, M.A. and Gunn, R.B., *Proton-sulfate cotransport: mechanism of H^+ and sulfate addition to the chloride transpoter of human red cells.* J. Gen. Physiol., 1982. **79**: 87-113.
86. Chernova, M.N., Jiang, L., Crest, M., Hand, M., Vandorpe, D.H., Strange, K., and Alper, S.L., *Electrogenic sulfate/chloride exchange in Xenopus oocytes mediated by murine AE1 E699Q.* J Gen Physiol, 1997. **109**(3): 345-360.
87. Bruce, L.J., Groves, J.D., Okubo, Y., Thilaganathan, B., and Tanner, M.J., *Altered band 3 structure and function in glycophorin A- and B-deficient (MkMk) red blood cells.* Blood, 1994. **84**(3): 916-922.
88. Groves, J.D. and Tanner, M.J., *Glycophorin A facilitates the expression of human Band 3-mediated anion transport in Xenopus oocytes.* J. Biol. Chem., 1992. **267**: 22163-22170.

89. Vince, J.W. and Reithmeier, R.A.F., *Carbonic anhydrase II binds to the carboxyl-terminus of human band 3, the erythrocyte Cl^-/HCO_3^- exchanger.* J. Biol. Chem., 1998. **273**(43): 28430-28437.
90. Vince, J.W. and Reithmeier, R.A., *Identification of the Carbonic Anhydrase II Binding Site in the Cl^-/HCO_3^- Anion Exchanger AE1.* Biochemistry, 2000. **39**(18): 5527-5533.
91. Sterling, D., Reithmeier, R.A., and Casey, J.R., *A Transport Metabolon. Functional Interaction of Carbonic Anhydrase II and Chloride/Bicarbonate Exchangers.* J. Biol. Chem., 2001. **276**(51): 47886-47894.
92. Piermarini, P.M., Kim, E.Y., and Boron, W.F., *Evidence against a Direct Interaction between Intracellular Carbonic Anhydrase II and Pure C-terminal Domains of SLC4 Bicarbonate Transporters.* J. Biol. Chem., 2007. **282**: 1409-1421.
93. Vince, J.W., Carlsson, U., and Reithmeier, R.A., *Localization of the Cl^-/HCO_3^- anion exchanger binding site to the amino-terminal region of carbonic anhydrase II.* Biochemistry, 2000. **39**(44): 13344-13349.
94. Loiselle, F.B., Alvarez, B.V., and Casey, J.R., *Regulation of the Human NBC3 Na^+/HCO_3^- co-transporter by Carbonic Anhydrase II and Protein Kinase A.* Am. J. Physiol., 2004. **286**(6): 307-317.
95. Bennett, V., *Spectrin-based membrane skeleton: a multipotential adaptor between plasma membrane and cytoplasm.* Physiol. Rev., 1990. **70**: 1029-1065.
96. Jay, D. and Cantley, L., *Structural aspects of the red cell anion exchange protein.* Ann. Rev. Biochem, 1986. **55**: 511-538.
97. Wang, D.N., *Band 3 protein: structure, flexibility and function.* FEBS Lett, 1994. **346**(1): 26-31.
98. Lepke, S., Fashold, H., Pring, M., and Passow, H., *A study of the relationship between inhibition of anion exchange and binding to the red blood cell membrane of DIDS and its dihydro deriviative.* J. Membr. Biol., 1976. **29**: 147-177.
99. Casey, J.R. and Reithmeier, R.A.F., *Transport activity of deglycosylated Band 3, the anion exchange protein of the erythrocyte membrane.* Glycoconjugate J., 1991. **8**: 138.
100. Casey, J.R., Pirraglia, C.A., and Reithmeier, R.A.F., *Enzymatic deglycosylation of human Band 3, the anion transport protein of the erythrocyte membrane: effect on protein structure and transport properties.* J. Biol. Chem., 1992. **267**: 11940-11948.
101. Toye, A.M., Bruce, L.J., Unwin, R.J., Wrong, O., and Tanner, M.J., *Band 3 Walton, a C-terminal deletion associated with distal renal tubular acidosis, is expressed in the red cell membrane but retained internally in kidney cells.* Blood, 2002. **99**: 342-347.
102. Sterling, D., Reithmeier, R.A.F., and Casey, J.R., *Carbonic Anhydrase Interaction Potentiates Chloride/ Bicarbonate Activity Of the Human AE1 Protein.* Gordon Research Conference on Mechanism of Membrane Transport Proteins, 2001.
103. Jennings, M.L. and Passow, H., *Anion transport across the erythrocyte membrane in situ proteoysis of Band 3 protein, and cross-linking of proteolytic fragments by 4,4'-diisothiocyano dihydrostilbene-2,2'-disulfonate.* Biochim. Biophys. Acta, 1979. **554**: 498-519.

104. Casey, J.R. and Reithmeier, R.A.F., *Analysis of the oligomeric state of Band 3, the anion transport protein of the human erythrocyte membrane, by size exclusion high performance liquid chromatography: oligomeric stability and origin of heterogeneity.* J. Biol. Chem., 1991. **266**: 15726-15737.
105. Salhany, J.M., *Erythrocyte Band 3 Protein.* 1990, Boca Raton, Florida: CRC Press: 213.
106. Liu, D., Kennedy, S.D., and Knauf, P.A., *^{35}Cl nuclear magnetic resonance line broadening shows that eosin-5- maleimide does not block the external anion access channel of band 3.* Biophys J, 1995. **69**(2): 399-408.
107. Tang, X.B., Fujinaga, J., Kopito, R., and Casey, J.R., *Topology of the region surrounding Glu681 of human AE1 protein, the erythrocyte anion exchanger.* J. Biol. Chem., 1998. **273**(35): 22545-22553.
108. Popov, M., Tam, L.Y., Li, J., and Reithmeier, R.A.F., *Mapping the ends of transmembrane segments in a polytopic membrane protein. Scanning N-glycosylation mutagenesis of extracytosolic loops in the anion exchanger, band 3.* J. Biol. Chem., 1997. **272**(29): 18325-18332.
109. Reithmeier, R.A.F., Chan, S.L., and Popov, M., *Structure of the erythrocyte band 3 anion exchanger*, in *Transport Processes in Eukaryotic and Prokaryotic Organisms*, W.N. Konings, H.R. Kaback, and J.S. Lolkema, Editors. 1996, Elsevier Science. 281-309.
110. Fujinaga, J., Tang, X.-B., and Casey, J.R., *Topology of the membrane domain of human anion exchange protein, AE1.* J. Biol. Chem., 1999. **274**: 6626-6633.
111. Kopito, R.R. and Lodish, H.F., *Primary structure and transmembrane orientation of the murine anion exchange protein.* Nature, 1985. **316**: 234-238.
112. Kuma, H., Shinde, A.A., Howren, T.R., and Jennings, M.L., *Topology of the Anion Exchange Protein AE1: The Controversial Sidedness of Lysine 743.* Biochemistry, 2002. **41**(10): 3380-3388.
113. Popov, M., Li, J., and Reithmeier, R.A., *Transmembrane folding of the human erythrocyte anion exchanger (AE1, Band 3) determined by scanning and insertional N-glycosylation mutagenesis.* Biochem. J., 1999. **339**(Pt 2): 269-279.
114. Wainwright, S.D., Tanner, M.J., Martin, G.E., Yendle, J.E., and Holmes, C., *Monoclonal antibodies to the membrane domain of the human erythrocyte anion transport protein. Localization of the C-terminus of the protein to the cytoplasmic side of the red cell membrane and distribution of the protein in some human tissues.* Biochem J, 1989. **258**(1): 211-220.
115. Zhang, D., Kiyatkin, A., Bolin, J.T., and Low, P.S., *Crystallographic structure and functional interpretation of the cytoplasmic domain of erythrocyte membrane band 3.* Blood, 2000. **96**(9): 2925-2933.
116. Wang, D.N., Sarabia, V.E., Reithmeier, R.A., and Kuhlbrandt, W., *Three-dimensional map of the dimeric membrane domain of the human erythrocyte anion exchanger, Band 3.* EMBO J., 1994. **13**(14): 3230-3235.
117. Lemieux, M.J., Reithmeier, R.A., and Wang, D.N., *Importance of detergent and phospholipid in the crystallization of the human erythrocyte anion-exchanger membrane domain.* J Struct Biol, 2002. **137**(3): 322-332.
118. Wang, D.N., Kuhlbrandt, W., Sarabia, V., and Reithmeier, R.A.F., *Two-dimensional structure of the membrane domain of human band 3, the anion transport protein of the erythrocyte membrane.* EMBO J., 1993. **12**: 2233-2239.

119. Cabantchik, Z.I. and Greger, R., *Chemical probes for anion transporters of mammalian membranes.* Am. J. Physiol., 1992. **262**: C803-C827.
120. Okubo, K., Kang, D., Hamasaki, N., and Jennings, M.L., *Red blood cell band 3. Lysine 539 and lysine 851 react with the same H_2DIDS (4,4'-diisothiocyanodihydrostilbene-2,2'-disulfonic acid) molecule.* J. Biol. Chem., 1994. **269**: 1918-1926.
121. Kaplan, J.H., Scorah, K., Fasold, H., and Passow, H., *Sidedness of the inhibitory action of disulfonic acids on chloride equilibrium exchange and net transport across the human erythrocyte membrane.* FEBS Lett, 1976. **62**(2): 182-185.
122. Jennings, M.L., Whitlock, J., and Shinde, A., *Pre-steady state transport by erythrocyte band 3 protein: uphill countertransport induced by the impermeant inhibitor H_2DIDS.* Biochem Cell Biol, 1998. **76**(5): 807-813.
123. Salhany, J.M., Sloan, R.L., and Schopfer, L.M., *Characterization of the stilbenedisulphonate binding site on band 3 Memphis variant II (Pro-854-->Leu).* Biochem J, 1996. **317**(Pt 2): 509-514.
124. Sorensen, T.L., Moller, J.V., and Nissen, P., *Phosphoryl transfer and calcium ion occlusion in the calcium pump.* Science, 2004. **304**(5677): 1672-1675.
125. Jidenko, M., Nielsen, R.C., Sørensen, T. L.-M., Møller, J., le Maire, M., Nissen, P., and Jaxel, C., *Crystallization of a mammalian membrane protein overexpressed in Saccharomyces cerevisiae.* Proc Natl Acad Sci U S A, 2005. **102**: 11687-11691.
126. Jin, X.R., Abe, Y., Li, C.Y., and Hamasaki, N., *Histidine-834 of Human Erythrocyte Band 3 Has an Essential Role in the Conformational Changes That Occur during the Band 3-Mediated Anion Exchange.* Biochemistry, 2003. **42**(44): 12927-12932.
127. Groves, J.D., Falson, P., le Maire, M., and Tanner, M.J., *Functional cell surface expression of the anion transport domain of human red cell band 3 (AE1) in the yeast Saccharomyces cerevisiae.* Proc Natl Acad Sci U S A, 1996. **93**(22): 12245-12250.
128. Lenoir, G., Menguy, T., Corre, F., Montigny, C., Pedersen, P. A., Thinès, D., le Maire, M., and Falson, P., *Overproduction in yeast and rapid and efficient purification of the rabbit SERCA1a Ca^{2+}-ATPase.* Biochim Biophys Acta, 2002. **1560**: 67-83.
129. Long, S.B., Campbell, E.B., and Mackinnon, R., *Crystal Structure of a Mammalian Voltage-Dependent Shaker Family K^+ Channel.* Science, 2005. **309**(5736): 897-903.
130. Jidenko, M., Lenoir, G., Fuentes, J., le Maire, M., and Jaxel, C., *Expression in yeast and purification of a membrane protein, SERCA1a, using a biotinylated acceptor domain.* Protein Expr Purif, 2006. **48**: 32-42.
131. Weiss, H.M., Haase, W., Michel, H., and Reilander, H., *Expression of functional mouse 5-HT5A serotonin receptor in the methylotrophic yeast Pichia pastoris: pharmacological characterization and localization.* FEBS Lett, 1995. **377**(3): 451-456.
132. Lewis, B.A. and Engelman, D.M., *Lipid bilayer thickness varies linearly with acyl chain length in phosphatidylcholine vesicles.* J. Mol. Biol., 1983. **166**: 211-217.

133. Roth, M., Lewit-Bentley, A., Michel, H., Diesenhofer, J., Huber, R., and Osterhelt, D., *Detergent structure in crystals of a bacterial photosynthetic reaction centre.* Nature, 1989. **340**: 659-662.
134. Sekler, I., Kopito, R.R., and Casey, J.R., *High level expression, partial purification and functional reconstitution of the human AE1 anion exchange protein in Saccharomyces cerevisiae.* J. Biol. Chem., 1995. **270**: 21028-21034.
135. Fukuda, M., Dell, A., Oates, J.E., and Fukuda, M.N., *Structure of the branched lactosaminoglycan, the carbohydrate moiety of Band 3 isolated from adult human erythrocytes.* J. Biol. Chem., 1984. **259**: 8260-8273.
136. Okubo, K., Hamasaki, N., Hara, K., and Kageura, M., *Palmitoylation of Cysteine 69 from the C-terminal of Band 3 protein in the human erythrocyte membrane.* J. Biol. Chem., 1991. **266**(25): 16420-16424.
137. Cheung, J.C. and Reithmeier, R.A., *Palmitoylation is not required for trafficking of human anion exchanger 1 to the cell surface.* Biochem J, 2004. **378**(Pt 3): 1015-1021.
138. Alper, S.L., Darman, R.B., Chernova, M.N., and Dahl, N.K., *The AE gene family of Cl^-/HCO_3^- exchangers.* J Nephrol, 2002. **15**(Suppl 5): S41-53.
139. Zolotarev, A.S., Townsend, R.R., Stuart-Tilley, A., and Alper, S.L., *HCO_3^--dependent conformational change in gastric parietal cell AE2, a glycoprotein naturally lacking sialic acid.* American Journal of Physiology, 1996. **271**(2 Pt 1): G311-321.
140. Tarentino, A.L., Gomez, C.M., and Jr., T.H.P., *Deglycosylation of asparagine-linked glycans by peptide:N-glycosidase F.* Biochem., 1985. **24**: 4665-4671.
141. Sui, H., Walian, P.J., Tang, G., Oh, A., and Jap, B.K., *Crystallization and preliminary X-ray crystallographic analysis of water channel AQP1.* Acta Crystallogr D Biol Crystallogr, 2000. **56**: 1198-1200.
142. Kuhlbrandt, W., *Three-dimensional crytallization of membrane proteins.* Quart. Rev. Biophys., 1988. **21**: 429-477.
143. Casey, J.R. and Reithmeier, R.A.F., *Detergent interaction with Band 3, a model polytopic membrane protein.* Biochem., 1993. **32**: 1172-1179.
144. Casey, J.R., Lieberman, D.M., and Reithmeier, R.A.F., *Purification and characterization of Band 3 protein.* Methods Enzymol., 1989. **173**: 494-512.
145. Waugh, D.S., *Making the most of affinity tags.* Trends Biotechnol, 2005. **23**: 316-320.
146. di Guan, C., Li, P., Riggs, P.D., and Inouye, H., *Vectors that facilitate the expression and purification of foreign peptides in Eschericia coli by fusion to maltose binding protein.* Gene, 1988. **67**: 21-30.
147. Wyborski, D.L., Bauer, J.C., Zheng, C-F., Felts, K., and Vaillancourt, P., *An Escherichia coli expression vector that allows recovery of proteins with native N-termini from purified calmodulin-binding peptide fusions.* Protein Expr Purif, 1999. **16**: 1-10.
148. Hochuli, E., Bannwarth, W., Döbeli, H., Gentz, R., and Stüber, D., *Genetic approach to facilitate purification of recombinant proteins with a novel metal chelate adsorbant.* Bio/technology, 1988. **6**: 1321-1325.
149. Smith, D.B., and Johnson, K.S., *One-step purification of polypeptides expressed in Escherichia coli as fusions with Glutathione S-transferase.* Gene, 1988. **67**: 31-40.

150. Porath, J., Carlsson, J., Olsson, I., and Belfrage, G., *Metal chelate affinity chromatography, a new approach to protein fractionation.* Nature, 1975. **258**(5536): 598-599.
151. Nygren, P.-A., Stahl, S., and Uhlen, M., *Engineering proteins to facilitate bioprocessing.* Trends Biotechnol, 1994. **12**: 184-188.
152. Wang, Q., and Chang, A., *Sphingoid base synthesis is required for oligomerization and cell surface stability of the yeast plasma membrane ATPase, Pma1.* Proc Natl Acad Sci U S A, 2002. **99**: 12853-12858.
153. Jones, E.W., *Tackling the protease problem in Saccharomyces cerevisiae.* Methods Enzymol., 1991. **194**: 428-453.
154. Pompon, D., Louerat, B., Bronine, A., and Urban, P., *Yeast Expression of Animal and Plant P450s in Optimized Redox Environments.* Methods Enzymol, 1996. **272**: 51-64.
155. Casey, J.R., Ding, Y., and Kopito, R.R., *The role of cysteine residues in the erythrocyte plasma membrane anion exchange protein, AE1.* J. Biol. Chem., 1995. **270**: 8521-8527.
156. Schiestl, R.H. and Gietz, D., *about yeast transformations.* Current Genetics, 1989. **16**: 339-346.
157. Gietz, R.H., Jean, A.S., Woods, R.A., and Schiestl, R.H., *Improved method for high efficiency transformation of yeast cells.* Nucl. Acids Res., 1992. **20**: 1425.
158. Eble, R., *A simple and efficeint procedure for transformation of yeasts.* Biotechniques, 1992. **13**: 18-20.
159. Bradford, M.M., *A rapid and sensitive method for the quantitation of microgram quantities of protein utilizing the pricinple of protein-dye binding.* Anal. Biochem., 1976. **72**: 248-254.
160. Smith, P.K., Krohn, R.I., Hermanson, G.T., Mallia, A.K., Gartner, F.H., Provenzano, M.D., Fujimoto, E.K., Goeke, N.M., Olson, B.J., and Klenk, D.C., *Measurement of protein using bicinchoninic acid.* Anal. Biochem., 1985. **150**: 76-85.
161. Grinstein, S., Ship, S., and Rothstein, A., *Anion transport in relation to proteolytic dissection of Band 3 protein.* Biochim. Biophys. Acta, 1979. **507**: 294-304.
162. Lee, B.S., Gunn, R.B., and Kopito, R.R., *Functional differences among nonerythroid anion exchangers expressed in a transfected human cell line.* J. Biol. Chem., 1991. **266**: 11448-11454.
163. Figler, R.A., Omote, H., Nakamato, R.K., and Al-Shawi, M.K., *Use of Chemical Chaperones in the Yeast Saccharomyces cerevisiae to Enhance Heterologous Membrane Protein Expression: High-Yield Expression and Purification of Human P-Glycoprotein.* Arch Biochem Biophys, 2000. **376**: 34-46.
164. Ealke, K.A., Kim, K.S., Kabalin, M.A., and Farley, R.A., *High-affinity oubain binding by yeast cells expressing Na^+,K^+-ATpase α subunits and the gastric H^+,K^+-ATPase β subunit.* J. Biol. Chem., 1992. **89**: 2834-2838.
165. Ruetz, S. and Gros, P., *Functional expression of P-glycoprotein in secretory vesicles.* J. Biol. Chem., 1994. **269**: 12277-12284.
166. Steck, T.L., Ramos, B., and Strapazon, E., *Proteolytic dissection of Band 3, the predominant transmembrane polypeptide of the human erythrocyte membrane.* Biochem., 1976. **15**: 1154-1161.

167. Kozak, M., *At least six nucleotides preceding the AUG initiator codon enhance translation in mammalian cells.* J Mol Biol, 1987. **196**: 947.
168. Tanner, M.J., Martin, P.G., and High, S., *The complete amino acid sequence of the human erythrocyte membrane anion-transport protein deduced from the cDNA sequence.* Biochem. J., 1988. **256**: 703-712.
169. Lux, S.E., John, K.M., and Bennett, V., *Analysis of cDNA for human erythrocyte ankyrin indicates a repeated structure with homology to tissue-differentiation and cell-cycle control proteins.* Nature, 1990. **344**: 36-42.
170. Drickamer, L.K., *Orientation of the Band 3 polypeptide from human erythrocyte membranes: identification of NH_2-terminal sequence and site of carbohydrate attachment.* J. Biol. Chem., 1978. **253**: 7242-7248.
171. Pimplikar, S.W. and Reithmeier, R.A.F., *Affinity chromatography of Band 3, the anion transport protein of erythrocyte membranes.* J. Biol. Chem., 1986. **261**: 9770-9778.
172. Knauf, P.A. and Mann, N.A., *Use of niflumic acid to determine the nature of the asymmetry of the human erythrocyte anion exchange system.* J Gen Physiol, 1984. **83**(5): 703-725.